

**NASA CONTRACTOR
REPORT**

NASA CR-634



NASA-GR

0060257

TECH LIBRARY KAFB, NM

**LOAN COPY: RETURN TO
AFWL (WLIL-2)
KIRTLAND AFB, N MEX**

**EFFECTS OF PERIODIC BLOWING
THROUGH FLUSH TRANSVERSE SLOTS
ON TURBULENT BOUNDARY LAYER
SKIN FRICTION**

by Jack G. Spangler

Prepared by
LING-TEMCO-VOUGHT, INC.
Dallas, Texas
for

NATIONAL AERONAUTICS AND SPACE ADMINISTRATION • WASHINGTON, D. C. • OCTOBER 1966



EFFECTS OF PERIODIC BLOWING THROUGH FLUSH TRANSVERSE SLOTS
ON TURBULENT BOUNDARY LAYER SKIN FRICTION

By Jack G. Spangler

Distribution of this report is provided in the interest of information exchange. Responsibility for the contents resides in the author or organization that prepared it.

Prepared under Contract No. NASw-956 by
LING-TEMCO-VOUGHT, INC.
Dallas, Texas

for

NATIONAL AERONAUTICS AND SPACE ADMINISTRATION

For sale by the Clearinghouse for Federal Scientific and Technical Information
Springfield, Virginia 22151 - Price \$2.50

EFFECTS OF PERIODIC BLOWING THROUGH
FLUSH TRANSVERSE SLOTS ON TURBULENT
BOUNDARY LAYER SKIN FRICTION

by Jack G. Spangler

SUMMARY

As part of an experimental investigation of techniques for reducing turbulent skin friction drag, small transverse disturbances were introduced into a turbulent boundary layer. The boundary layer was formed on the test section wall of a facility designed especially for low-speed boundary layer studies. Periodic jets of air were injected into the boundary layer from a continuous circumferential slot in the test section wall resulting in reduced values of skin friction drag and boundary layer turbulence. Skin friction measurements, velocity profiles, and turbulence intensity measurements are presented as a function of blowing rate, pulse frequency, and location in the flow field. The experiments show an interesting relation between turbulence intensity and skin friction drag, but no promise is shown for realizing a net drag reduction due to the power requirements of the particular system.

INTRODUCTION

The turbulent boundary layer has long posed a problem to aerodynamicists and others concerned with the performance of vehicles operating in a viscous medium. The high skin friction drag and heat transfer rates in turbulent flow, relative to those in laminar flow, are sufficiently detrimental to vehicle performance to have justified the interest of numerous investigators in searching for ways to maintain a fully laminar boundary layer. Unfortunately, in spite of these efforts, most practical situations involve the eventual occurrence of turbulent flow, and consequently the engineer or scientist is constantly trying to find methods for minimizing the undesirable characteristics of the turbulent boundary layer.

The Aerophysics Group of the LTV Research Center has been conducting a study of the effects of introducing discrete vortices into a fully developed turbulent boundary layer. The initial effort in this study was an investigation of the effects of continuous longitudinal vortices, particularly on the skin friction drag. The results of these experiments have been reported in reference 1.

This report deals with the results to date of a study on the effects of periodically occurring transverse vortices in a fully developed turbulent boundary layer. Interest in this study arose

from the results of an investigation by Eggers and Hermach (reference 2) in which they concluded that reductions in turbulent heat transfer rate by as much as 22 percent on a supersonic body were due to the periodic passage through the boundary layer of large scale vortical motions. Assuming the validity of the analogy between heat transfer and momentum transfer to hold for this case, the results of reference 2 imply that similar reductions in skin friction drag were effected although they were not measured or reported.

Based on these findings, an experiment was designed wherein transverse vortices would be introduced into a turbulent boundary layer formed in the boundary layer channel facility of the LTV Research Center. If skin friction reductions were accomplished, the results would be analyzed to determine the mechanism involved. Analyses would also be made to determine if the energy consumed in generating the vortices would be small enough to allow a net reduction in the system drag to be realized.

SYMBOLS

A	test section surface area
C_f	average skin friction coefficient, $\frac{1}{X} \int_0^X \tau_o/q \, dX$
ΔC_f	change in C_f due to blowing
ΔC_{f_p}	equivalent increase in C_f due to power requirements
P	power consumed in blowing
Δp	pressure differential across blowing slot
Q	volume flow rate of blowing
q	stream dynamic pressure, $\frac{1}{2} \rho U_\infty^2$
t	time
u	local mean velocity
u'_{RMS}	rms value of longitudinal velocity fluctuation
U_∞	local free stream velocity
u_τ	friction velocity, $\sqrt{\frac{\tau_o}{\rho}}$
V	hot-wire signal
X	longitudinal distance downstream of blowing slot
y	distance normal to wall
τ_{o_B}	wall shear stress with blowing

τ_{oNB}	wall shear stress with no blowing
$\Delta\tau_o$	percentage change in τ_o due to blowing, $100 (\tau_{oB} - \tau_{oNB})/\tau_{oNB}$
ω	pulse frequency
f	frequency of turbulent velocity fluctuations
λ	bandwidth
ν	kinematic viscosity
ρ	density

EXPERIMENTAL FACILITY AND INSTRUMENTATION

A. BOUNDARY LAYER CHANNEL

The basic experimental facility used for the vortex-boundary layer experiments is an open-circuit wind tunnel designed for study of the boundary layer produced on the test section wall. A complete description of this facility (shown by sketch in Figure 1) may be found in references 1 and 3 and only a brief review will be given here.

The test section of the boundary layer channel is 25 feet long with an inside diameter of 8.030 inches. The test section is an assembly of six transparent plexiglas tubes bored, honed, and polished to an overall tolerance in diameter of $\pm .001$ -inch and a wall waviness of .001-inches per inch of length. Air is drawn through the channel by a Roots-Connersville vacuum blower isolated from the test section by a choked sonic throat. Damping screens and a 20:1 area ratio entrance nozzle reduce the turbulence level of the incoming air to a very low value. For turbulent flow studies one section of the channel is replaced by an assembly of interlocking rings which can be interchanged to allow various instrumentation to be placed at any azimuthal or longitudinal location in the channel.

B. SKIN FRICTION BALANCE

The primary objective of this study was to determine the effects of periodic transverse vortices on the turbulent skin friction. Thus it was desirable to be able to measure skin friction values directly and accurately. At the beginning of this program a skin friction balance was designed and built for this purpose. This instrument is described in detail in reference 4. Briefly, the skin friction balance is of the floating element type with an interacting electrical current and magnetic field providing a restoring force which may be controlled to null out the skin friction drag force. The drag force is thus a linear function of the electrical current required to null the balance. A schematic of the balance is shown in Figure 2. This

instrument is capable of measuring wall shear stress values from 10^{-6} to 10^{-4} lb/in² with an accuracy of ± 1 percent for turbulent boundary layer flows.

C. HOT-WIRE ANEMOMETER

Measurements of time-averaged mean velocities and fluctuating velocity components were made with constant-temperature hot-wire anemometers. These instruments are transistorized circuits of the Kovasznay type. Output linearizers for the hot-wire signals were available but were not used because of unsatisfactory stability. The remainder of the circuit including the bridge and amplifier were quite stable and gave very repeatable results. All of the hot-wire probes were made of .0002-inch diameter tungsten wire spot welded to sewing needle supports.

D. PRESSURE MEASUREMENTS

All pressure measurements were made with a Transonics Type 121 Equibar Pressure Meter which employs a fast response differential capacitance transducer. This instrument was used along with appropriate probes for determining channel flow rates, blowing chamber pressures, and calibrating all hot-wire probes.

PRELIMINARY EXPERIMENTS

A. FORMATION OF TRANSVERSE VORTICES

In the quest for a means of producing transverse vortices, the best thought that came to mind was to simulate the action that would be created by a transverse fence mounted perpendicularly on the test section wall that could be alternately extended and retracted. In this way transverse vortices would be formed behind the fence when it was extended and would shed and be swept downstream when the fence was retracted. Because of the axi-symmetrical configuration of the boundary layer channel, a mechanical fence would have to be quite complex and any mechanical system would undoubtedly cause intolerable vibrations. Consequently a system was devised that would simulate the action of a fence by the periodic injection into the boundary layer of a thin jet of air through a continuous circumferential slot in the test section wall. It was hoped that the momentary pulses of air would interact with the vorticity in the boundary layer to cause the periodic formation of transverse vortices. It should be pointed out that in the axi-symmetric boundary layer channel transverse vortices are actually continuous rings which, as will be shown later, are unstable and frequently add complications to the experiments.

As a first step in the development of an air pulsing system, a pilot model chamber was built. Compressed air was fed into the chamber through a throttling valve and a rotating "on-off" valve which

gave a ratio of flow on to flow off of 1:9. The rotary valve was belt driven by a variable speed A-C motor. The chamber was a rectangular box with inside dimensions which could be altered by the arrangement of dummy walls. A slot was provided in one exterior wall. The length and width of the slot could also be varied.

A hot wire probe was placed in the chamber slot to monitor the pulse form of the emerging air jet. After a series of tests, a suitable combination of chamber volume and slot size was obtained which gave a single sharp air pulse that was uniform along the length of the slot for each half cycle of the rotary valve.

The proportions determined in the rectangular box were incorporated into an annular chamber which was co-axially mounted in the boundary layer channel. Different sets of lips for the circumferential slot allowed the pulsed air jet to be directed either normal to the wall, tangentially upstream, or tangentially downstream in the boundary layer. The incoming air to the system was regulated to 80 psig which kept the metering needle valve choked. The system was calibrated so that the total mass injection into the boundary layer was known at all times. A schematic of the system is shown in Figure 3. Originally the pulses from the rotary valve were introduced into the annular plenum chamber at one location, but a check showed uniformity of the jet around the circumference of the test section to be unsatisfactory. Subsequently a manifold was incorporated to distribute the air to four equally spaced inlets to the plenum chamber which gave acceptable results. Once the uniformity of the pulse shape was established two fixed hot-wire probes were permanently mounted inside the chamber slot to allow continuous monitoring of the periodic jet flow.

B. INITIAL TESTS

The first measurements of the effects of the periodic blowing into the turbulent boundary layer revealed a multitude of resonance problems in the system. Since the boundary layer channel is essentially a long straight tube, it has a fundamental "organ pipe" frequency and harmonics. The fundamental frequency is about 10 cycles per second. When the injected air was pulsed at frequencies less than 100 cycles per second the tube resonated at the expected frequencies. This was a potential problem since the experiments were planned for this frequency range. The reasoning here was that to simulate the vortex spacing encountered in reference 2 the injected air should be pulsed at about 20 cycles per second. Also, considering the spectral distribution of the energy of fluctuations in a turbulent boundary layer, almost all of the energy, at the test conditions used, occurred at frequencies below 100 cycles per second.

It was somewhat surprising to find that initial measurements with the skin friction balance showed pulsing frequencies less than 200 cycles per second to be ineffective on the skin friction and

frequencies in the neighborhood of 300 cycles per second were necessary to get significant changes. Thus the organ pipe resonance of the channel was not too important but two other problems came to light.

The enclosure of the skin friction balance was found to respond as a Helmholtz resonator when air was pulsed into the boundary layer channel. Consequently the mass of air in the clearance space around the floating element would oscillate. The configuration was such that partial rectification of this oscillatory flow occurred causing a resultant force to act normal to the floating element and thus introduced an error into the balance reading. Several modifications were made to the balance to correct this situation. The most important modification was to mount the balance at the bottom of the boundary layer channel and eliminate the internal air volume by filling the entire enclosure with oil. This essentially eliminated resonance problems with the balance but it restricted the placement of the balance to the bottom of the channel and made handling and operation of the instrument considerably more tedious.

The other resonance problem concerned the annular plenum chamber. It was found that the chamber and slot configuration also behaved as a Helmholtz resonator with certain resonance frequencies that strongly affected the pulsed air jet. More will be said about this in the discussion of the results.

C. INITIAL RESULTS

Skin friction measurements were made at several locations downstream from the slot for numerous settings of blowing rate and pulse frequency. The first measurements were made for the case of blowing normal to the wall which was expected to be the best method for producing transverse vortices and reducing friction drag. To the contrary, no reductions in skin friction were found and in some instances slight increases were noticed. Tangential blowing was then tried for situations with the jet pulses being directed along the wall either upstream or downstream. Again the upstream blowing caused no favorable effects, but the downstream blowing created local skin friction reductions that were dependent on both blowing rate and pulse frequency and were as large as 20 percent in some instances.

As mentioned previously, the plenum chamber was designed for operation at frequencies under 100 cycles per second but significant drag reductions required pulse rates on the order of 300 pulses per second. The hot-wire probes mounted in the slot showed that the pulse form was quite different at these frequencies from what had been desired. It seemed logical that refining the chamber to give single sharp pulses in the high frequency range rather than ill defined pulses with considerable harmonic content would improve the effect on skin friction. This was accomplished by altering the internal volume of the chamber and adding packing material for damping. A reasonable pulse form was obtained but the maximum jet velocities were reduced and the best possible local skin friction reductions were then only

7 percent. A compromise setup was finally reached by removing the packing material. This left a somewhat irregular pulse form but skin friction reductions of 20 percent were once more possible.

While trying to determine the variation of skin friction with frequency it was found that in each of several narrow bandwidths the balance would show large increases in the measured drag force. With the earlier resonance problems still in mind it was suspected that these anomalies were again due to balance resonance. However, a hot-wire probe placed in the boundary layer just above the floating balance element showed that the local velocity also increased sharply when the measured drag increased and likewise the velocity decreased as the drag decreased. The two instruments checked qualitatively and quantitatively verifying that the anomalies were actually in the flow.

Inspection of the signal from the hot-wires in the slot showed that the jet velocities became much larger at these anomalous points in the frequency range even though the total mass flow through the blowing system was held constant. Also the apparent frequency of the large pulses was doubled at these points. It was concluded that these were resonance points in the plenum chamber and the result was a strong oscillatory flow in and out of the slot superimposed on the regular pulse flow. The hot-wires, being equally sensitive to flow in or out of the slot acted as rectifiers indicating twice the true pulse frequency. The result was a very strong jet pulse outward followed by a slightly weaker pulse inward. The difference in the two mass flows was the amount being let into the chamber through the calibrated flow system. This was verified by integrating the pulse profile over a period of one cycle, assuming the slightly weaker pulses to be in the inward direction. Agreement with the measured mass input was good. Further inspection of the hot-wire signals showed that this phenomenon occurred to a lesser extent over most of the frequency range above 200 pulses per second. The integrated difference between the inward and outward pulses always agreed reasonably well with the measured net flow rate and the individual pulses became very large only at the aforementioned resonance frequencies.

Up to this time no information had been obtained concerning the action in the boundary layer caused by the jet pulses, i.e., were vortices being formed or not? Signals from hot-wire probes did not show any regular disturbance pattern in the boundary layer except within a region extending about two inches downstream from the slot. In this region very small oscillations appeared in the signal when the probe was near the wall. The signal generally had the form of a rectified sine wave, but at the resonance frequencies of the plenum chamber the signal broke up into strong irregular fluctuations typical of turbulent bursts.

At this point an attempt was made to render the jet pulses visible. It will be recalled that the test section of the boundary layer channel is completely transparent except for the plenum chamber and the mounting rings for the skin friction balance and hot-wire traverse. Also a collimated, high-intensity light beam can be directed down the tube axis through a window in the transition section near the sonic throat. This allows flow patterns to be observed visually by

injecting smoke into the air stream. Due to the rapid diffusive action of the turbulent boundary layer nothing could be learned about the action of the jet pulses by flooding the boundary layer with smoke. Instead smoke was injected into the plenum chamber so that each pulse that came out was actually a puff of smoke. A mechanical chopper was used to interrupt the light beam to achieve a strobe effect. With this set up, the emerging jet pulses could be seen but they were very faint.

Several interesting discoveries came out of the flow visualization studies. First and most surprising was the size of the transverse disturbances. Vortices of the same order in size as the boundary layer thickness were desired, but with downstream tangential blowing the only distinct transverse disturbances that could be seen were very small, appearing to be approximately 1/10 to 1/8-inch in thickness, and occurring only for particular values of blowing rate and pulse frequency. These disturbances could be seen originating at the blowing slot and continuing downstream a distance of two to three inches. At this distance they faded out and it could not be determined conclusively whether the disturbances died out or the smoke just became too diffused to see any more. The disturbances were very uniform around the entire channel circumference and appeared to be stable. The distance of the disturbances from the wall seemed to be approximately 1/10-inch. It was also noted that the occurrence of these small disturbances coincided with reductions in skin friction as indicated by the balance.

Similar tests with other blowing rates and frequencies gave very different results. Instead of transverse disturbances being shown by the smoke, various longitudinal patterns appeared. In most cases these patterns seemed to consist of longitudinal vortices of various strengths depending on the amount of blowing and the pulse frequency. In some cases the vortex streamers lay right on the wall originating at the slot. In other cases the longitudinal vortices could be seen to arise out of the break-up of an initially transverse disturbance. In general the flow pattern indicated an instability in the transverse disturbances which led to the formation of longitudinal vortices. These patterns were somewhat difficult to identify at the normal channel flow rates, but by slowing the channel down to very low flow rates the action was quite clear.

When the pulsing frequency was set at one of the previously mentioned resonance points of the plenum chamber, the smoke showed very large disturbances coming out of the slot which broke up into large longitudinal vortices and regions of strong turbulence. It was this action that was responsible for the anomalous high skin friction drag readings for these frequencies.

Further attempts were made to identify the nature of the small, well defined transverse disturbances. The smoke had shown them to be uniform and stable but no definite vortex rotation could be seen due to the small size. A hot-wire probe was placed in the flow such that the disturbance centers passed over it. The probe signal showed small double pips each time a disturbance passed. This would be indicative of a vortex since the hot-wire should show a signal increase as the leading and trailing edges of the vortex passed it. Also the mean velocities measured by the hot-wire showed a slightly higher value in the upper

region of the disturbances and a slightly lower value in the lower region as compared to the case of no disturbances. This result agrees with the concept of a vortex in a steady flow rotating in a direction such as to effectively be rolling downstream. These observations all suggest that the small transverse disturbances were vortices but this has still not been proved conclusively.

Although the cases of blowing normal to the wall and blowing tangentially upstream were found to give no benefits and were eliminated from the final investigations, one additional comment should be made about them. While the apparatus was set up for flow visualization studies, these two cases were examined with smoke and hot-wires for periodic disturbances in the same manner as described for the downstream blowing. No discrete periodic disturbances were found at any conditions for the upstream blowing. For the normal blowing a few combinations of blowing rate and frequency were found which caused the appearance of periodic disturbances very similar in all respects to those that were formed by the downstream blowing. However, the disturbances for normal blowing were always about one half of an inch off of the wall which was well outside of the viscous sublayer region. The fact that these disturbances had no effect on skin friction, despite their similarity to the ones near the wall, suggests that it is essential that the interaction mechanism of the disturbances with the mean flow occur near the wall.

FINAL EXPERIMENTS

A. TEST ENVIRONMENT

During the preliminary experiments, the effects of the periodic blowing on skin friction drag were investigated for several different flow rates in the boundary layer channel. The largest percentage reductions in skin friction occurred over the middle portion of the channel operating range. Due to the large number of variables which seemed to affect the results it was decided to fix as many parameters as possible in order to keep the scope of the experiments within reason. Consequently a single channel flow rate was arbitrarily picked and maintained during all further testing. This particular flow rate (4.0 ft.³/sec) provided a fully developed turbulent boundary layer with a local thickness and free stream velocity at the slot station of 2.5 inches and 13.8 feet per second respectively.

B. SKIN FRICTION DISTRIBUTIONS

The first detailed investigation was the determination of the skin friction drag as a function of position, blowing rate, and pulse frequency. Data were taken with the skin friction balance at stations 3.3, 5.3, 6.9, 15.7, and 26.0 inches downstream from the blowing slot. Two sets of data were taken at each station; one set for a fixed pulse frequency with various blowing rates and the other set for a fixed blowing rate and variable pulse frequency. In each case the wall shear

stress was measured with the skin friction balance, the pressure drop across the blowing slot was measured, and oscilloscope records were made of the hot-wire signal in the slot. The shear stress data for the first four stations are shown in Figures 4 and 5 plotted as percentage change in shear stress based on the local shear stress for the case of no blowing. Negative values indicate shear stress reductions and positive values indicate shear stress increases. Time averaged values of the pressure differential across the slot are also shown in Figure 5. The pressure differential is the difference between the average values of the plenum chamber pressure and the free stream static pressure. More will be said about the pressure differential in the discussion of power requirements.

The data in Figure 4 were obtained by tuning the pulse frequency to give a good skin friction reduction at a nominal blowing rate and then holding this frequency (340 pps) and varying the blowing rate over its full range. The effect is similar at each of the measuring stations with the maximum reduction shifting to higher blowing rates as the distance from the slot increases. It may be seen that the maximum reduction in skin friction occurs in the middle portion of the test region of the boundary layer channel. The maximum reduction increases from 16% at the 3.3-inch station to 20% at the middle stations, dropping off to 6.5% at the 15.7-inch station. No data are shown for the 26.0-inch station as there was no measurable effect persisting this far downstream.

The data in Figure 5 were taken at a fixed blowing rate of $26.4 \times 10^{-3} \text{ ft}^3/\text{sec}$. The frequency range from 100 to 370 pulses per second was covered. The data show that the skin friction varies considerably with frequency. The primary reason for this is because of the change in the pulse with frequency. One exception is a sharp drag reduction indicated near 210 pulses per second which was caused by a resonant condition in the balance due to a low oil level. It was confirmed that this particular effect did not exist in the flow and should be neglected. The shape of the pulse does not seem to be as critical as the magnitude of the jet velocity and, as mentioned previously, the velocity is very sensitive to resonance conditions in the plenum chamber. For instance a large skin friction increase occurs at the forward stations between 220 and 280 pulses per second. The pressure differential across the slot also shows a local peak. Several oscilloscope pictures of the signal from the hot-wire in the slot are shown in Figure 6 which help to explain this situation. It should be kept in mind that the scope shows the hot-wire voltage which is approximately proportional to the one-fourth power of velocity. The center of the grid is the base line for zero velocity and velocity increases downward in the pictures. The scope does not show the signal returning to the base line when the flow is reversed because of the frequency cut-off characteristics of the hot-wire amplifier.

Picture (a) in Figure 6 shows the pulse form at a frequency of 190 pulses per second. Two pulses are shown for each cycle indicating that the flow in the slot was oscillating. The stronger pulse is the outward flow with a velocity of 29.2 feet per second. Picture (b) was taken at a frequency of 300 pulses per second and in general is similar to picture (a). The outward flow velocity in (b) is 27.2 feet per

second. Pictures (c) and (d) are at 240 and 270 pulses per second respectively. The outward velocities are 53.7 and 45.2 feet per second even though the blowing rate is the same as in (a) and (b). Referring to Figure 5 the skin friction is seen to be increased by approximately 30% in this region. By reducing the blowing rate to 9.6×10^{-3} ft³/sec and repeating the measurements at 240 and 270 pulses per second, the skin friction was found to decrease. The shear stress and pressure differential data for this blowing rate are also shown in Figure 5 and identified by *. Figure 6, (e) and (f) show the hot-wire signal for the reduced blowing rate. The velocities are now 32.9 and 29.2 feet per second respectively, the shear stress is reduced by 10%, and the pressure differential is decreased from .038 to .014 millimeters of mercury. This indicates that driving the plenum chamber at a resonant point gives a more efficient operation but more will be said about this in the discussion of power requirements.

Some of the data from Figures 4 and 5 are combined and shown in Figure 7 to illustrate the shear stress distribution downstream from the slot at various blowing rates. Unfortunately the skin friction balance could not be placed closer to the slot than the 3.3-inch station. The lower blowing rates show the skin friction increasing from this station on downstream. A minimum may occur in these curves at a station closer to the slot but this is only speculation. The curves for the higher blowing rates show a progressively higher skin friction at the forward station with a minimum occurring near the 6.0-inch station. The skin friction increases from this point downstream until the effect of the blowing vanishes for all conditions at the 26.0-inch station.

The total reduction in skin friction drag at any blowing rate may be found by integrating the shear stress curves in Figure 7 over the surface area of the boundary layer channel in which the reductions exist. To do this, some assumption must be made about the shear stress in the region between the slot and the 3.3-inch station. The data imply that the shear stress is actually increased in this region but for evaluation purposes the curves for the lower blowing rates are assumed to drop off to zero effect at the slot. If anything, this gives a liberal estimate of the total skin friction reduction for these blowing rates.

A blowing rate of 26.4×10^{-3} cubic feet per second at 340 pulses per second was picked for detailed studies of the mechanism involved in the skin friction reduction. The data for this blowing rate give an average skin friction reduction of 6.1% when integrated in the manner described above.

C. POWER REQUIREMENTS

One of the questions that comes to mind when a technique is found for reducing drag concerns the penalty that must be paid. This penalty can be thought of in terms of an effective drag increase by converting the power consumed in the system to an equivalent drag as follows. Since the type of drag in question is skin friction drag, it is convenient to work with the skin friction coefficient given as

$$C_f = \frac{2 \tau_o \text{ avg}}{\rho U_\infty^2} \quad (1).$$

The net skin friction coefficient may be expressed as

$$C_{f \text{ net}} = C_f - \Delta C_f + \Delta C_{f_p} \quad (2).$$

The percentage change in net drag may be indicated by re-writing equation (2)

$$\frac{C_{f \text{ net}}}{C_f} = 1 - \frac{\Delta C_f}{C_f} + \frac{\Delta C_{f_p}}{C_f} \quad (3).$$

The power consumed is given by

$$P = Q \Delta p \quad (4).$$

Dividing the power by the free stream velocity gives the effective drag and normalizing this by the product of free stream dynamic pressure and surface area gives the equivalent drag coefficient for the power. Thus

$$\Delta C_{f_p} = \frac{D}{qA} = \frac{P}{qAU_\infty} = \frac{2Q\Delta p}{\rho AU_\infty^2} \quad (5).$$

There is one problem in using this analysis and that is knowing the correct value for the pressure differential. In these tests, it was fairly easy to measure the time averaged pressure but nothing was known about the actual pressure level during the 10% of the cycle that the blowing takes place. A conservative estimate of the power requirement may be made by using the average pressure differential. If this technique does not show a net drag decrease then there is no need to look further because the actual pressure differential will cause an even higher net drag.

Application of equation (3) to all of the data shows that no net drag reduction was realized at any condition except the previously mentioned plenum chamber resonant point with reduced blowing. The result for this case was a net drag decrease of 4% based on the average pressure differential. The fact that the net drag was decreased justified a closer look at the actual blowing power being used. An attempt was made to determine the damping characteristics of the plenum chamber so that the true power required to drive it at its resonant frequency could be calculated. The results showed the damping rate to be so large as to require a lengthy investigation. The feeling at this point was that it would be of more value to study the mechanism involved in the skin friction reduction than to try to optimize the system. It should be emphasized that any effort toward developing a practical system for drag reduction would necessitate a much more thorough study of the technique for producing the disturbances.

D. MEAN VELOCITY MEASUREMENTS

The skin friction data have shown conclusively that periodic blowing in the manner described reduces the wall shear stress in a turbulent boundary layer. The problem now becomes one of determining how this is accomplished. A change in wall shear stress requires a corresponding change in the shape of the velocity profile. To find what changes were effected by the periodic blowing mean velocity profiles were measured at the 3.3, 6.9, and 15.7-inch stations with and without blowing. A single element hot-wire probe was used for all measurements. These data are shown plotted in the universal law of the wall form in Figure 8. The solid curve in the figure shows the empirical profile expression derived by Coles (reference 5) for incompressible flow and widely used as a standard for turbulent boundary layers. The data for no blowing are in good agreement with the empirical curve.

The velocity profiles with blowing (26.4×10^{-3} cubic feet per second, 340 pulses per second) show two interesting features. The sublayer region appears to be extended by an amount related to the local shear stress reduction, and the turbulent region appears to have the same shape and slope as the standard turbulent profile. This implies that the sublayer is effectively thickened without the outer turbulent layer being affected. This result does not agree with the effects that would be expected if the skin friction reduction were due to large scale vortex-boundary layer interactions as hypothesized in the beginning of the study.

E. TURBULENCE EFFECTS

The fact that the mean velocity profiles were affected only in the sublayer stimulated interest in the behavior of the turbulent structure of the boundary layer. Since the sublayer is actually a region in which turbulent velocity fluctuations are damped, any change in its thickness indicates a corresponding change in the turbulent energy structure of the boundary layer.

The boundary layer turbulence was examined by measuring spectral distributions and integrated totals of the turbulent, u' , velocity fluctuations. The data were measured with the same hot-wire probe used for the mean velocity measurements. Spectral distributions were obtained using a Hewlett-Packard 302A wave analyzer as a notch filter and recording its output on a Flow Corporation 12A1 random signal voltmeter. The 12A1 was used directly to measure average totals of the turbulent, u' , fluctuations. These data are presented in Figures 9 through 14.

Figures 9, 11, and 13 compare the root-mean-square values of the longitudinal turbulence intensity across the flow field with and without the periodic blowing. The blowing data show a slight trend toward a reduced turbulence level in the inner portion of the boundary layer but in general no strong effect shows up.

Figures 10, 12, and 14 compare the spectral distribution of the turbulent, u' , energy at various positions in the boundary layer with and without blowing. The data are plotted as the square of the rms value of, u' , divided by the bandwidth over which they were measured. This bandwidth was 6.5 cycles per second for the 302A wave analyzer. The data were presented in this form so that the spectral curves could be integrated to get the total energy for comparison with the values measured with the 12A1 random signal voltmeter.

The turbulence spectra with blowing are consistently below the spectra without blowing in the inner region of the boundary layer, and the difference in the two diminishes with increasing distance down the channel. At the 3.3-inch station the turbulent energy reduction varies from approximately 25% at 20 cycles per second to 50% at 100 cycles per second. Beyond 150 cycles per second there is no significant effect. The turbulence reduction decreases with increasing distance from the wall. Figure 10 shows some effect at 1.000 inch from the wall but the stronger effects are within .250 inches. Figure 12 shows the effect to be within .050 inches from the wall, and Figure 14 shows an appreciable effect only at .010 inches. These data indicate that the periodic blowing has reduced the turbulence level throughout a significant portion of the boundary layer near the station where blowing is applied, and the turbulence intensifies from this reduced level as the flow progresses down the channel until the intensity is back up to the values for no blowing.

A curious feature of these data is that the spectral distributions show a much larger reduction than the total, u' , component of Figures 9, 11, and 13. Also the integrated values of each spectra are consistently lower than the corresponding values measured directly with the random signal voltmeter. The probable reason for this discrepancy lies in the low frequency range of the energy spectra. The 12A1 voltmeter responds to fluctuations down to a frequency of 2 cycles per second but the 302A wave analyzer is operable only down to 15 cycles per second. The fact that all integrated spectra are lower than the totals measured with the 12A1 implies that large contributions to the total turbulent energy lie in the frequency range below 15 cycles per second. Also, the discrepancies in the turbulence reduction as indicated by the spectral curves and the total measurements suggest that a possible cross-over of the spectral curves with and without blowing occurs at some low frequency. In other words, although the turbulence level is consistently reduced above 20 cycles per second with periodic blowing it possibly is increased at lower frequencies. Further investigations are necessary to resolve this question.

F. EFFECTS OF CONTINUOUS BLOWING

The data obtained for the case of periodic blowing into the turbulent boundary layer raise many questions and do not provide sufficient answers to determine conclusively the mechanism causing the skin friction reduction. The idea of large scale vortices causing a reduction in the slope of the velocity profile at the wall due to a simple super-position of flow fields is discounted because of the

extremely small observed size of the actual disturbances. A more reasonable hypothesis is that the turbulence reduction is due to an altered mixing process in the boundary layer caused by the small disturbances.

It was known that the Reynolds number of the periodic flow in the slot was always below the critical value such that the jet pulses were laminar in all cases. Thus each pulse was actually a small quantity of very low turbulence air which mixed into the turbulent flow of the boundary layer. The net effect should have been a reduced turbulence level in the boundary layer as observed. The reduced turbulence level would then allow the sublayer to thicken and hence reduce the shear stress at the wall. If this hypothesis is correct then any introduction of low turbulence air into the boundary layer should cause a similar effect. This is to say the periodicity of the blowing is not essential to the mechanism.

To test this idea some additional experiments were performed with continuous instead of periodic blowing. Skin friction reductions were again accomplished but only at higher blowing flow rates than were necessary with the periodic blowing. The 26.4×10^{-3} cubic feet per second flow rate had no effect. As the flow rate was increased the skin friction decreased until local reductions as large as 24% were obtained. This occurred at a blowing rate of 60×10^{-3} cubic feet per second. As the blowing rate was further increased the skin friction increased until values higher than those for no blowing were finally reached.

Some of the data for steady blowing at 60×10^{-3} cubic feet per second are shown in Figures 15 and 16. Figure 15 again compares the velocity profiles in the law of the wall form. The data for continuous blowing are seen to be quite similar to the data for periodic blowing shown in Figure 8. Figure 16 shows an example of the turbulence reduction at two continuous blowing rates. Again the results for the higher blowing rate are similar to the results in Figure 10 for periodic blowing. Notice that the steady blowing at 26.4×10^{-3} ft³/sec has no effect on the turbulence as compared with pulsing at the same blowing rate in Figure 10 (b). The power requirement for continuous blowing was found to be four to five times as high as for periodic blowing in order to achieve comparable skin friction reductions.

An investigation of similar effects has been conducted at NASA, Langley Research Center (references 6 and 7) for continuous blowing through slots in supersonic flow. The effectiveness of single and multiple slots, both flush and rearward facing steps, as compared to distributed blowing through a porous surface was studied. An exact comparison of the LTV and NASA data is difficult because of insufficient local skin friction measurements in the NASA tests. However, average skin friction reductions of the same order as reported here were found for some of the flush slot configurations. It is interesting to note that the NASA investigators also place emphasis on the exact mixing

process of the injection air with the boundary layer in determining the skin friction.

CONCLUSIONS

These experiments are by no means sufficient to completely describe the mechanism responsible for reducing skin friction drag. A thorough understanding of the phenomenon will require much more work. However, several conclusions may be drawn from the results presented herein.

1. A skin friction reduction has been accomplished by the introduction of low turbulence air into a turbulent boundary layer. The fact that this is possible with either periodic or continuous blowing discredits the importance of any vortical motion for the size disturbances used in this study.
2. The turbulence intensity near the wall is reduced coincident with the skin friction. This effect, along with the effects on the law of the wall, indicate that the skin friction reduction is due to a thickening of the viscous sublayer rather than a gross modification of the velocity profile as might be expected with large scale vortices such as in reference 2.
3. The power required to accomplish the skin friction reduction is prohibitively large to allow a net drag decrease except possibly for certain resonant conditions in the system. This suggests that further work toward developing a more efficient mechanical apparatus might be worthwhile.
4. The turbulence reduction is probably due to the mixing of low turbulence air with the turbulent flow in the boundary layer. The fact that stronger effects occur with periodic rather than continuous blowing at a given blowing rate suggests that a more efficient mixing process is achieved with the former due to the higher jet velocities.

ACKNOWLEDGEMENTS

The work reported herein is part of a project supported jointly by independent research and development funds of Ling-Temco-Vought, Inc., and the National Aeronautics and Space Administration under Contract No. NASw-956 (Fluid Physics Branch of the Research Division, OART).

REFERENCES

1. Spangler, J. G., and Wells, C. S., "Effects of Spiral Longitudinal Vortices on Turbulent Boundary Layer Skin Friction", NASA CR-145, (1964); also LTV Research Center Report No. O-71000/4R-19 (1964).
2. Eggers, A. J., and Hermach, C. A., "Initial Experiments on the Aerodynamic Cooling Associated with Large-scale Vortical Motions in Supersonic Flow", NASA RM A54LL3 (1955).

3. Wells, C. S., and Spangler, J. G., "A Facility for Basic Boundary Layer Experiments", LTV Research Center Report No. O-71000/2R-32. (1962).
4. Spangler, J. G., "A Sensitive Magnetic Balance for the Direct Measurement of Skin Friction Drag", LTV Research Center Report No. O-71000/3R-29, (1963).
5. Coles, D., "Measurements in the Boundary Layer on a Smooth Flat Plate in Supersonic Flow", Ph.D. Thesis, California Institute of Technology, 1953.
6. McRee, D. I., Peterson, J. B., Jr., and Braslow, A. L., "Effect of Air Injection Through a Porous Surface and Through Slots on Turbulent Skin Friction at Mach 3", NASA TN D-2427, August 1964.
7. Peterson, J. B., Jr., McRee, D. I., Adcock, J. B., and Braslow, A. L., "Further Investigation of Effect of Air Injection Through Slots and Porous Surfaces on Flat-plate Turbulent Skin Friction at Mach 3", NASA TN D-3311, March 1966.

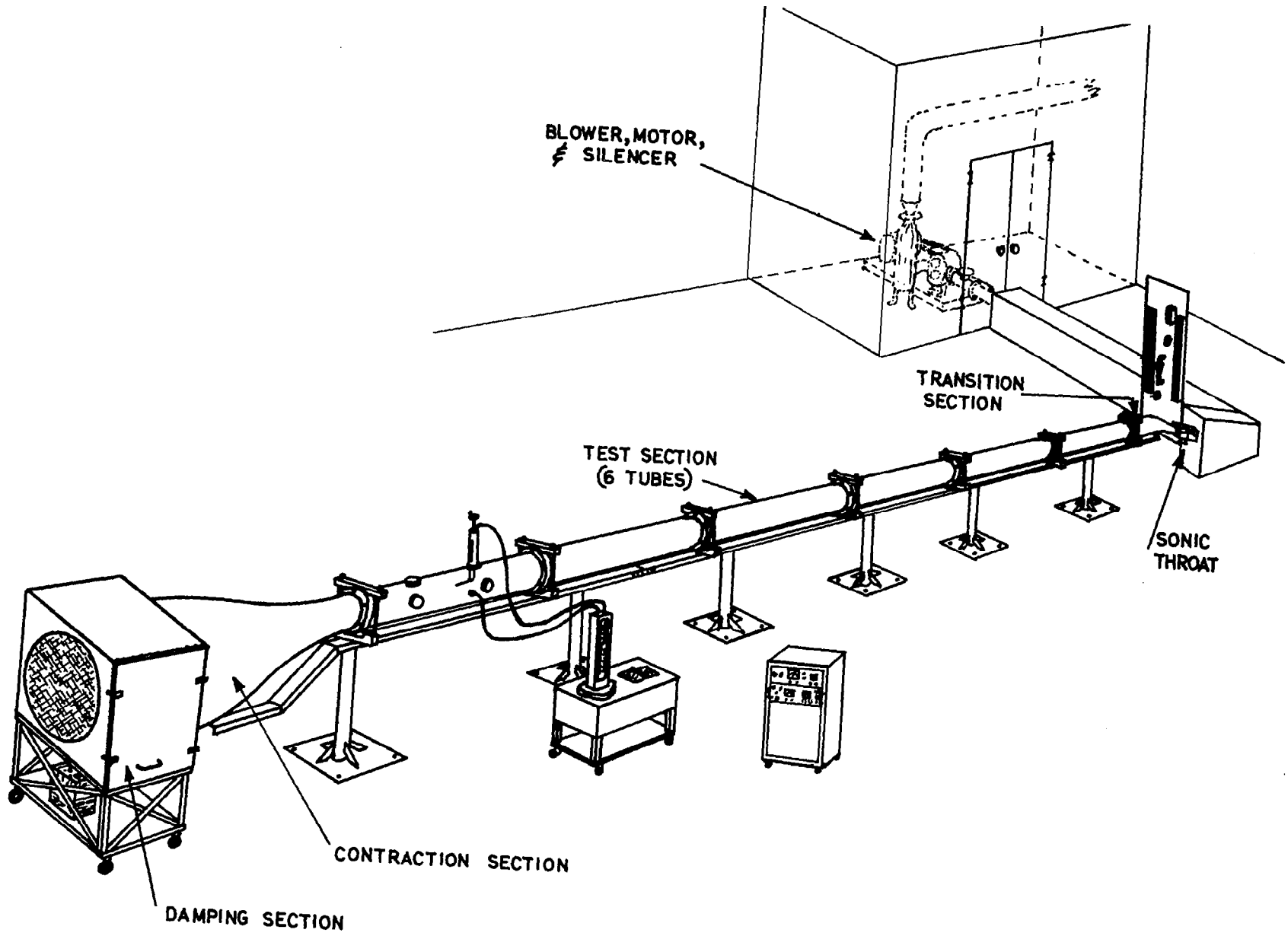


Figure 1 Boundary layer channel facility

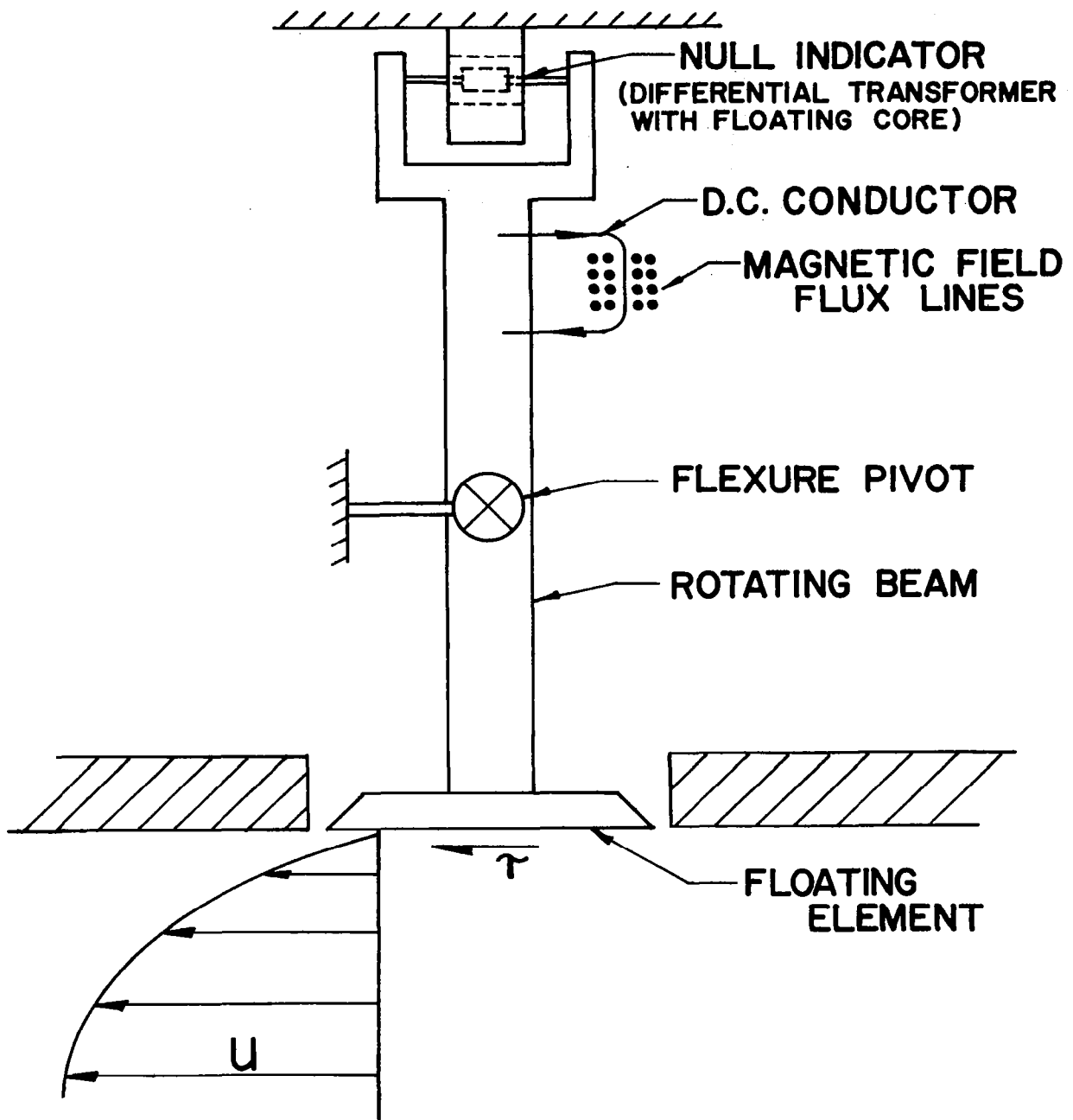


Figure 2 Schematic of skin friction balance.

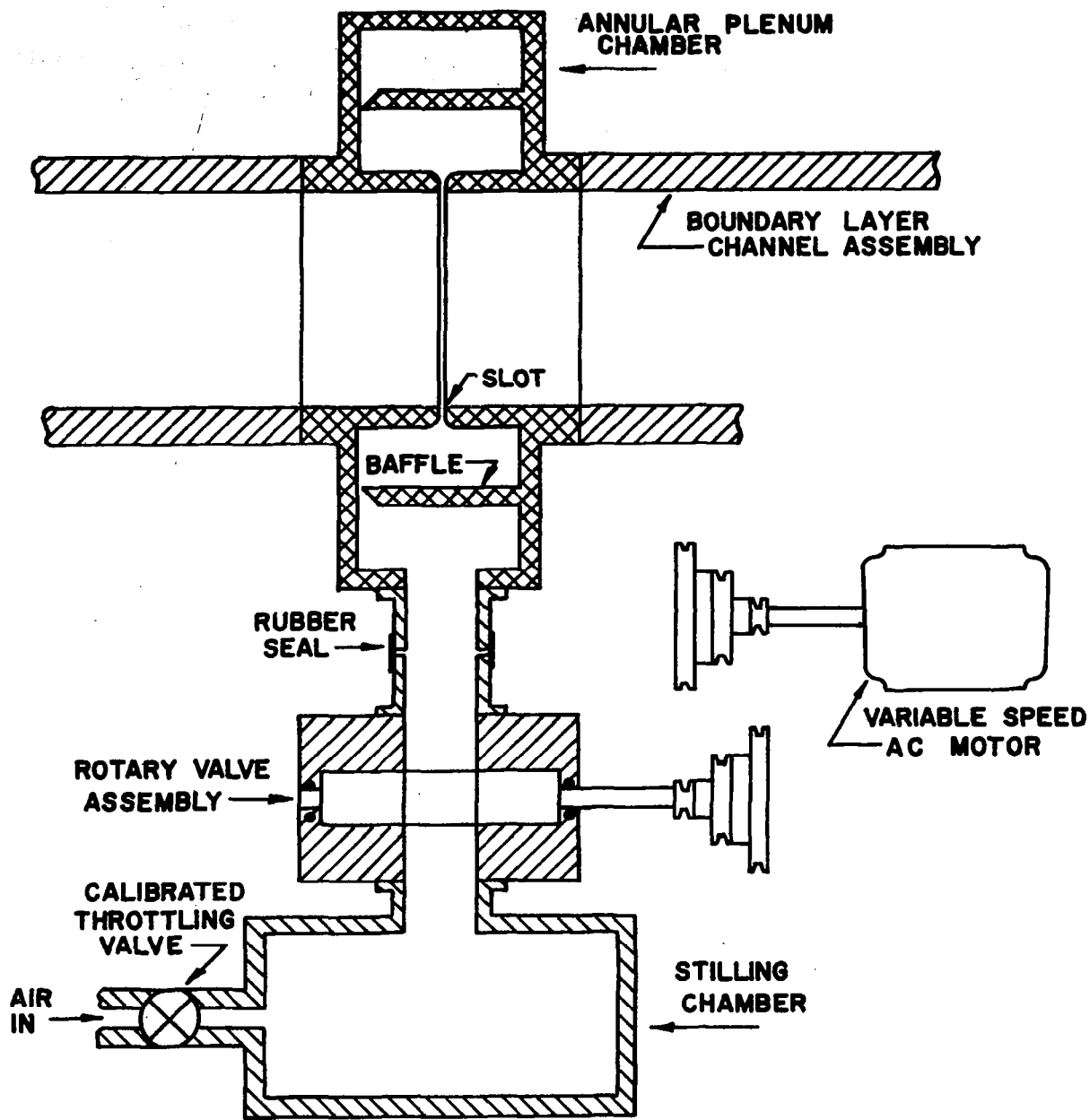
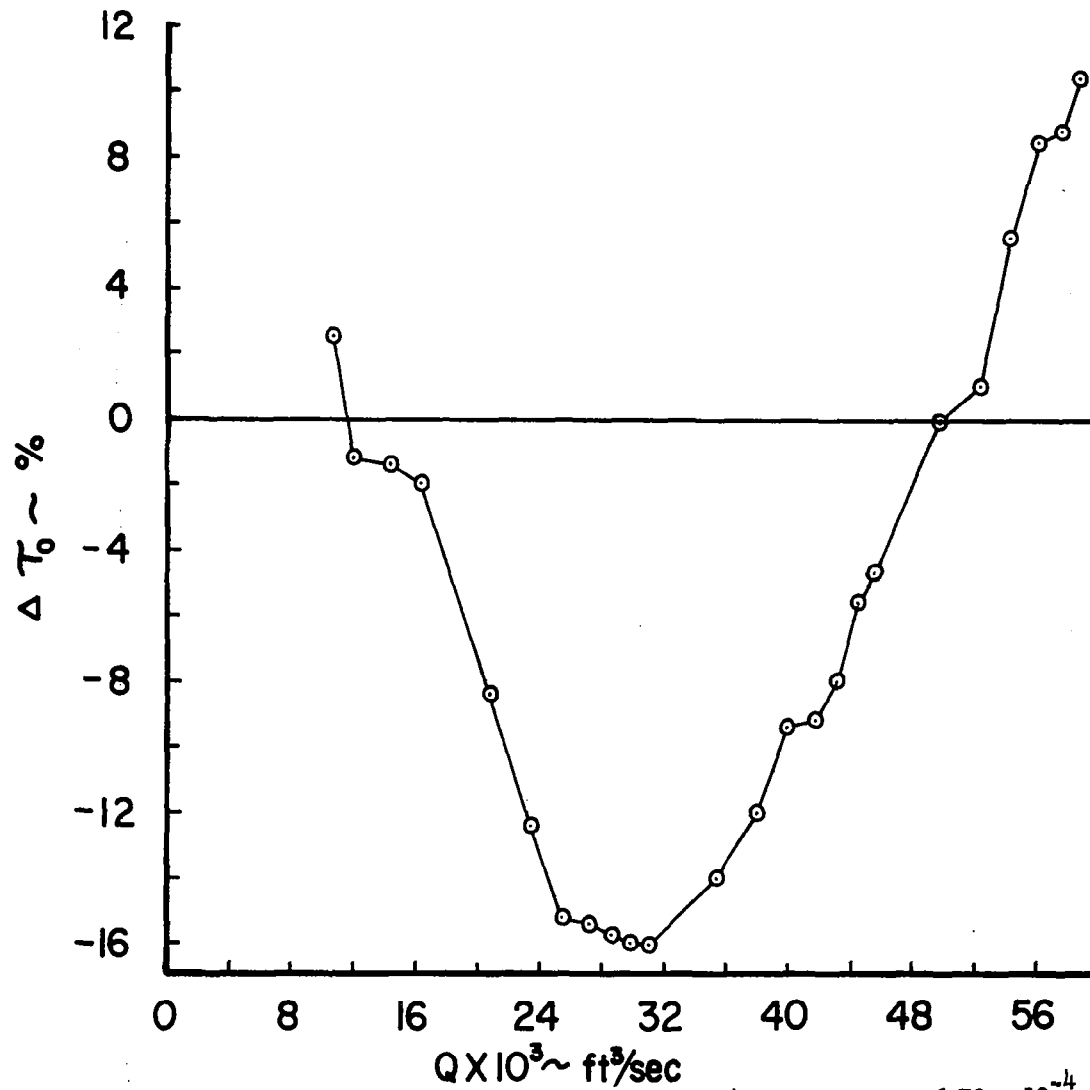
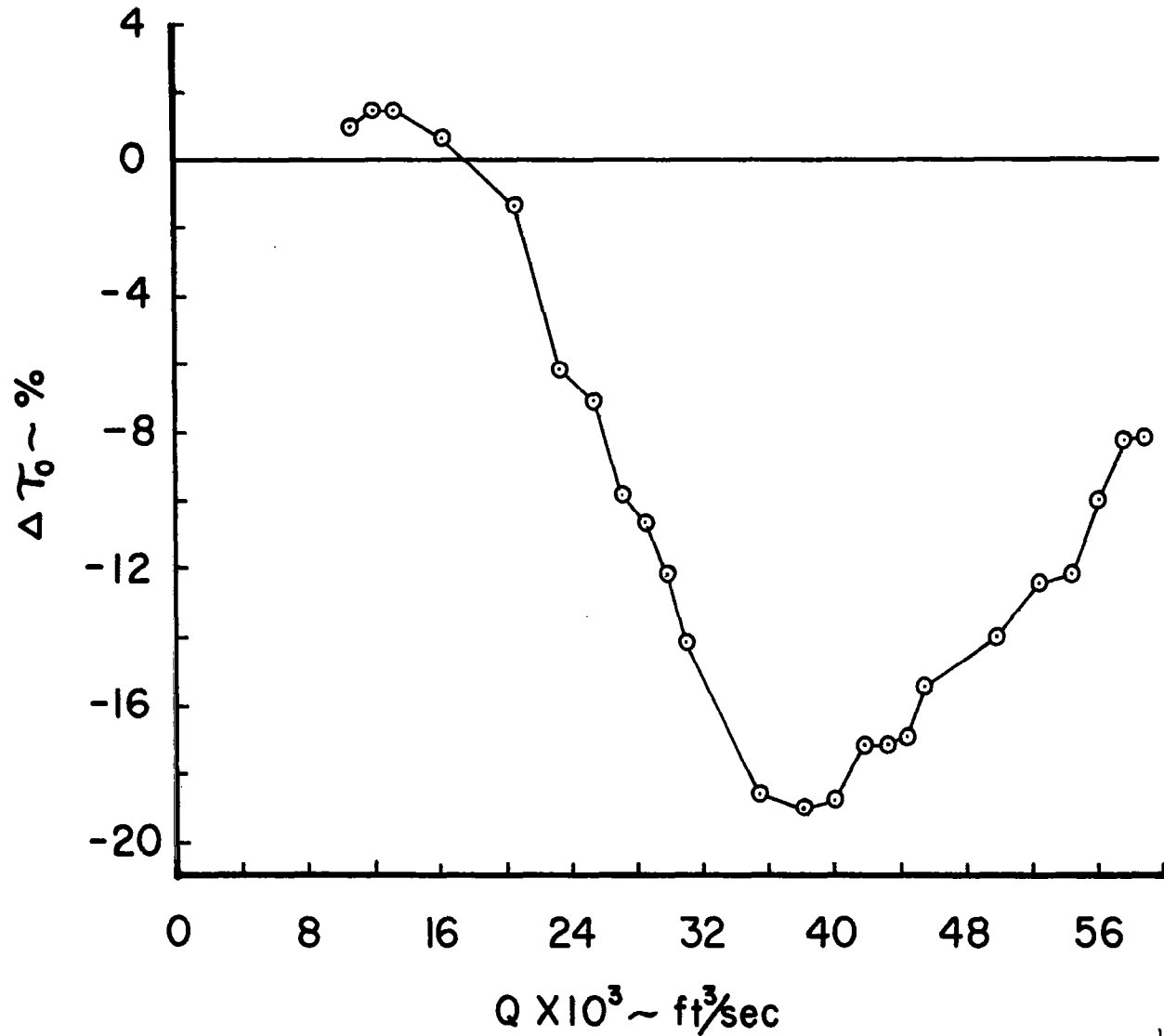


Figure 3 Periodic blowing apparatus.



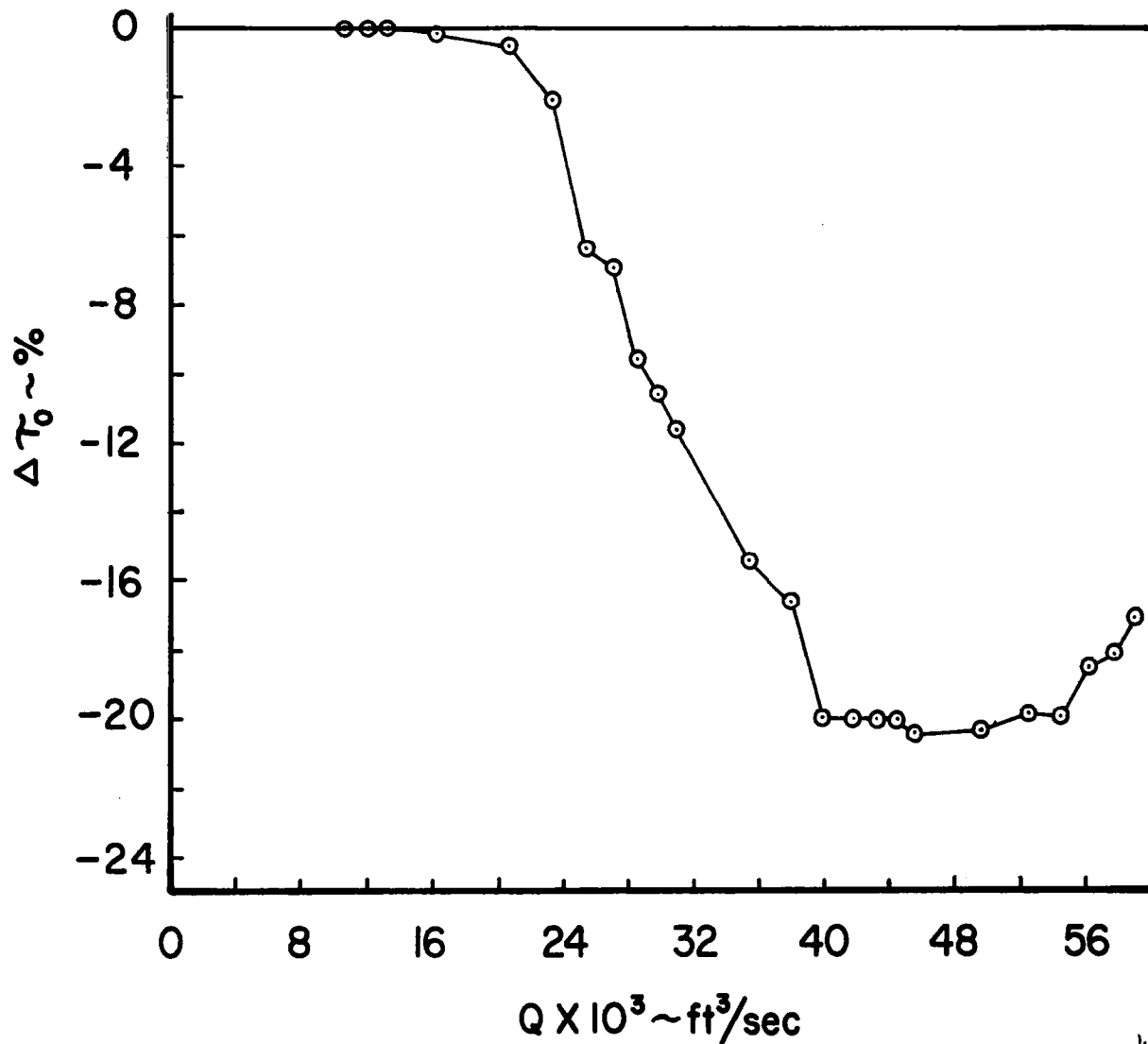
(a) Station 3.3 inches, $\omega = 340$ pps, $\tau_{0NB} = 6.72 \times 10^{-4}$ lb/ft²

Figure 4 Variation of wall shear stress with blowing rate.



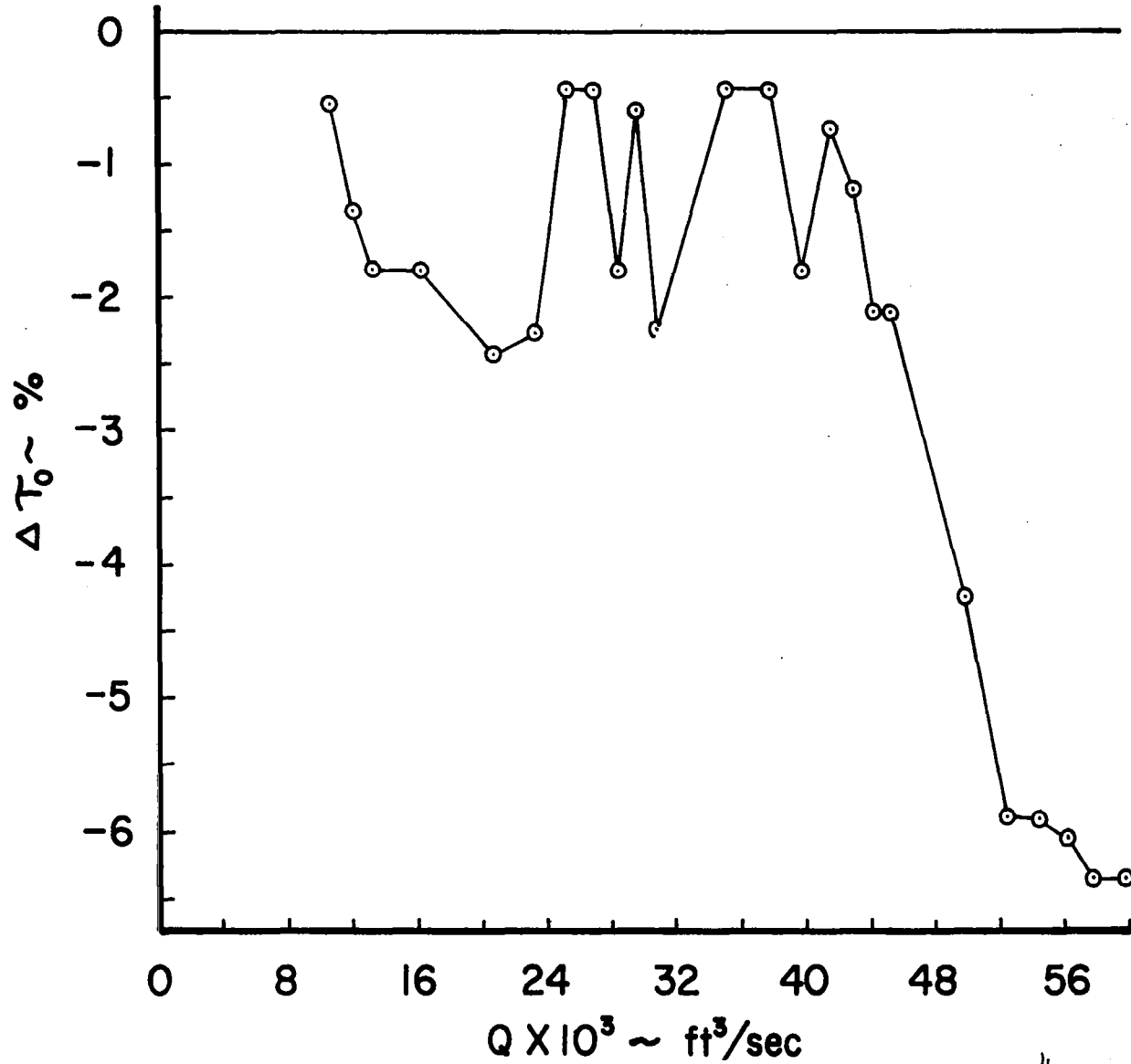
(b) Station 5.3 inches, $\omega = 340$ pps, $\tau_{o_{NB}} = 6.68 \times 10^{-4}$ lb/ft²

Figure 4 (Continued) Variation of wall shear stress with blowing rate.



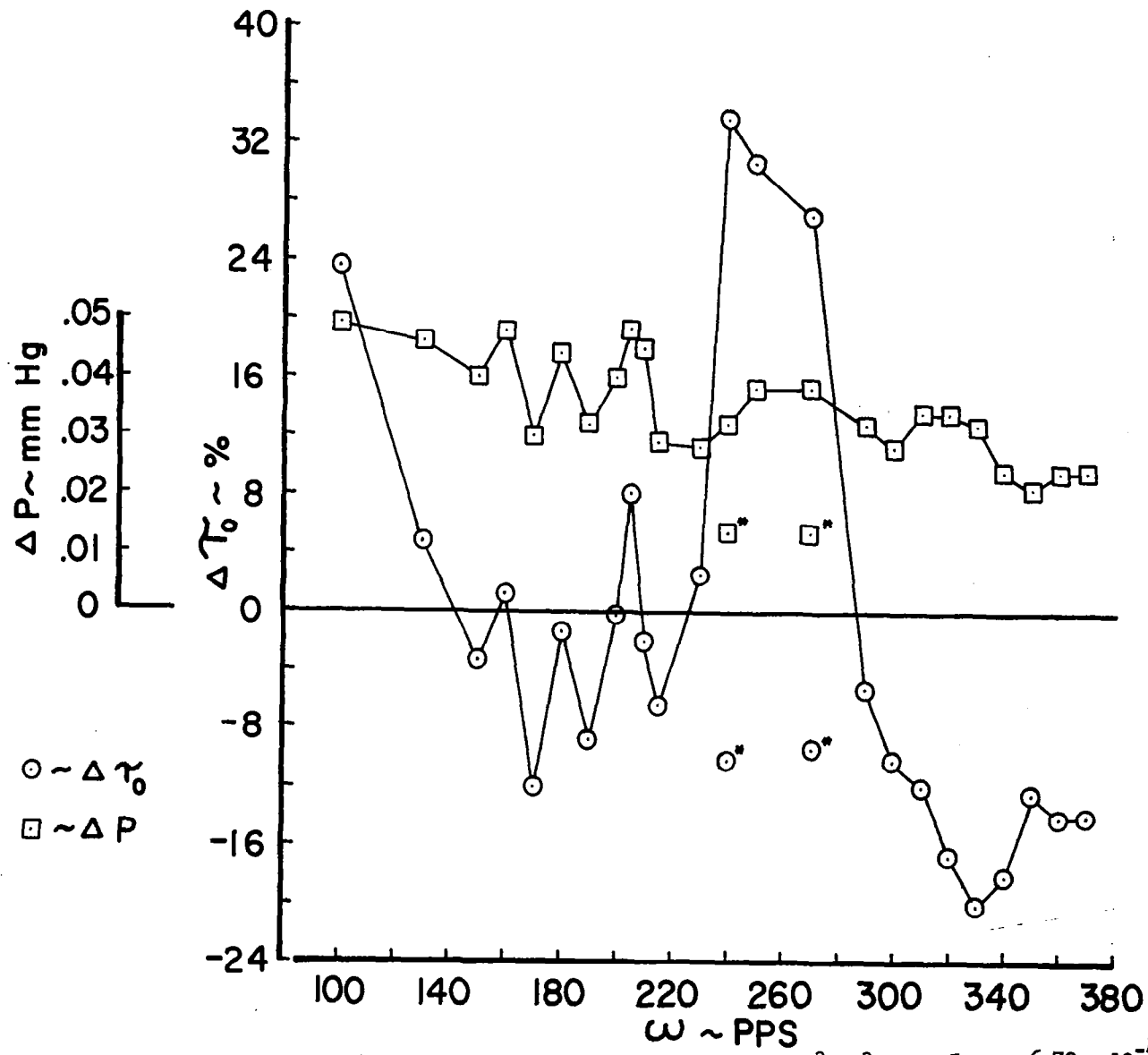
(c) Station 6.9 inches, $\omega = 340$ pps, $\tau_{0_{NB}} = 6.68 \times 10^{-4}$ lb/ft²

Figure 4 (Continued) Variation of wall shear stress with blowing rate.

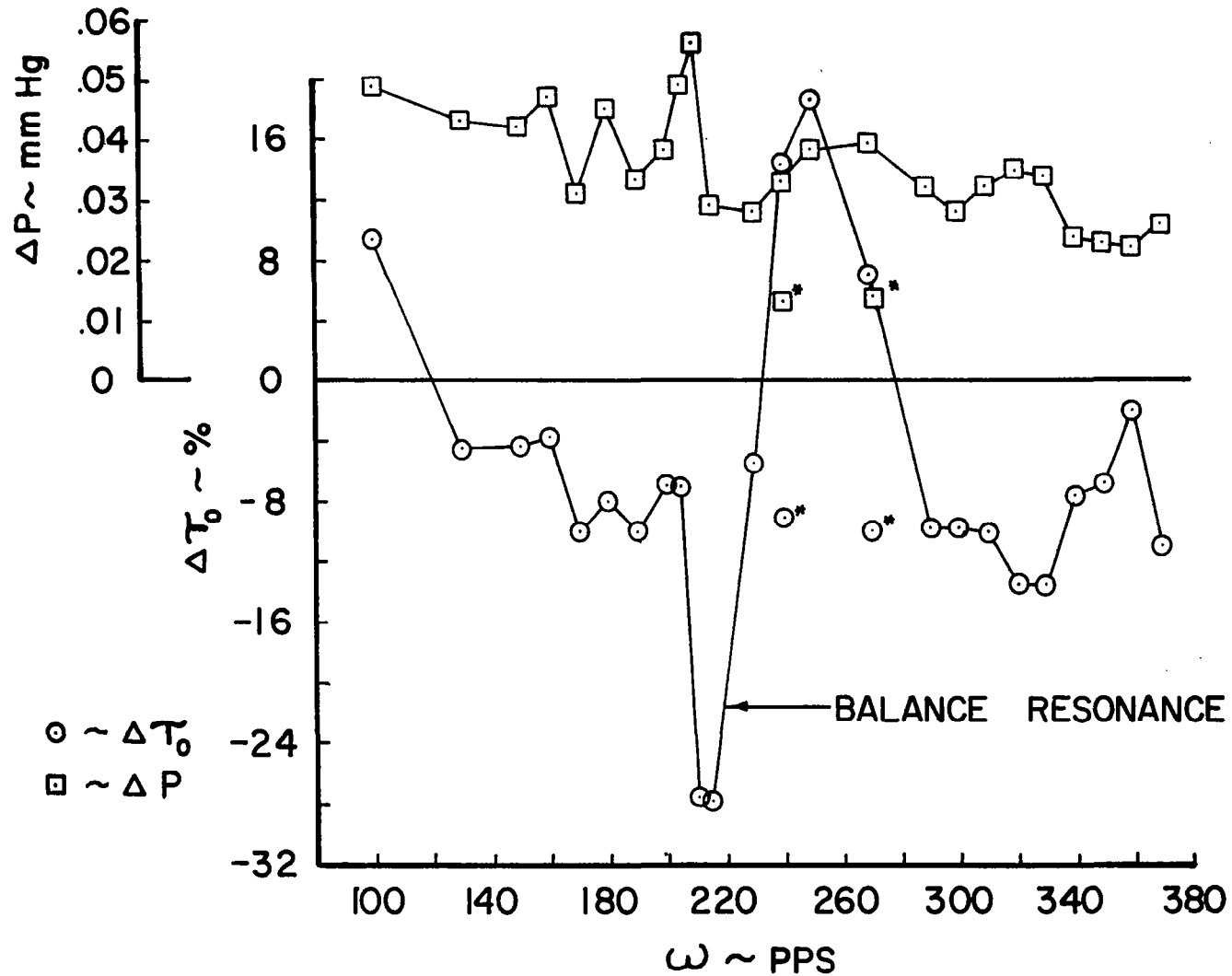


(d) Station 15.7 inches, $\omega = 340$ pps, $\tau_{0NB} = 6.59 \times 10^{-4}$ lb/ft²

Figure 4 (Concluded) Variation of wall shear stress with blowing rate.

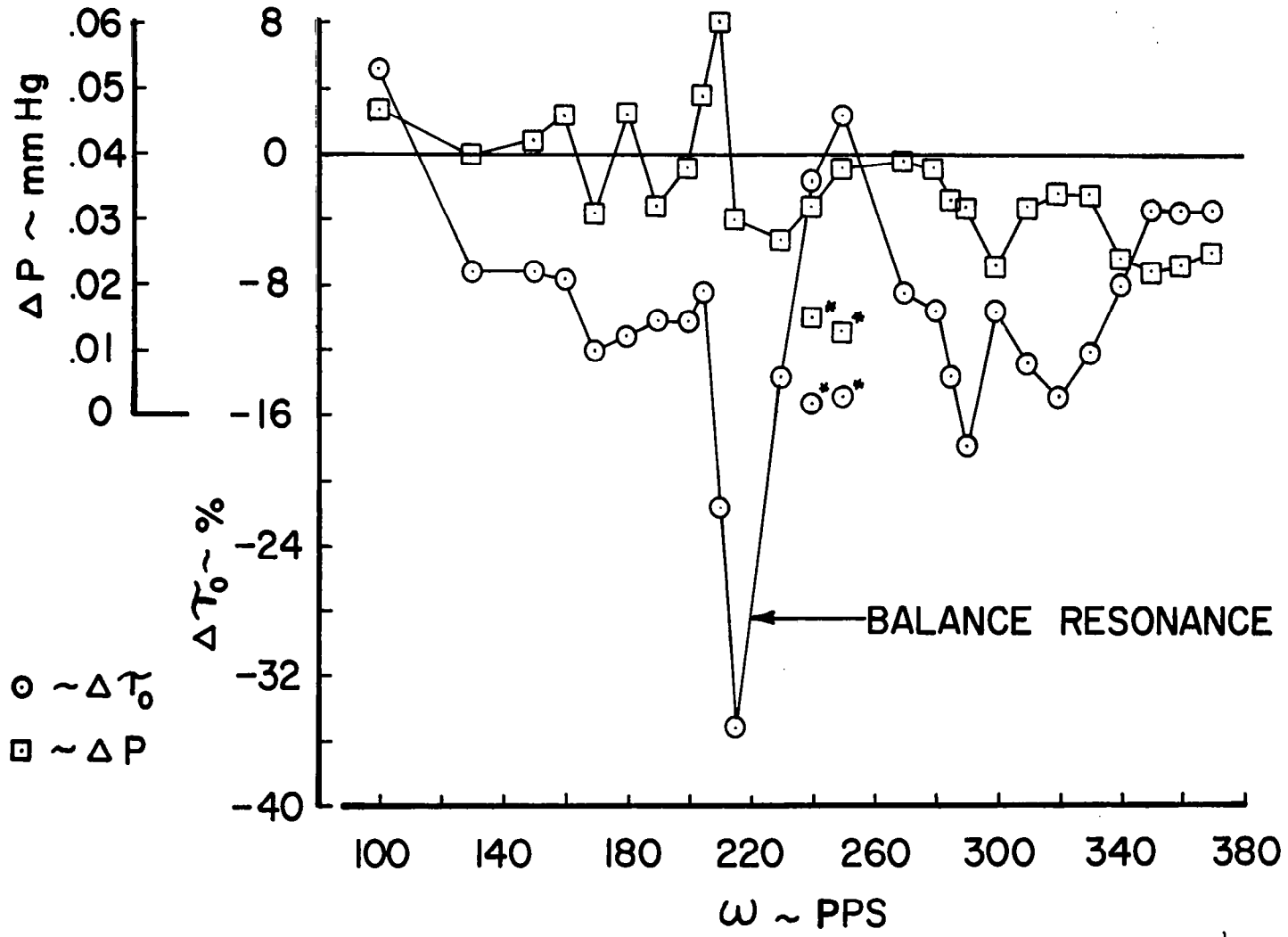


(a) Station 3.3 inches, $Q = 26.4 \times 10^{-3} \text{ ft}^3/\text{sec}$, $\tau_{0, NB} = 6.72 \times 10^{-4} \text{ lb/ft}^2$
 Figure 5 Variation of wall shear stress and pressure differential across blowing slot with pulse frequency.



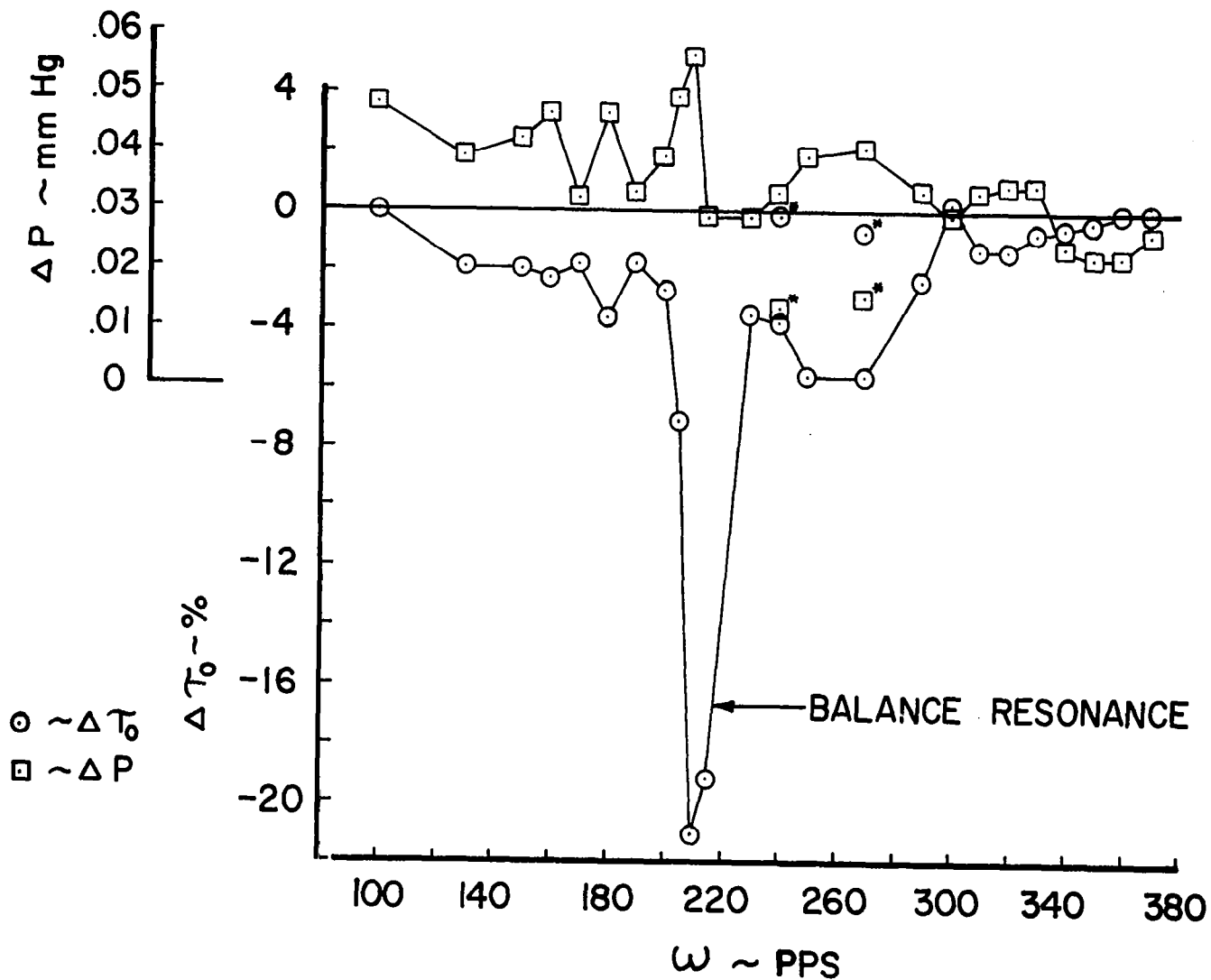
(b) Station 5.3 inches, $Q = 26.4 \times 10^{-3} \text{ ft}^3/\text{sec}$, $\tau_{0NB} = 6.68 \times 10^{-4} \text{ lb/ft}^2$

Figure 5 (Continued) Variation of wall shear stress and pressure differential across blowing slot with pulse frequency.

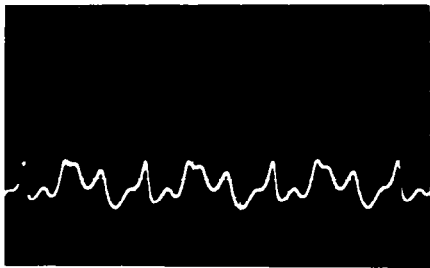


(c) Station 6.9 inches, $Q = 26.4 \times 10^{-3} \text{ ft}^3/\text{sec}$, $\tau_{0NB} = 6.68 \times 10^{-4} \text{ lb/ft}^2$

Figure 5 (Continued) Variation of wall shear stress and pressure differential across blowing slot with pulse frequency.

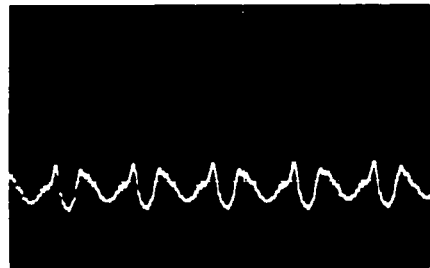


(d) Station 15.7 inches, $Q = 26.4 \times 10^{-3}$ ft³/sec, $\tau_{0NB} = 6.59 \times 10^{-4}$ lb/ft²
 Figure 5 (Concluded) Variation of wall shear stress and NB pressure differential across blowing slot with pulse frequency.



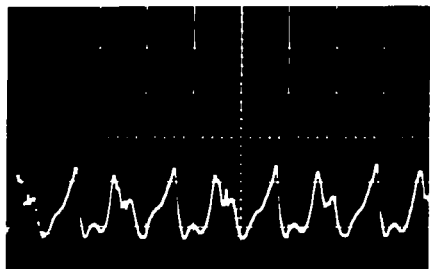
(a)

$\omega = 190$ PPS
 $Q = 26.4 \times 10^{-3}$ ft³/sec



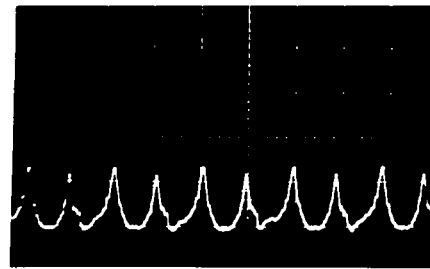
(b)

$\omega = 300$ PPS
 $Q = 26.4 \times 10^{-3}$ ft³/sec



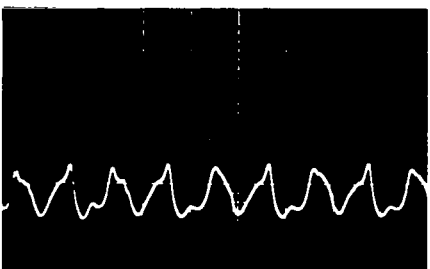
(c)

$\omega = 240$ PPS
 $Q = 26.4 \times 10^{-3}$ ft³/sec



(d)

$\omega = 270$ PPS
 $Q = 26.4 \times 10^{-3}$ ft³/sec



(e)

$\omega = 240$ PPS
 $Q = 9.6 \times 10^{-3}$ ft³/sec



(f)

$\omega = 270$ PPS
 $Q = 9.6 \times 10^{-3}$ ft³/sec

Figure 6 Pulse forms as measured by a hot-wire probe in the blowing slot. Gain = 0.5 volts/cm, sweep = .002 sec/cm.

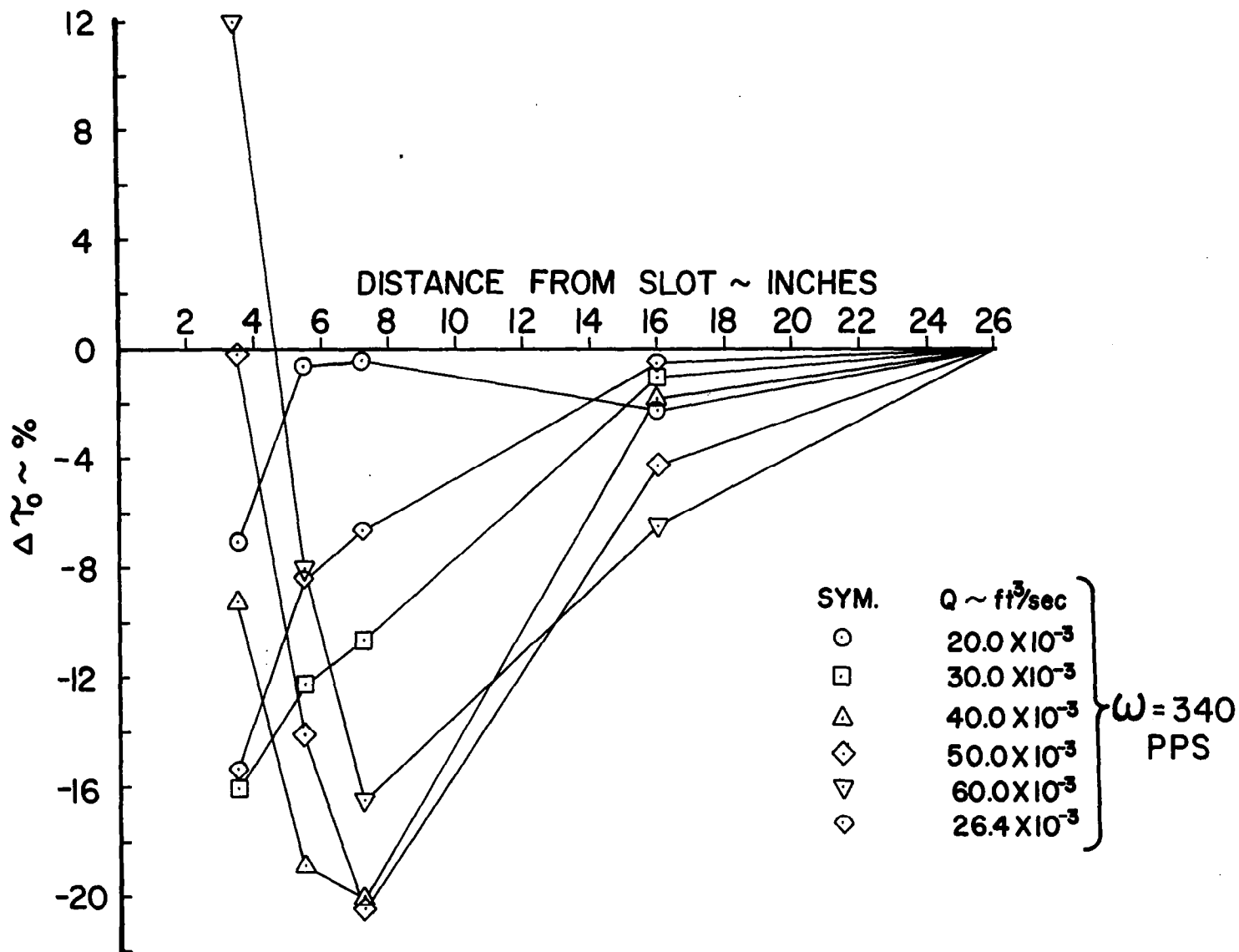
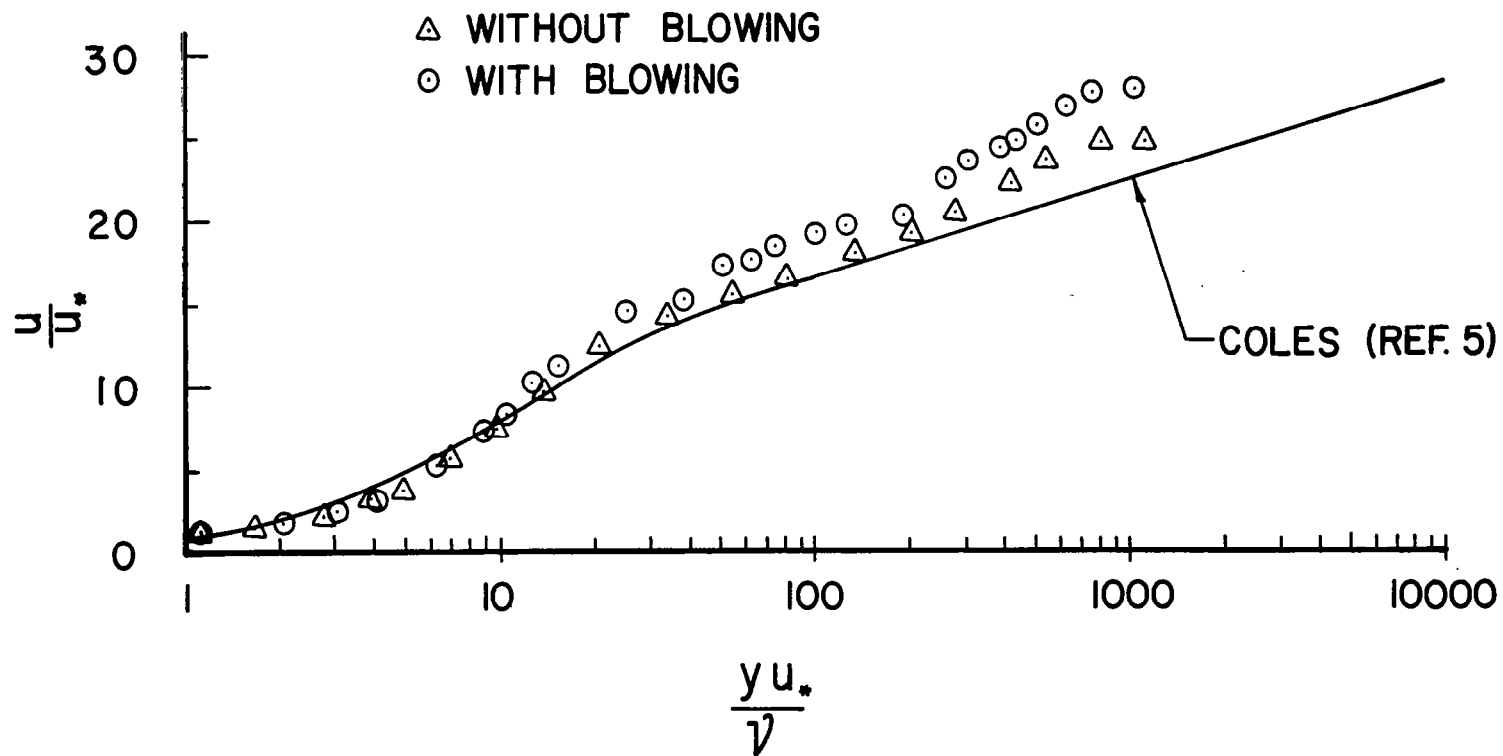
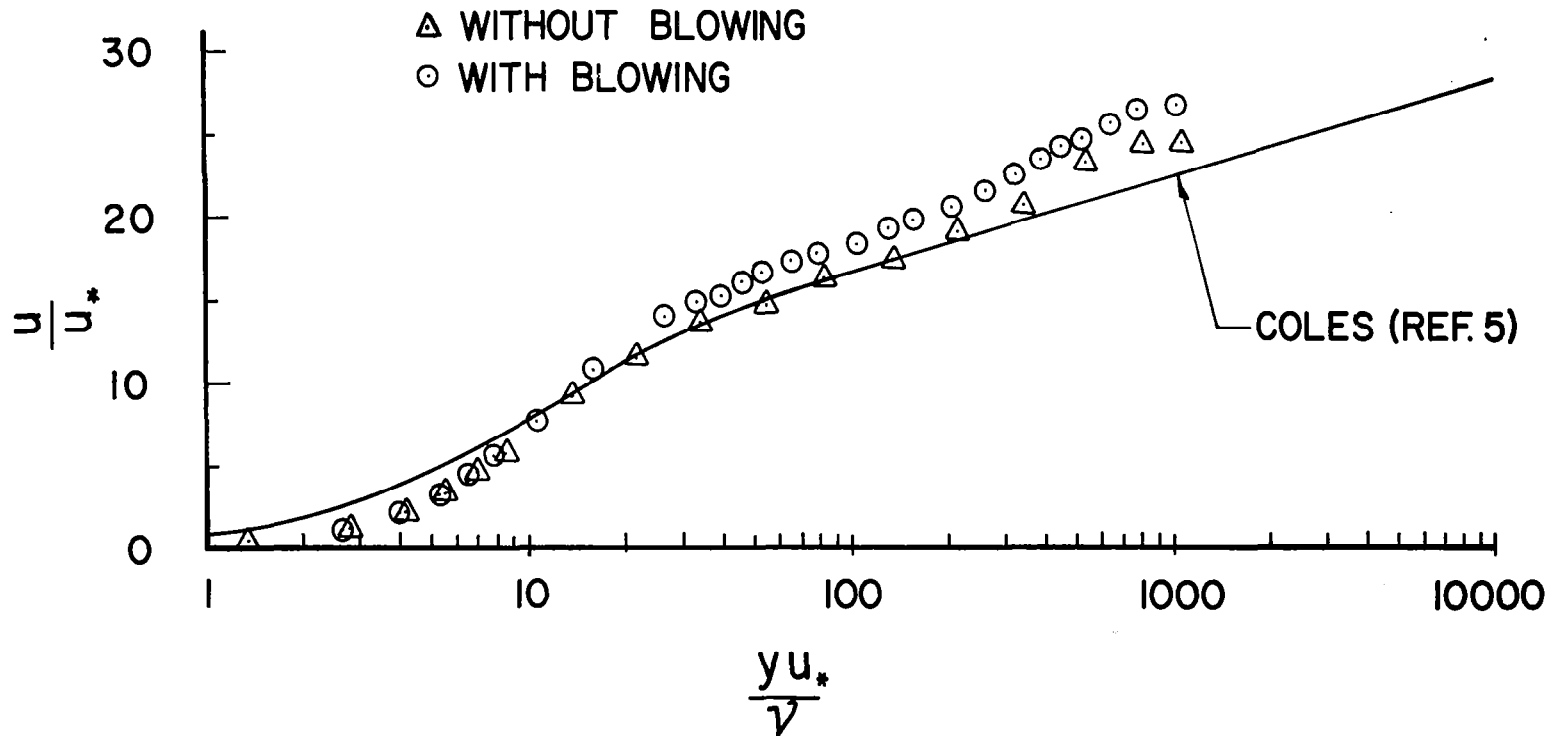


Figure 7 Longitudinal wall shear stress distributions.



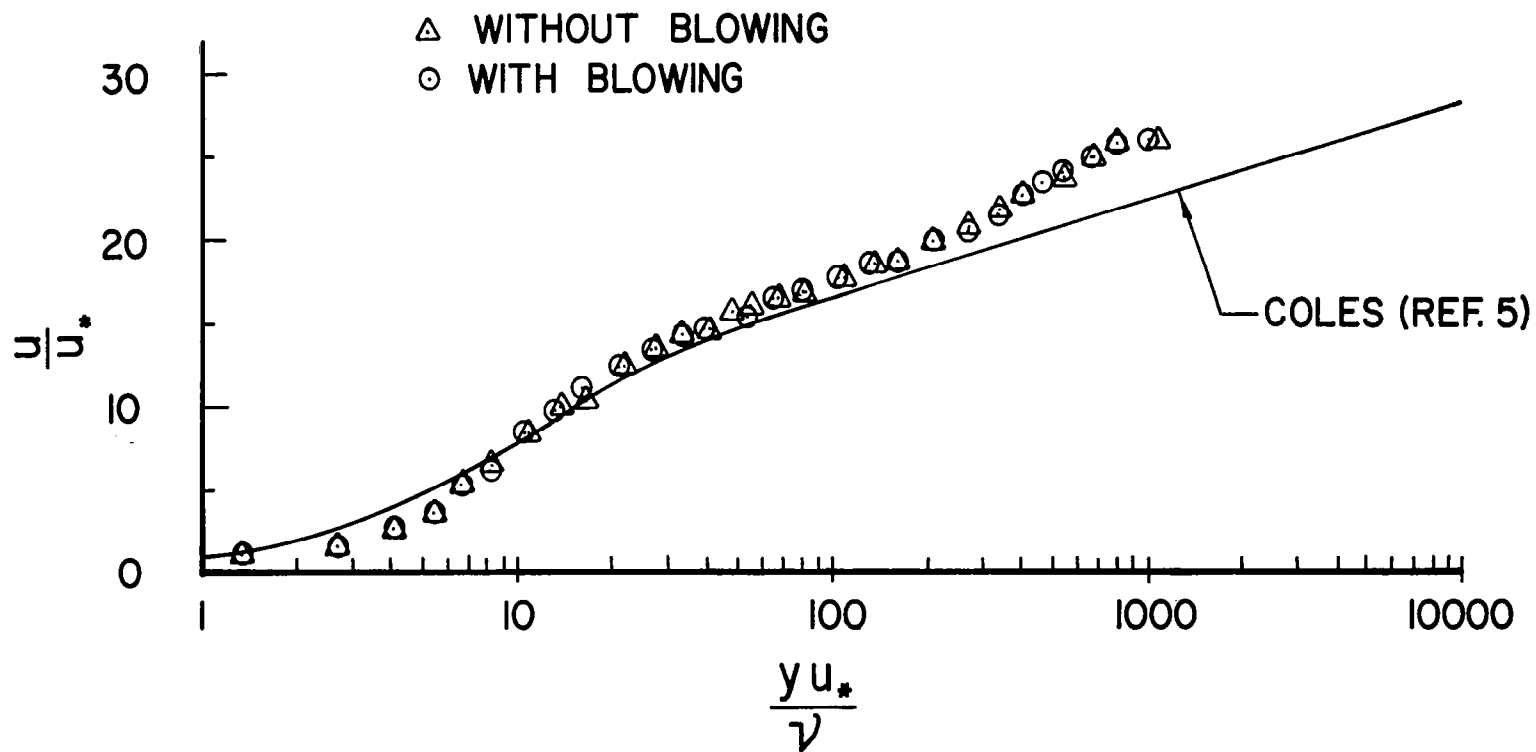
(a) Station 3.3 inches, $\omega = 340$ pps, $Q = 26.4 \times 10^{-3}$ ft³/sec,
 $\Delta \tau_0 = -16.2\%$, $\tau_{0NB} = 6.72 \times 10^{-4}$ lb/ft².

Figure 8 Law of the wall velocity profile.



(b) Station 6.9 inches, $\omega = 340$ pps, $Q = 26.4 \times 10^{-3}$ ft³/sec,
 $\Delta\tau_0 = -8.2\%$, $\tau_{0NB} = 6.68 \times 10^{-4}$ lb/ft²

Figure 8 (Continued) Law of the wall velocity profile.



(c) Station 15.7 inches, $\omega = 340$ pps, $Q = 26.4 \times 10^{-3}$ ft³/sec,
 $\Delta\tau_o = -3.2\%$, $\tau_{oNB} = 6.59 \times 10^{-4}$ lb/ft².

Figure 8 (Concluded) Law of the wall velocity profile.

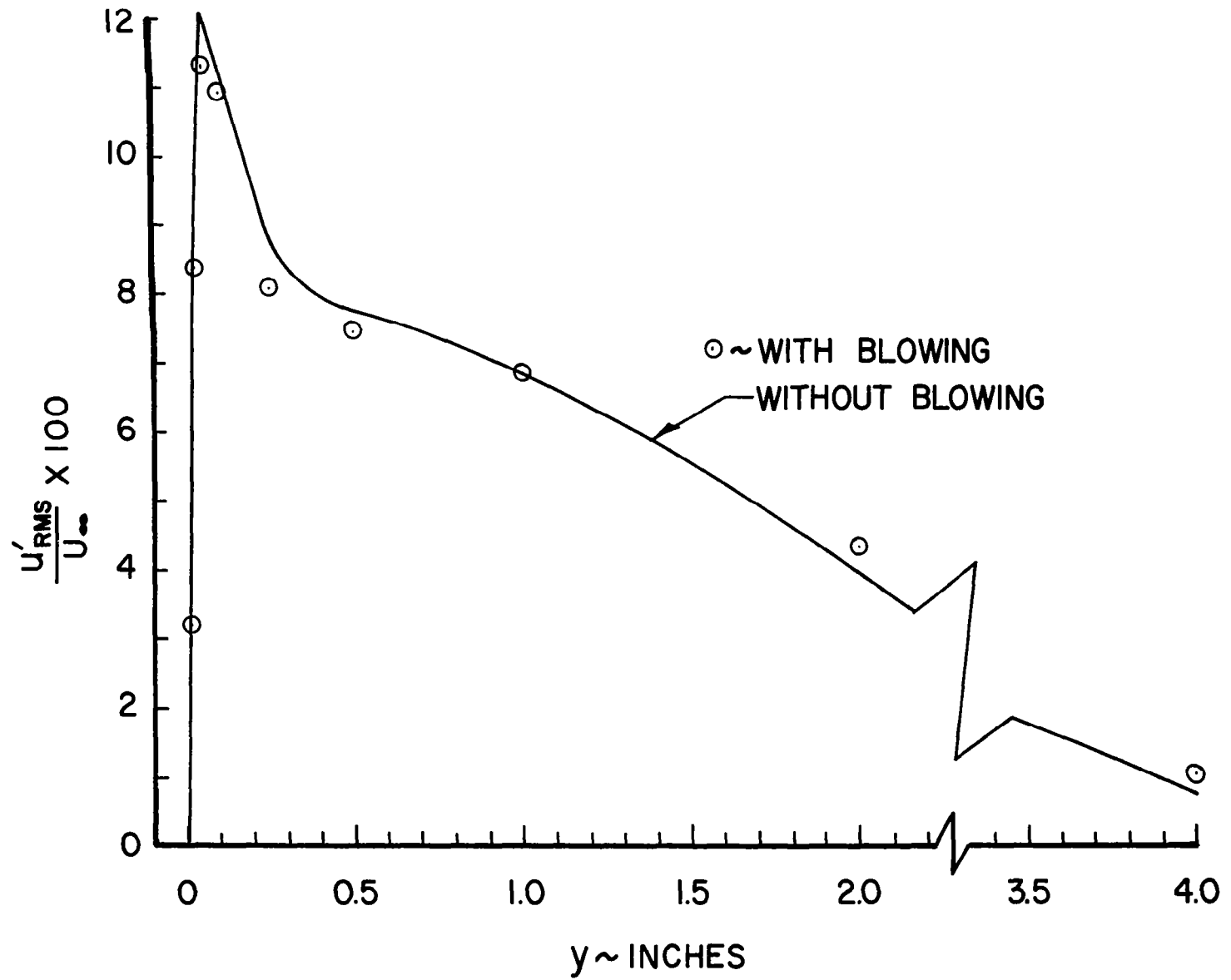
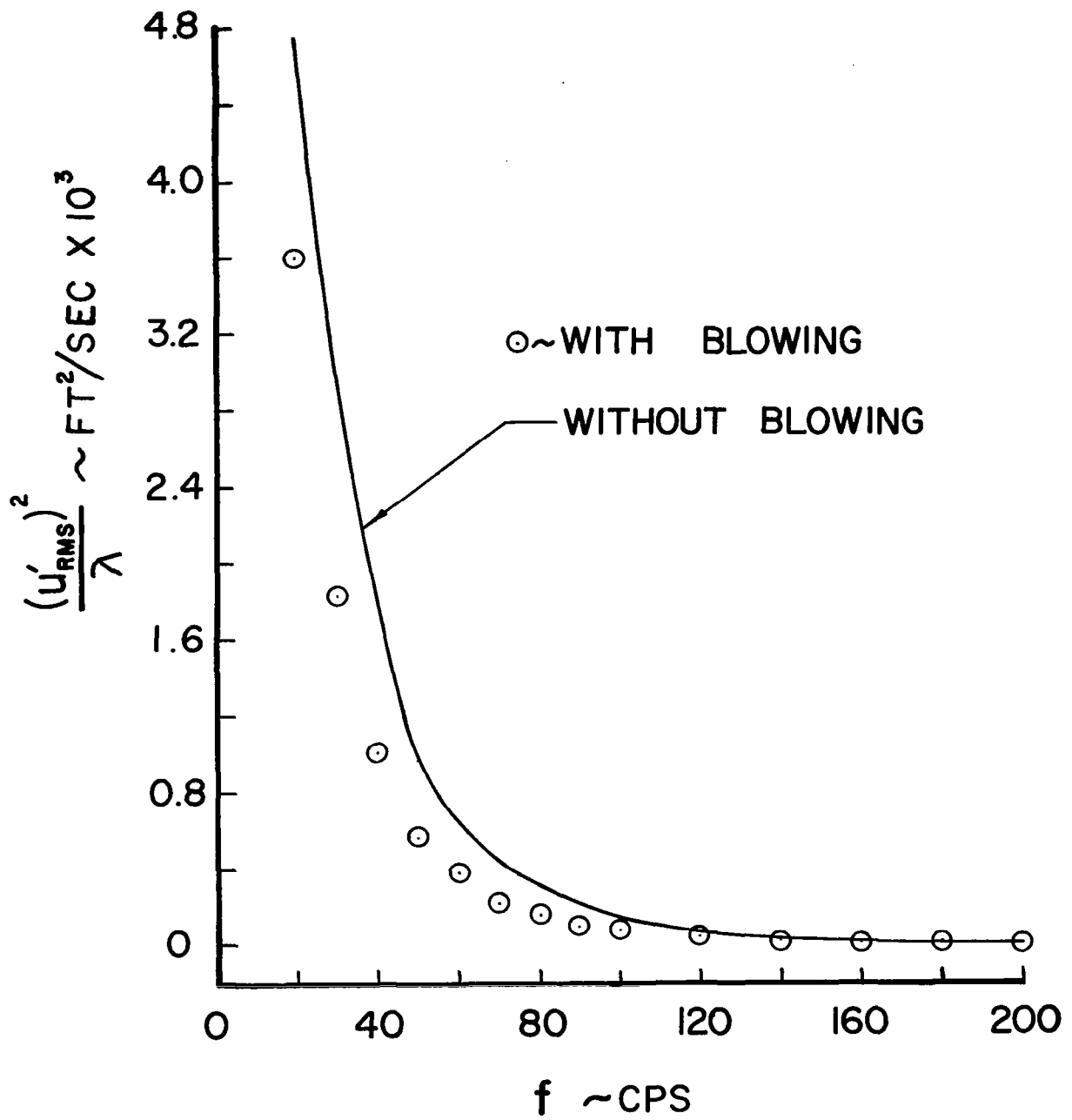
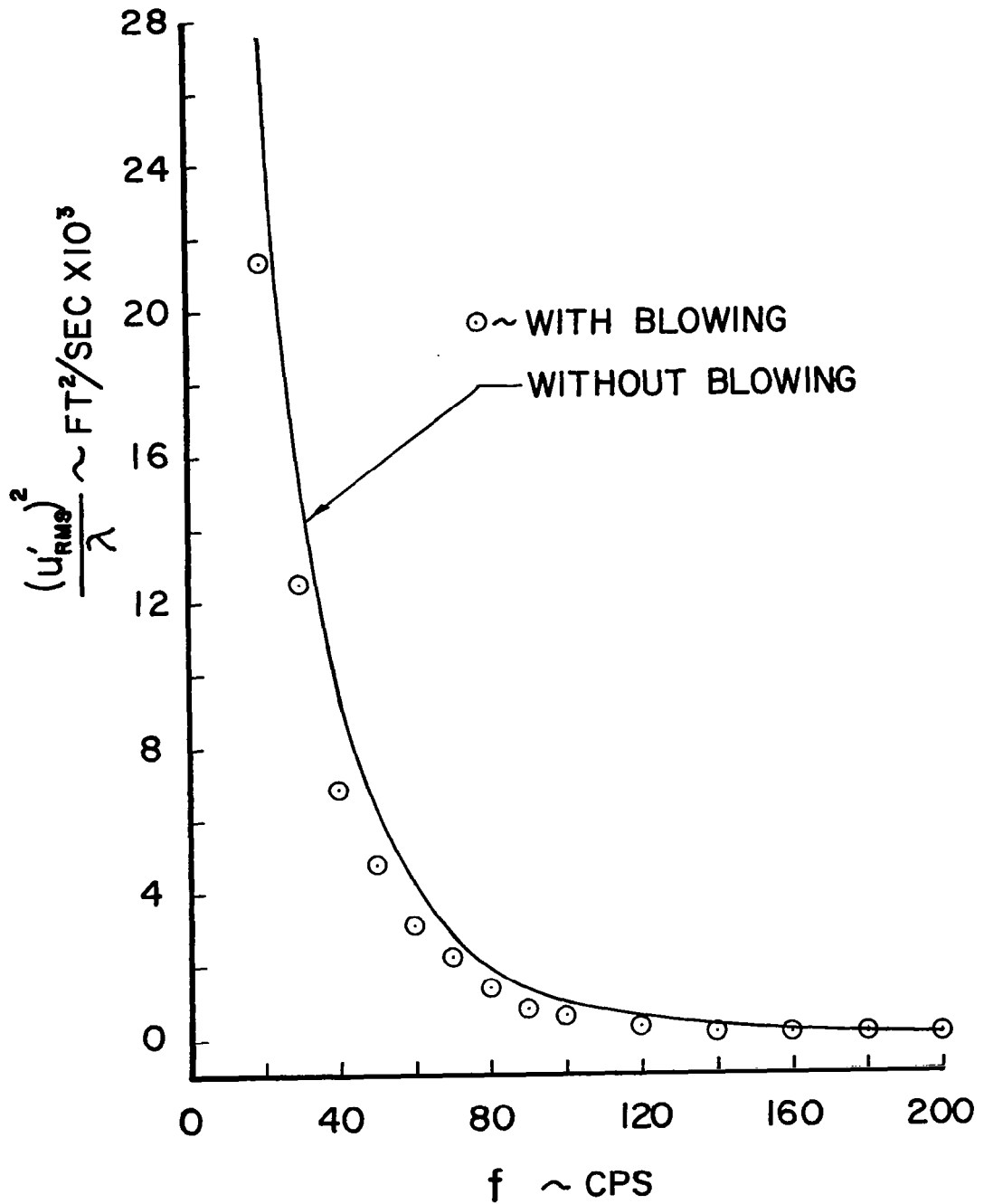


Figure 9 Longitudinal turbulence intensity, station 3.3 inches.



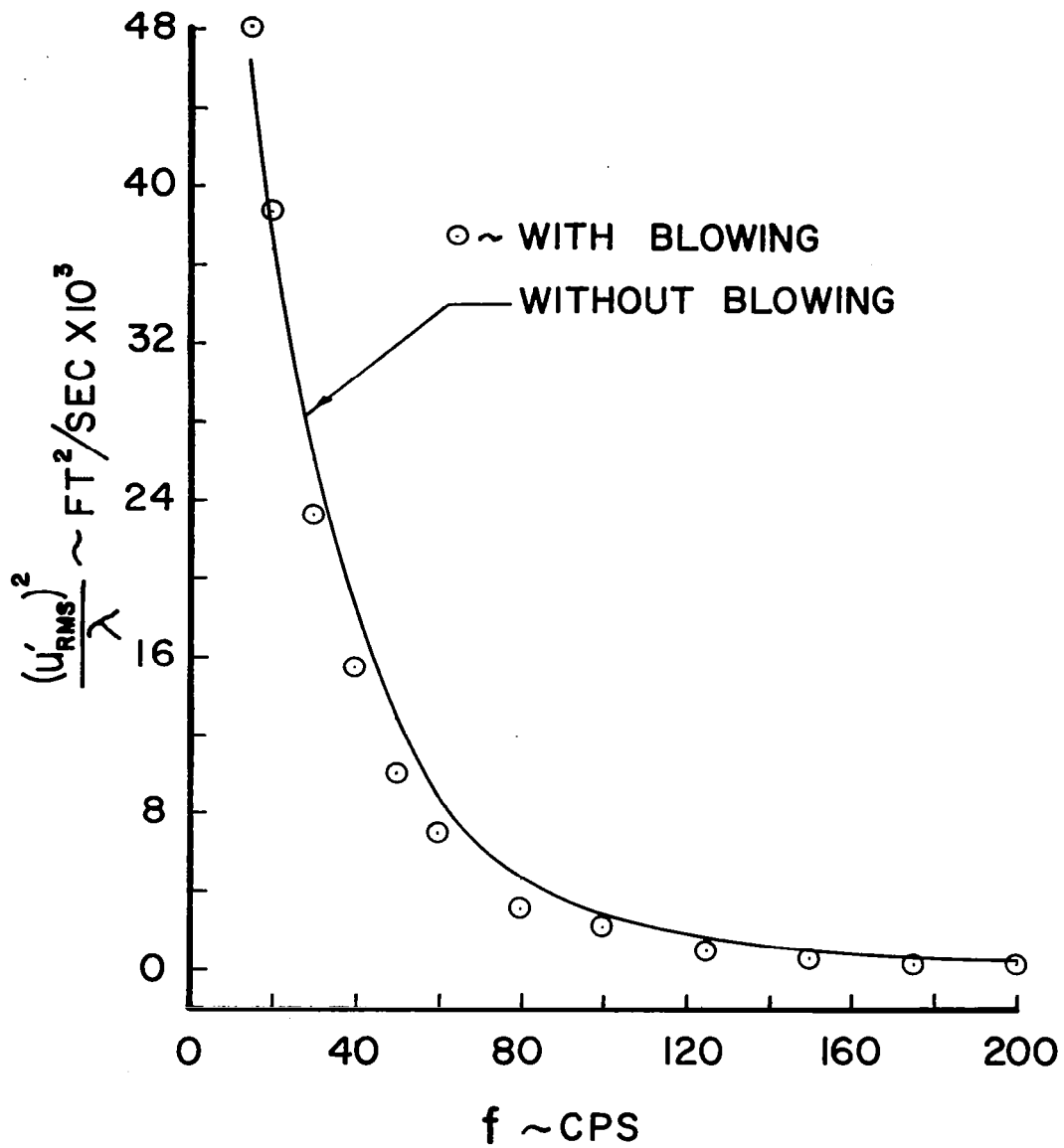
(a) Station 3.3 inches, $y = 0.010$ inches

Figure 10 Longitudinal turbulence spectrum.



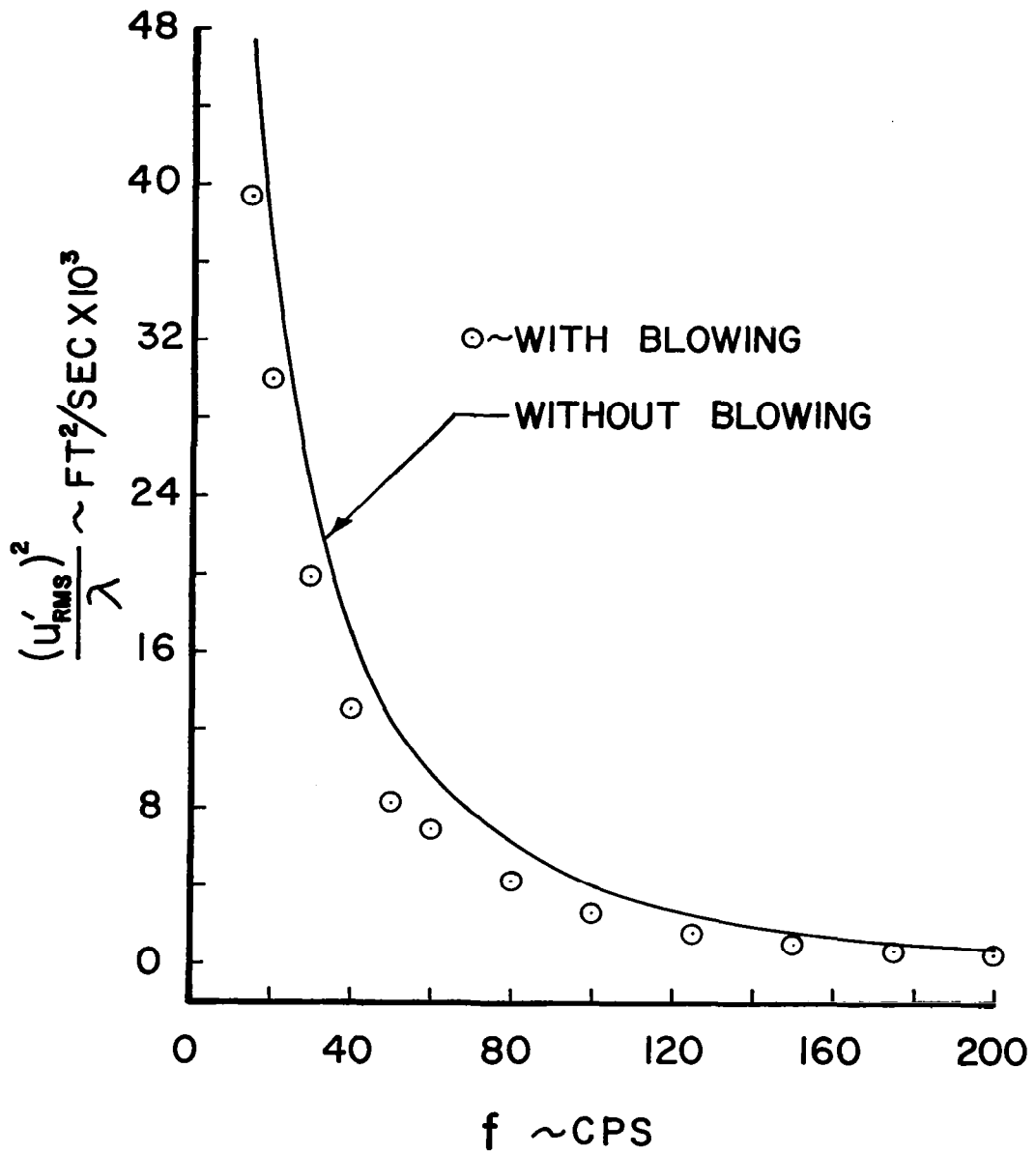
(b) Station 3.3 inches, y = 0.025 inches

Figure 10 (Continued) Longitudinal turbulence spectrum.



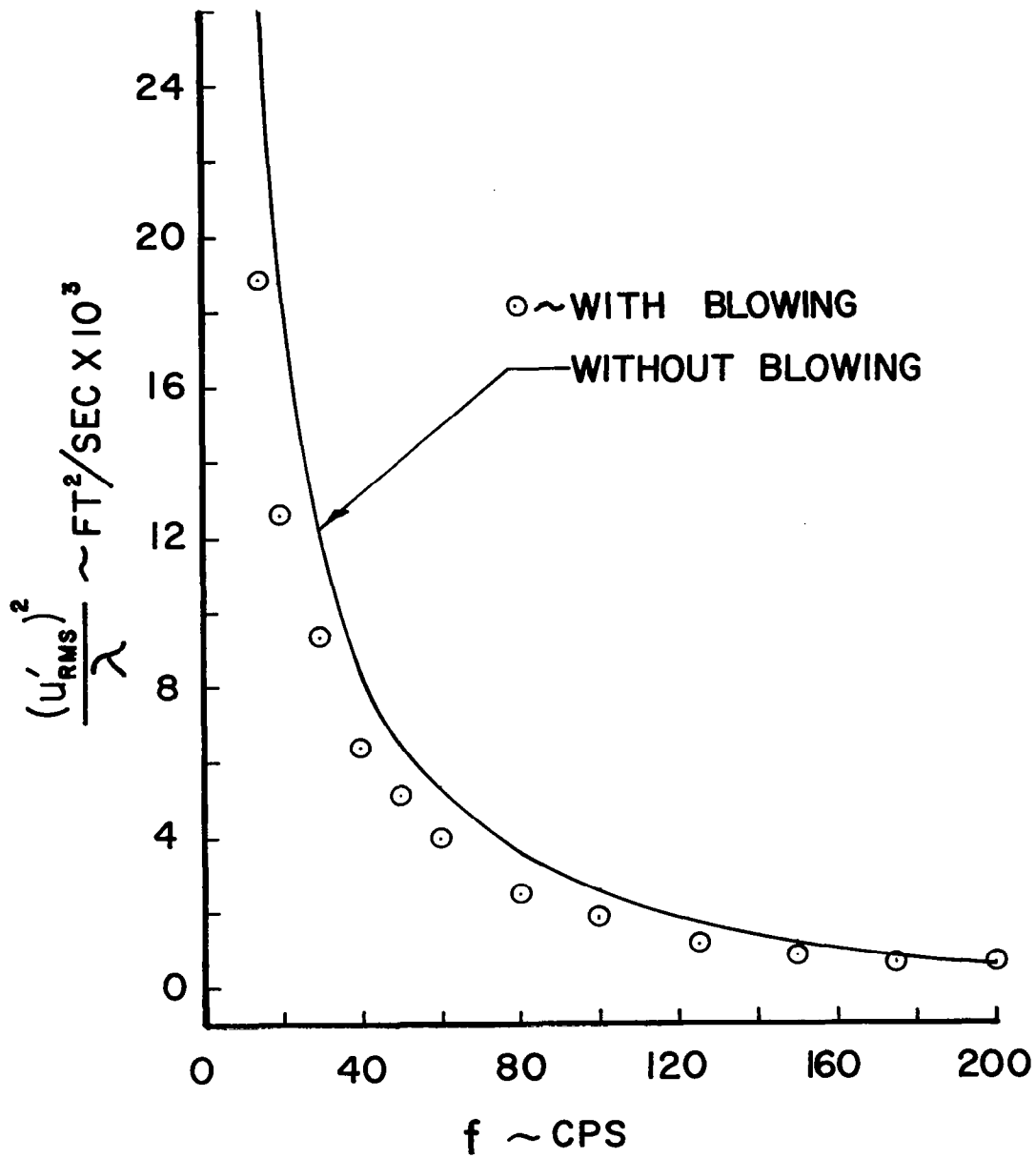
(c) Station 3.3 inches, $y = 0.050$ inches

Figure 10 (Continued) Longitudinal turbulence spectrum.



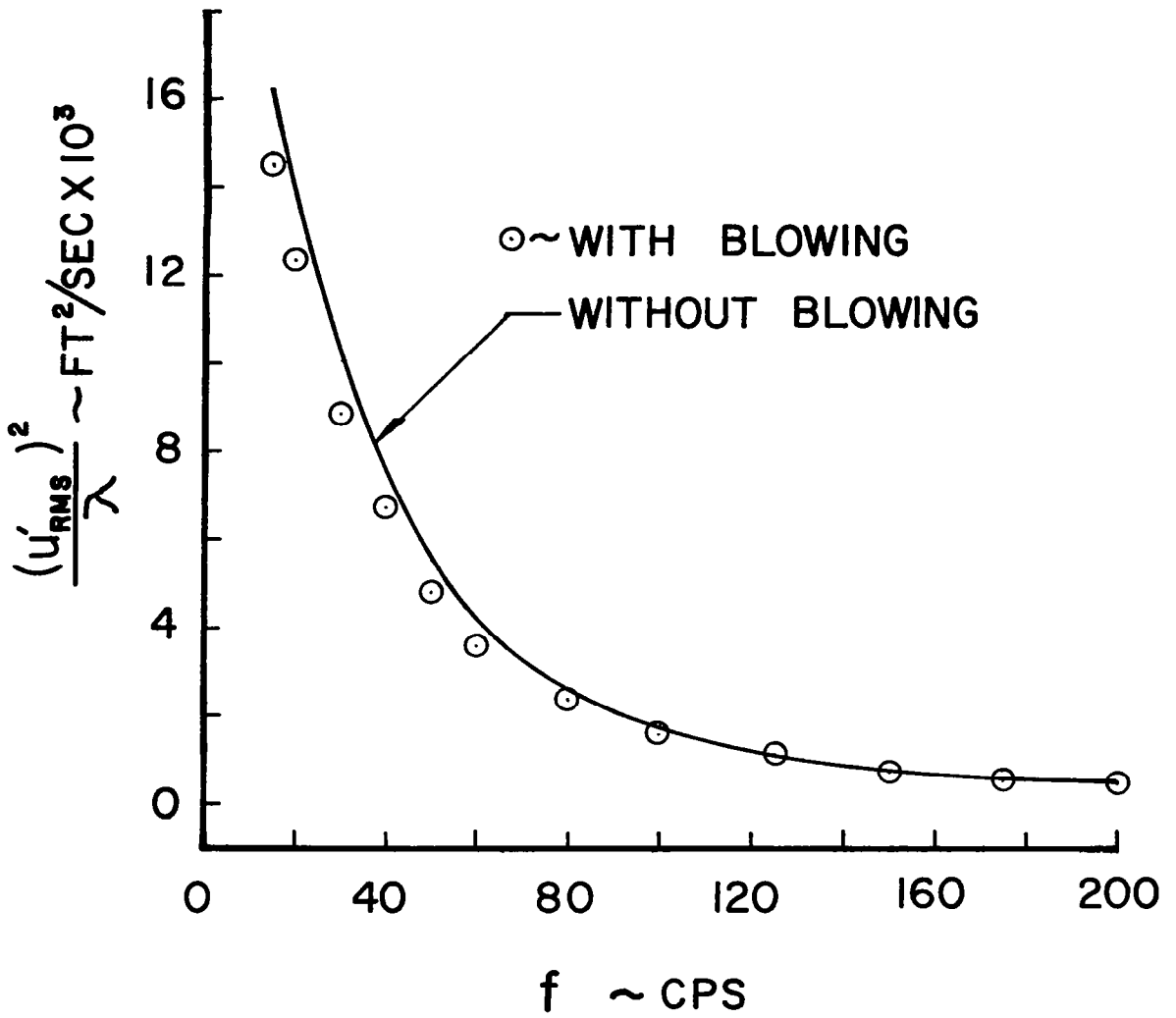
(d) Station 3.3 inches, $y = 0.100$ inches

Figure 10 (Continued) Longitudinal turbulence spectrum.



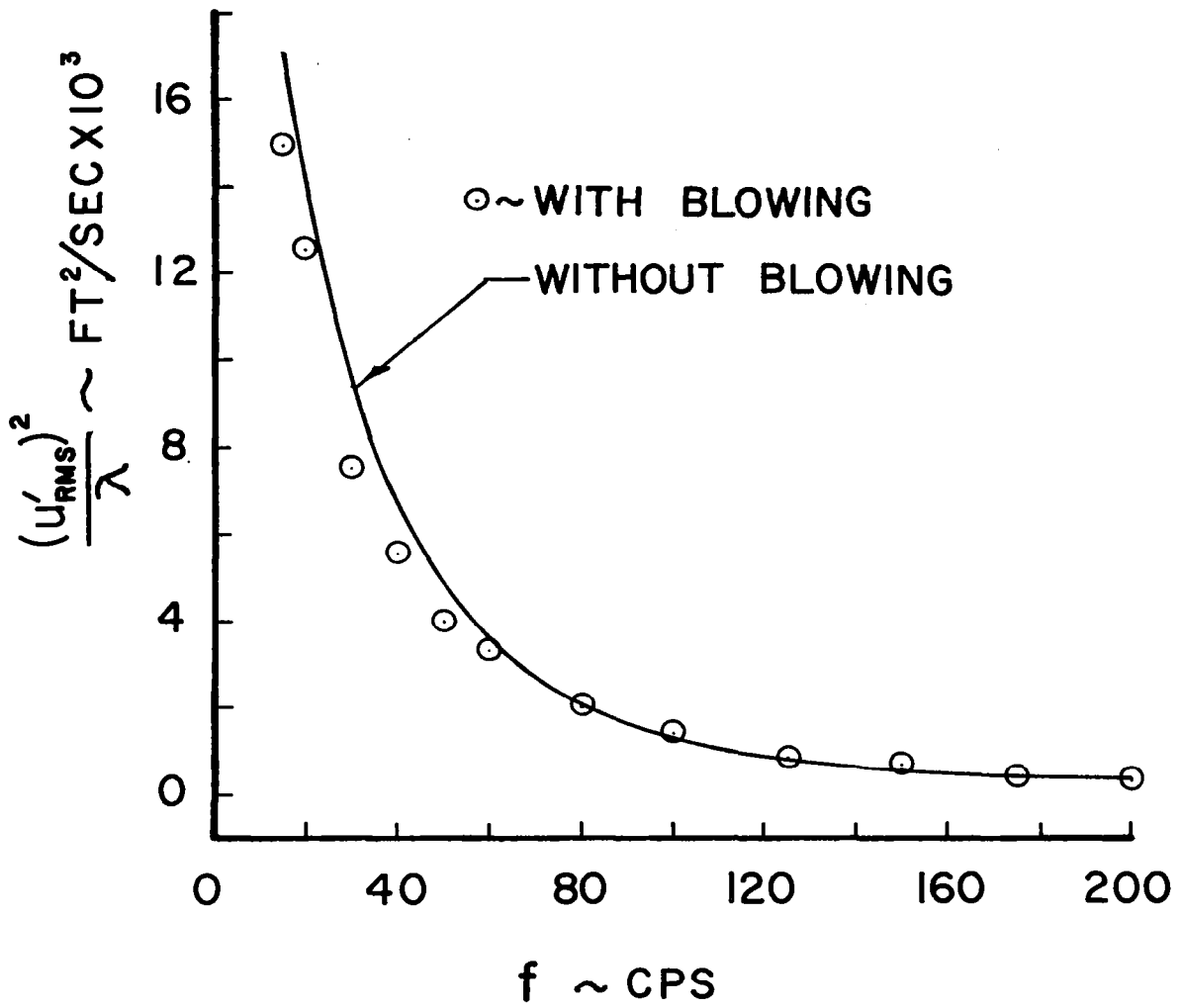
(e) Station 3.3 inches, $y = 0.250$ inches

Figure 10 (Continued) Longitudinal turbulence spectrum.



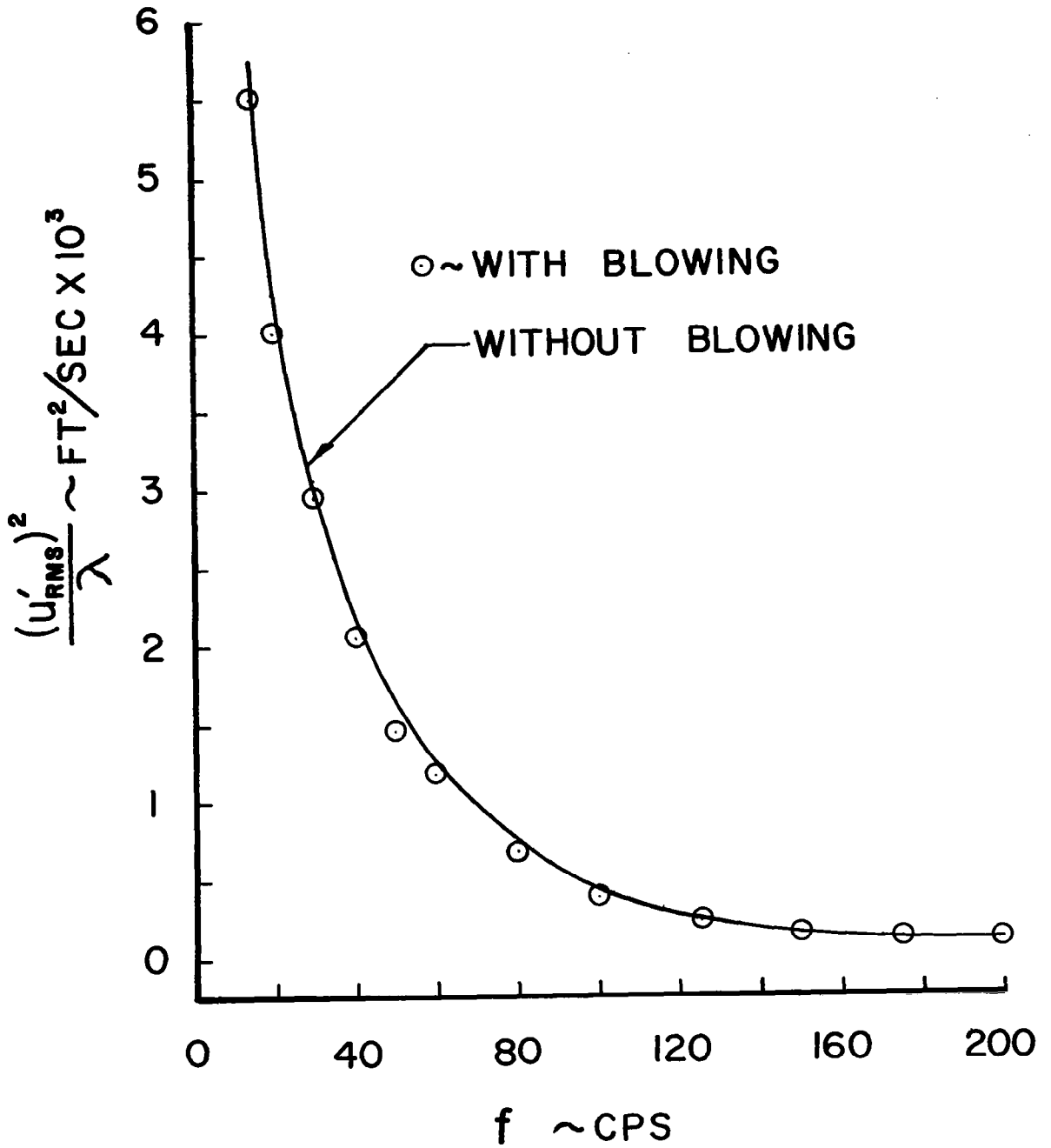
(f) Station 3.3 inches, $y = 0.500$ inches

Figure 10 (Continued) Longitudinal turbulence spectrum.



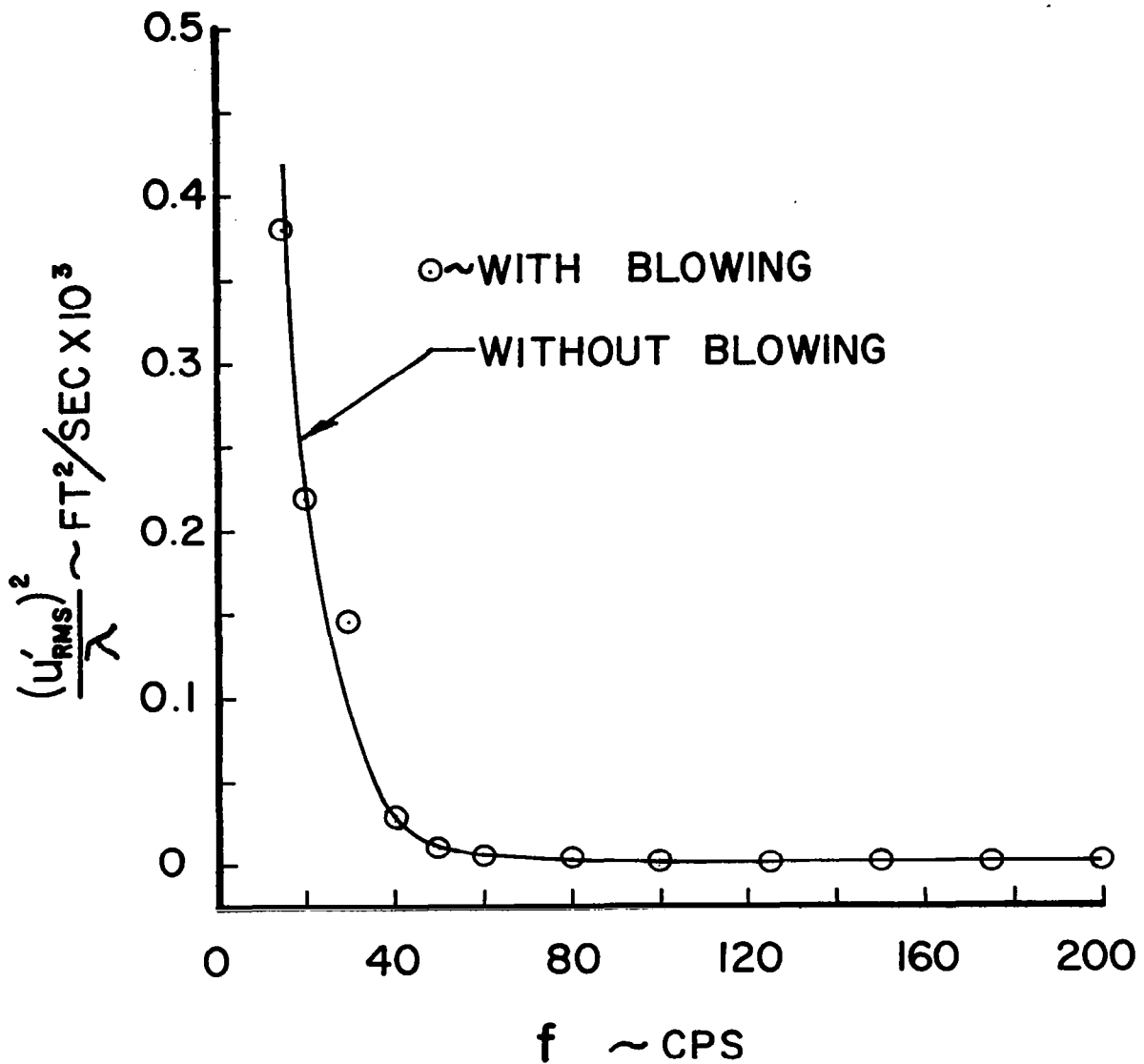
(g) Station 3.3 inches, $y = 1.000$ inches

Figure 10 (Continued) Longitudinal turbulence spectrum.



(h) Station 3.3 inches, $y = 2.000$ inches

Figure 10 (Continued) Longitudinal turbulence spectrum.



(1) Station 3.3 inches, $y = 4.015$ inches (channel centerline)

Figure 10 (Concluded) Longitudinal turbulence spectrum.

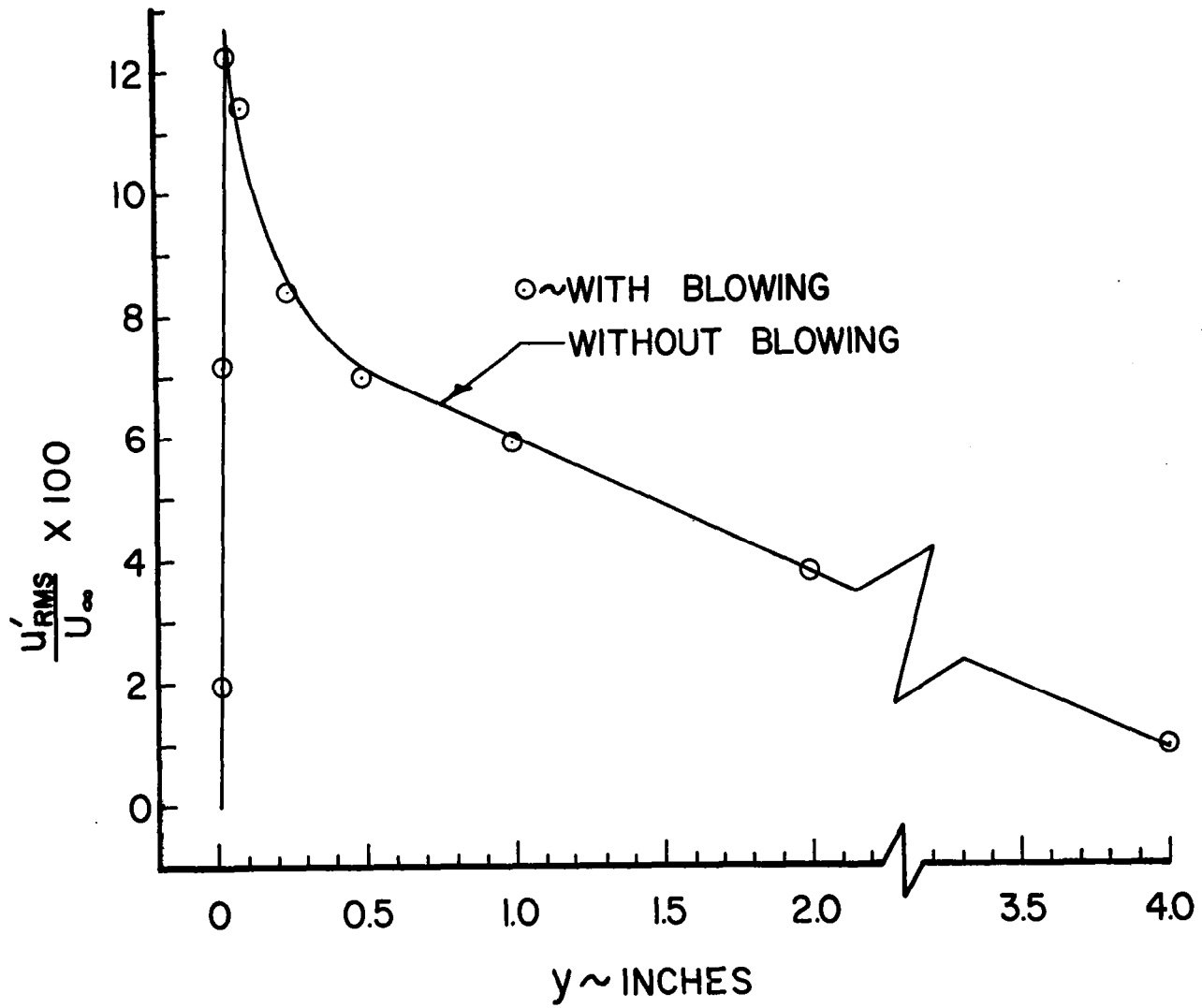
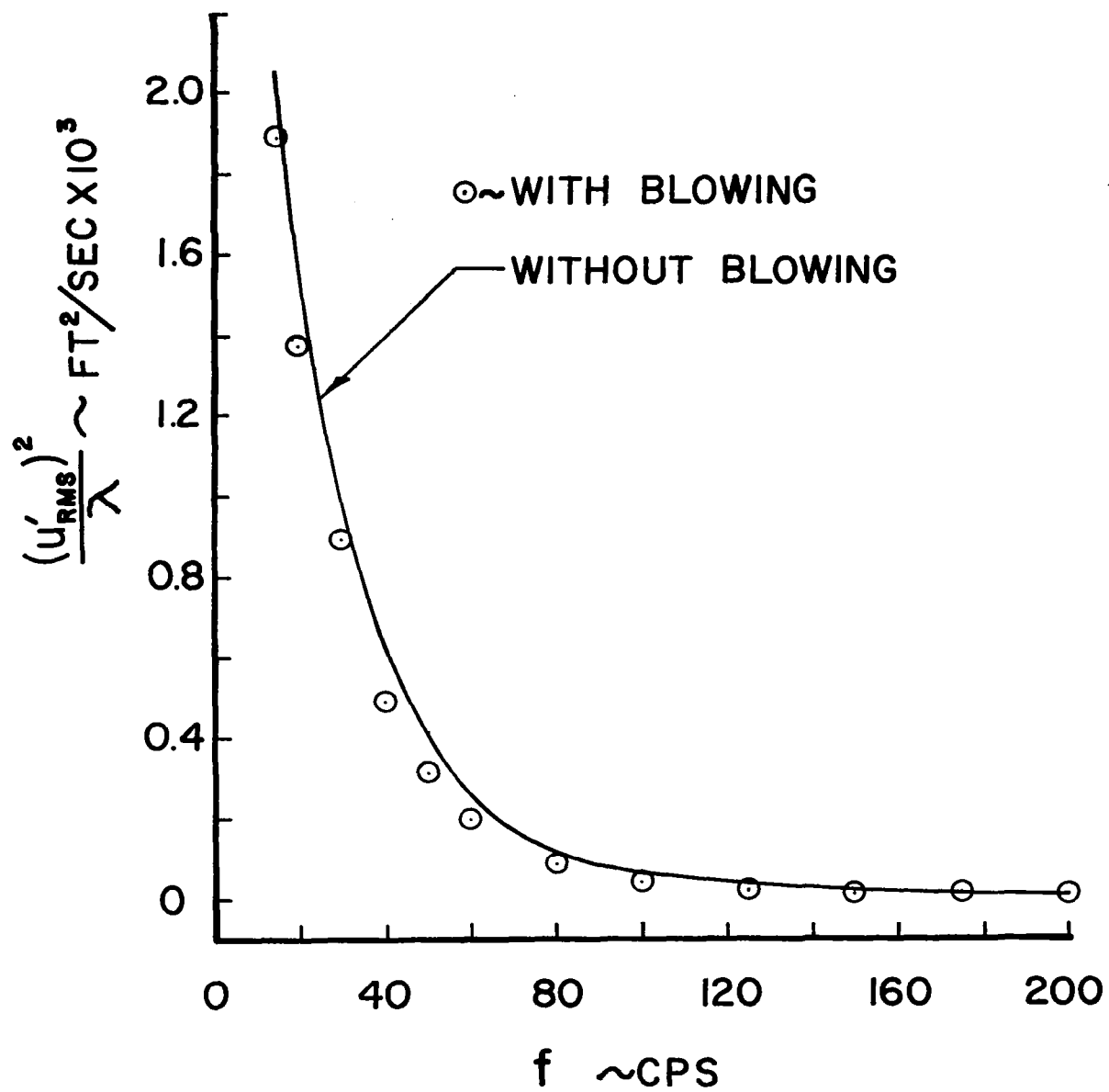
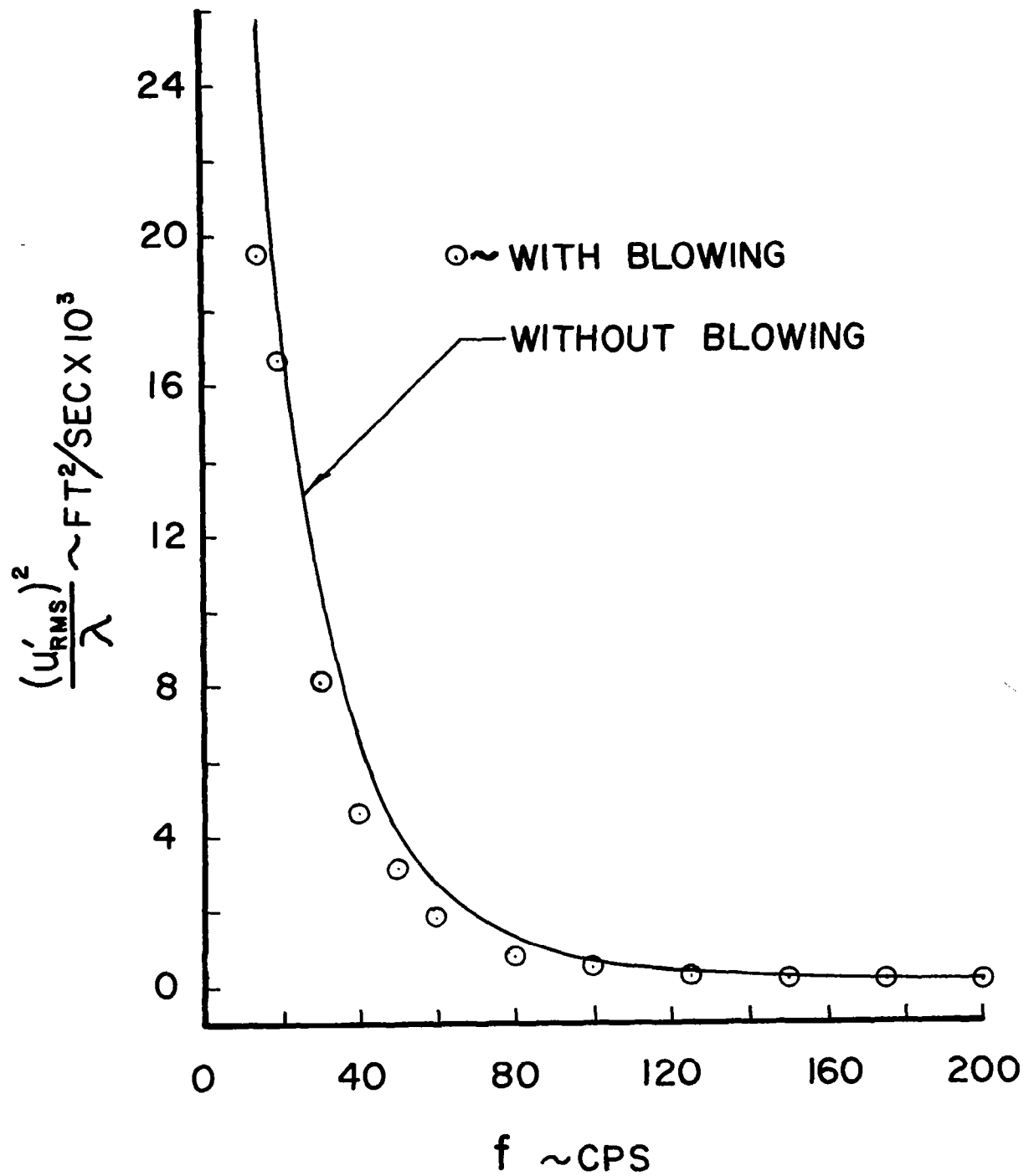


Figure 11 Longitudinal turbulence intensity, station 6.9 inches.



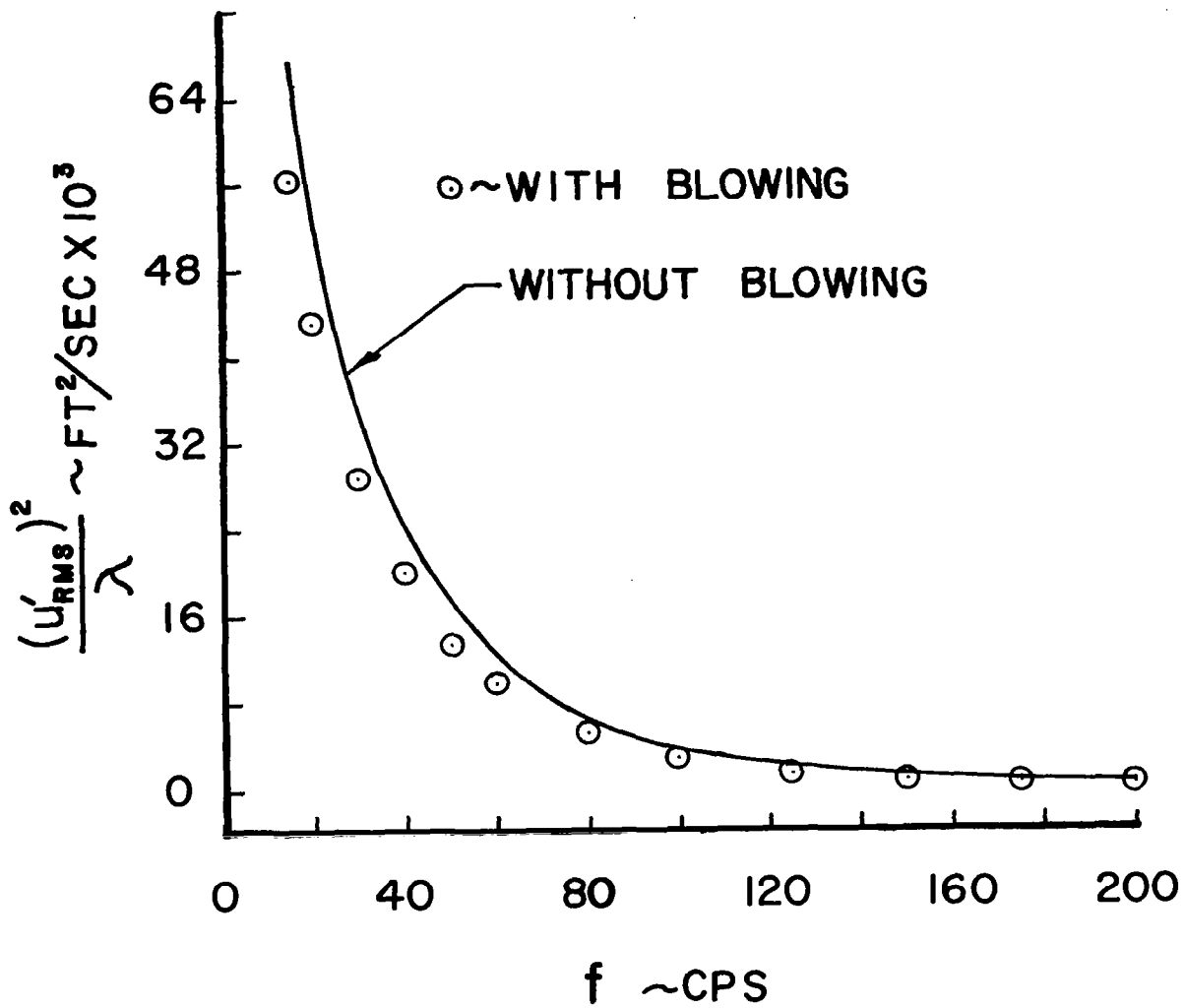
(a) Station 6.9 inches, $y = 0.010$ inches

Figure 12 Longitudinal turbulence spectrum.



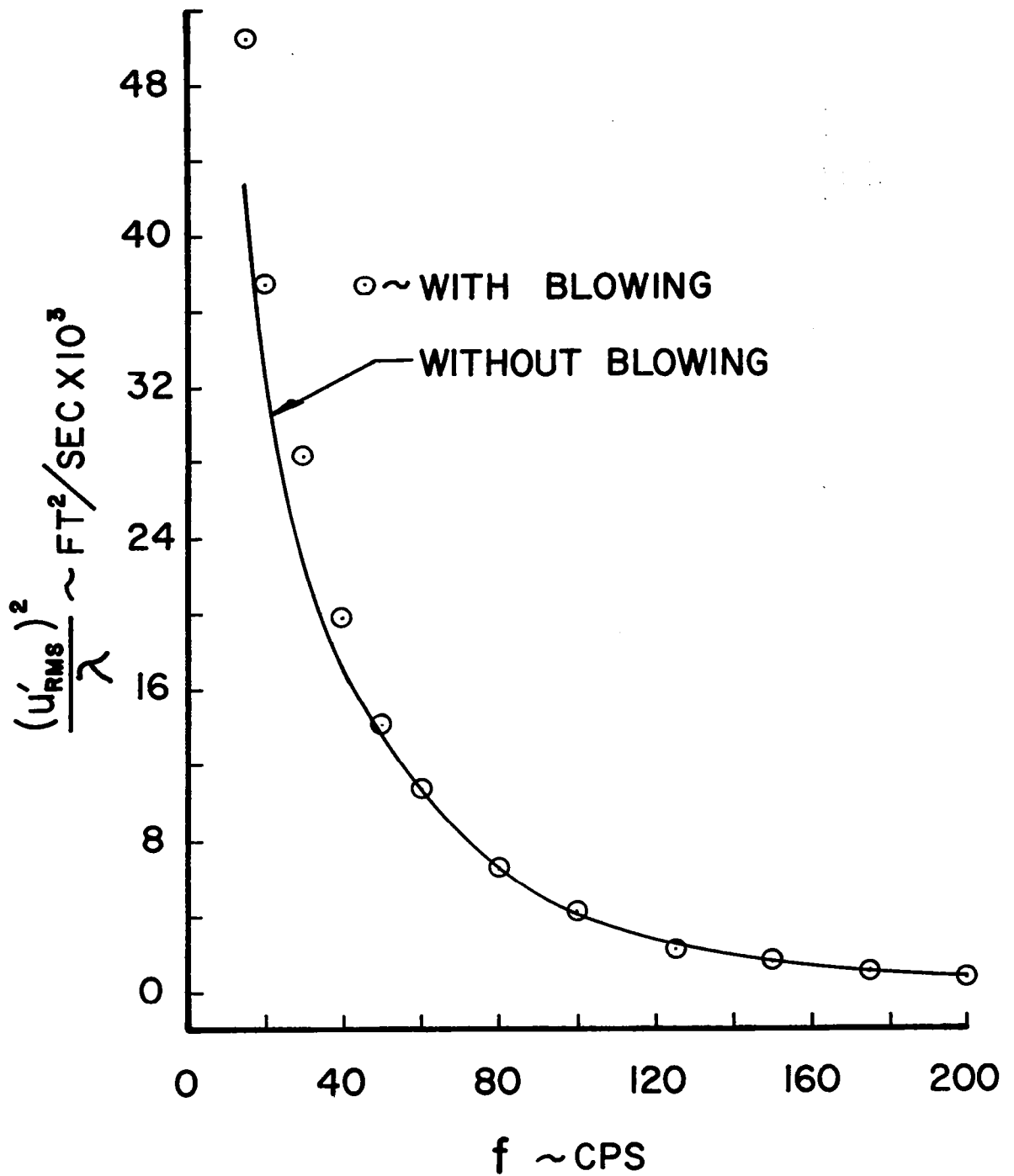
(b) Station 6.9 inches, $y = 0.025$ inches

Figure 12 (Continued) Longitudinal turbulence spectrum.



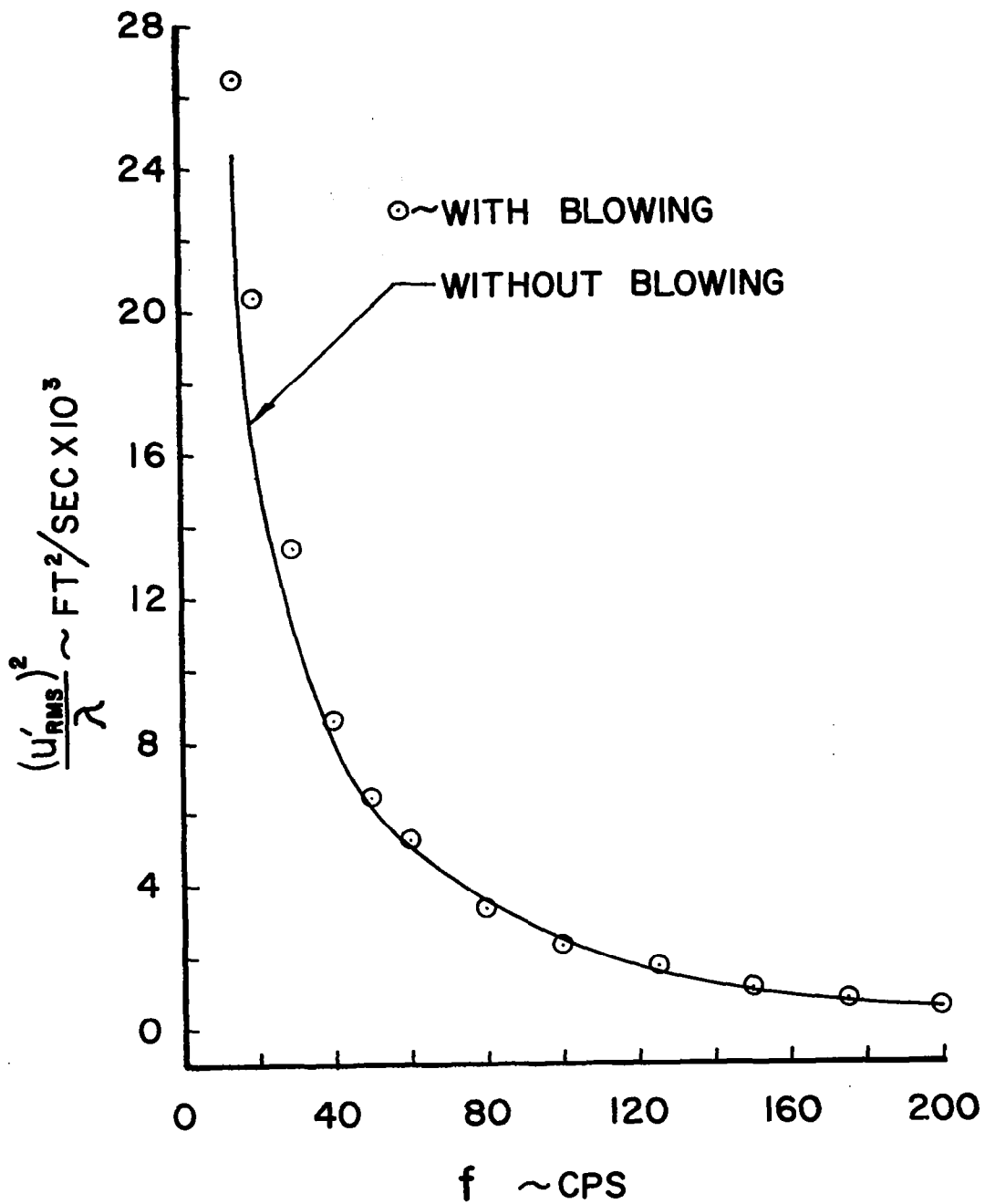
(c) Station 6.9 inches, $y = 0.050$ inches

Figure 12 (Continued) Longitudinal turbulence spectrum.



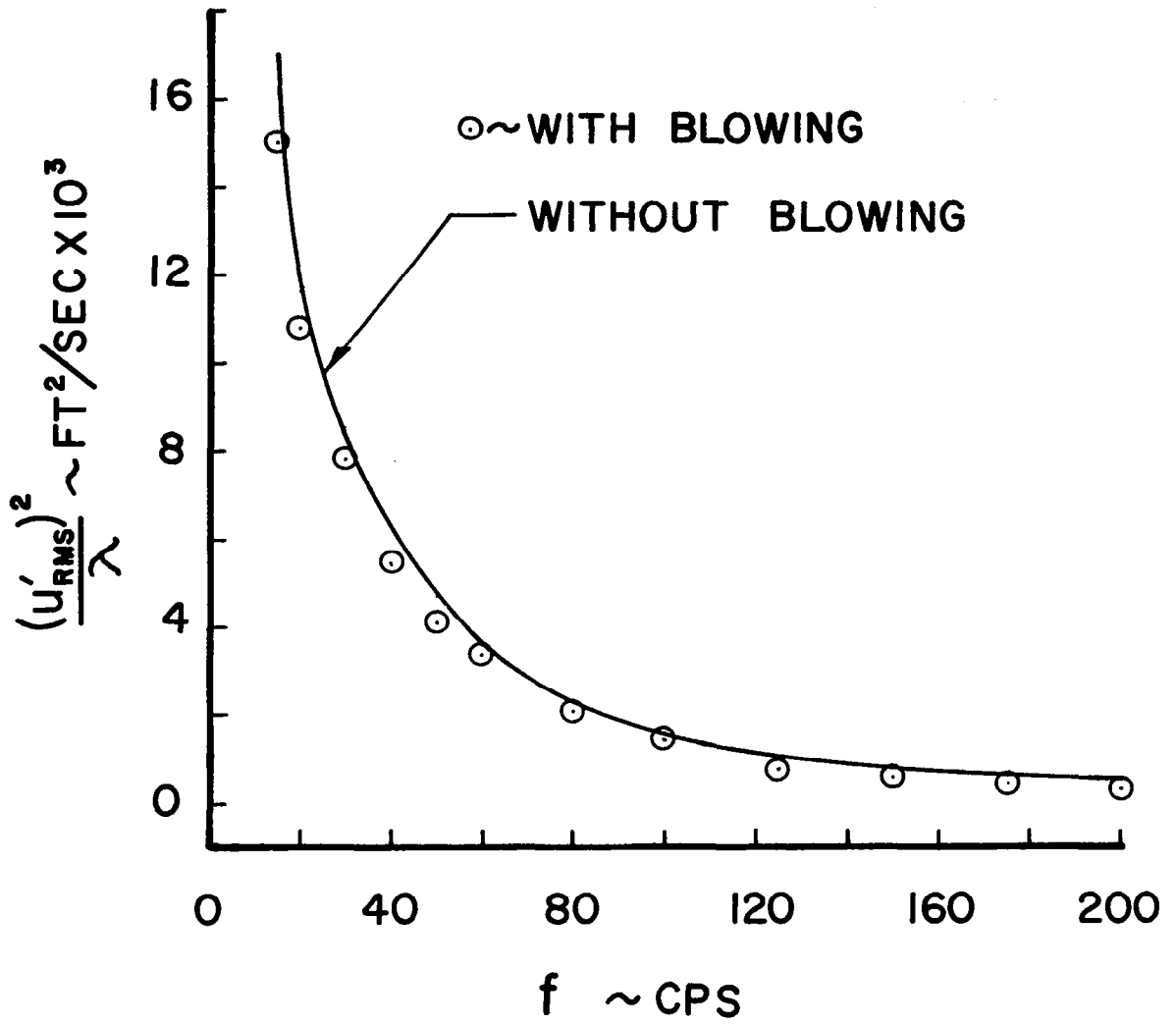
(d) Station 6.9 inches, $y = 0.100$ inches

Figure 12 (Continued) Longitudinal turbulence spectrum.



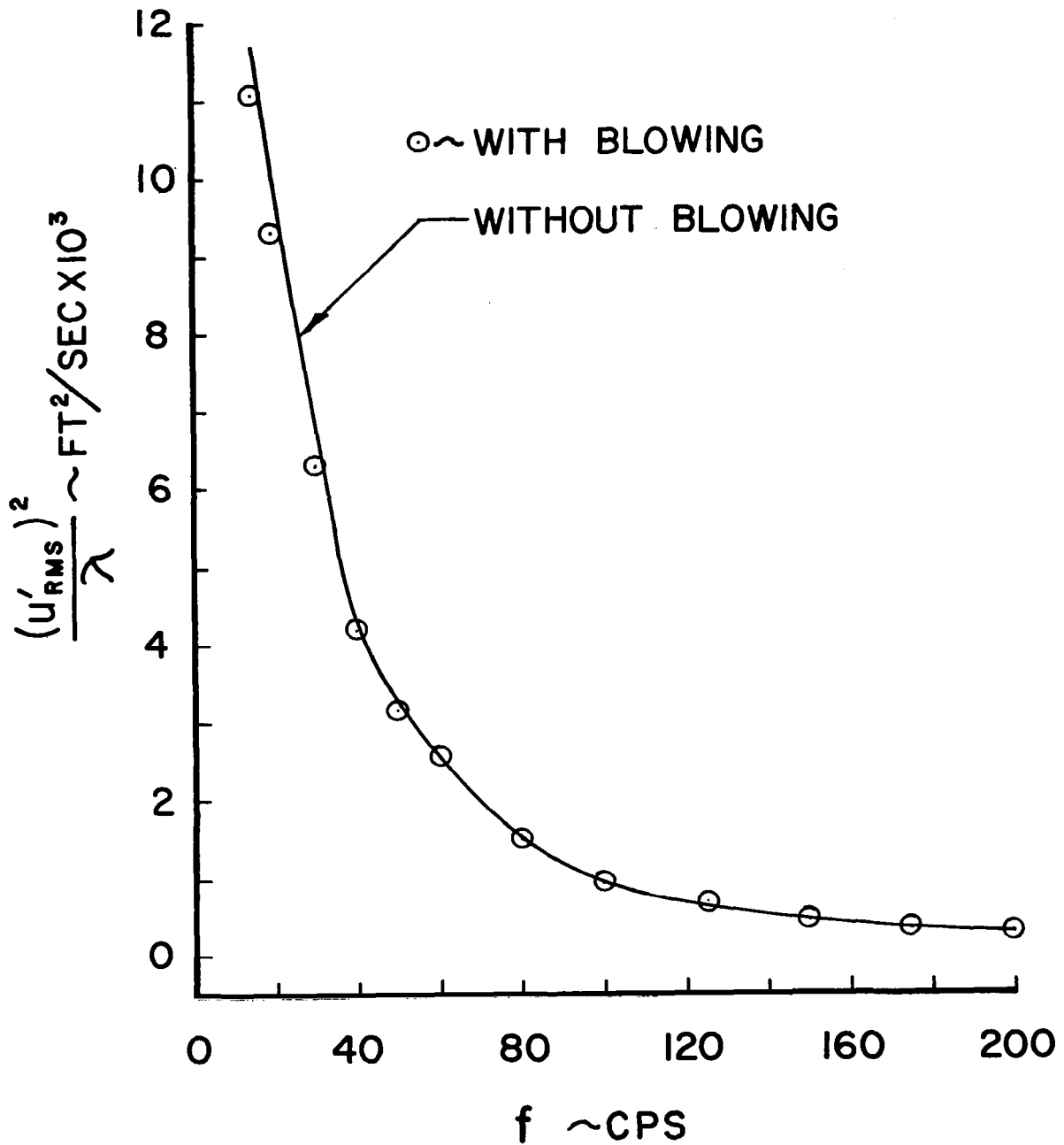
(e) Station 6.9 inches, $y = 0.250$ inches

Figure 12 (Continued) Longitudinal turbulence spectrum.



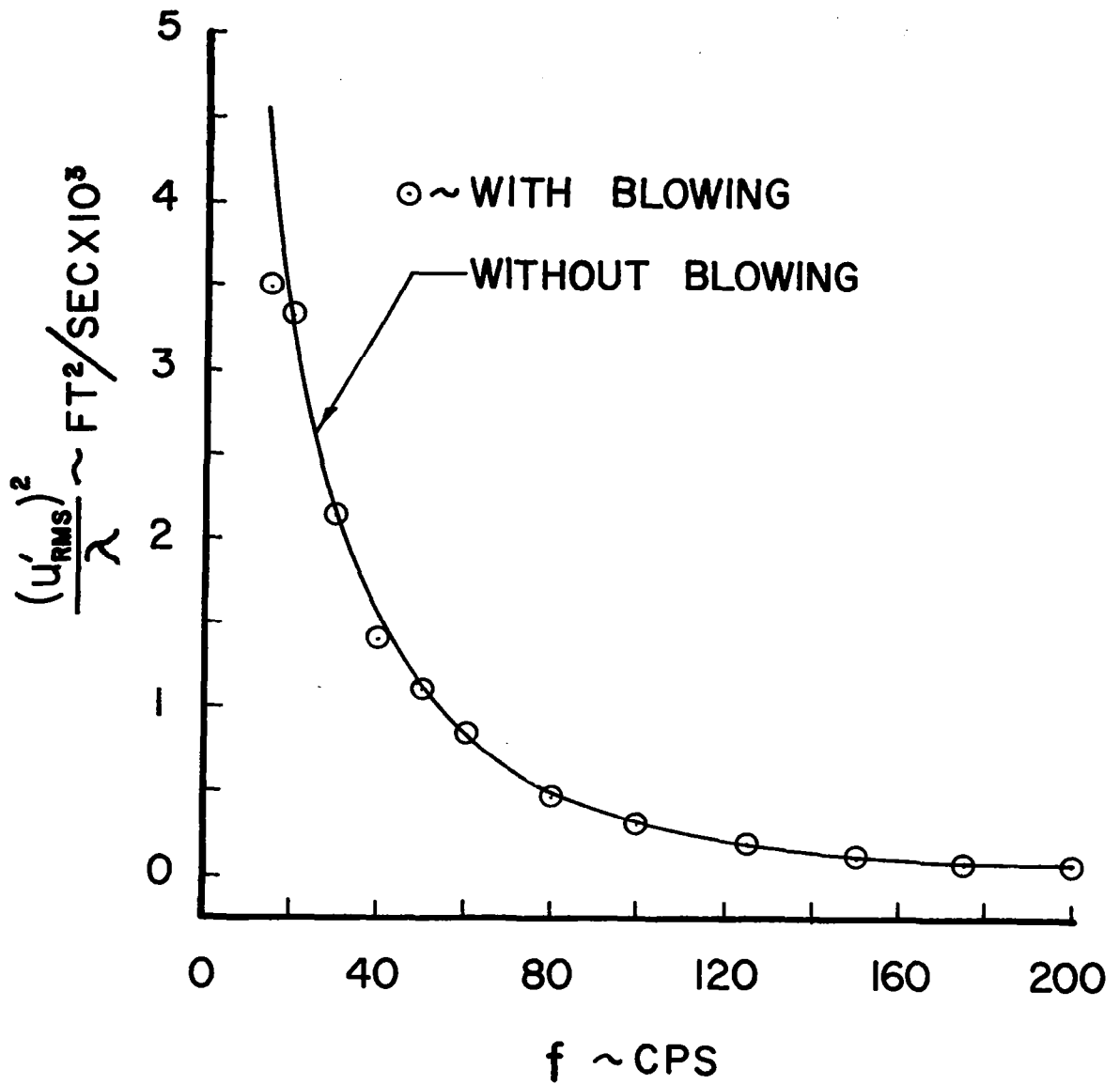
(f) Station 6.9 inches, y = 0.500 inches

Figure 12 (Continued) Longitudinal turbulence spectrum.



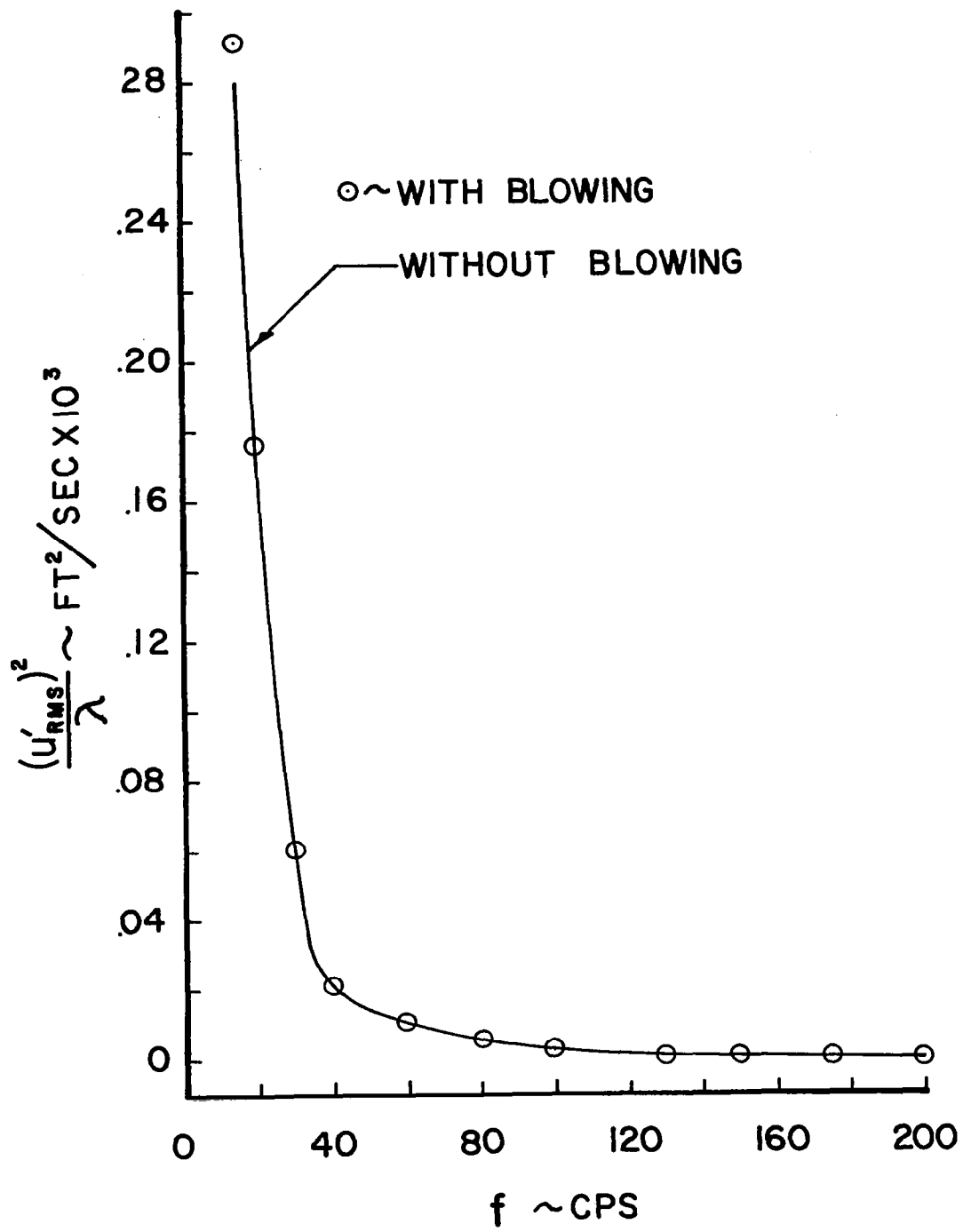
(g) Station 6.9 inches, $y = 1.000$ inches

Figure 12 (Continued) Longitudinal turbulence spectrum.



(h) Station 6.9 inches, y = 2.000 inches

Figure 12 (Continued) Longitudinal turbulence spectrum.



(1) Station 6.9 inches, $y = 4.015$ inches (channel centerline)

Figure 12 (Concluded) Longitudinal turbulence spectrum.

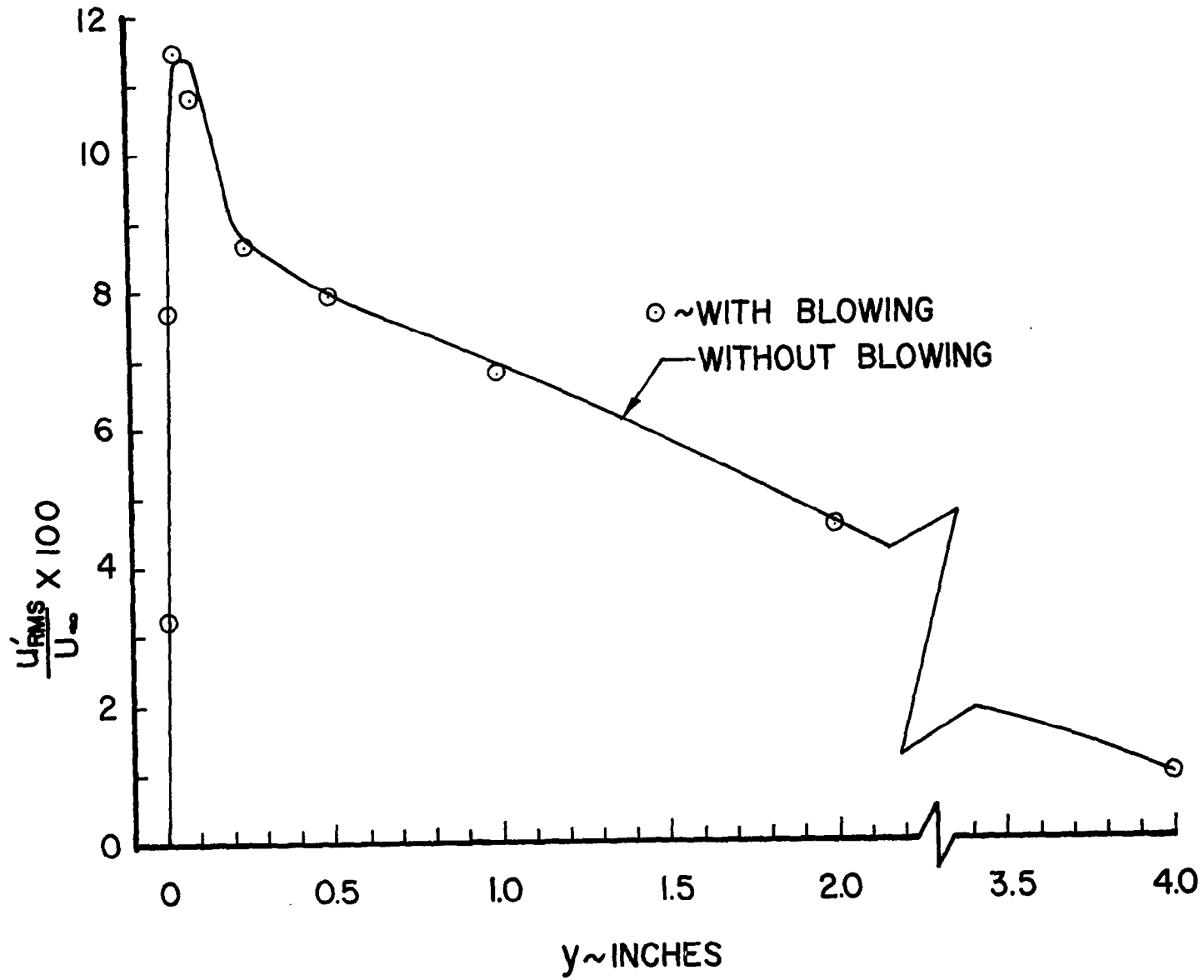
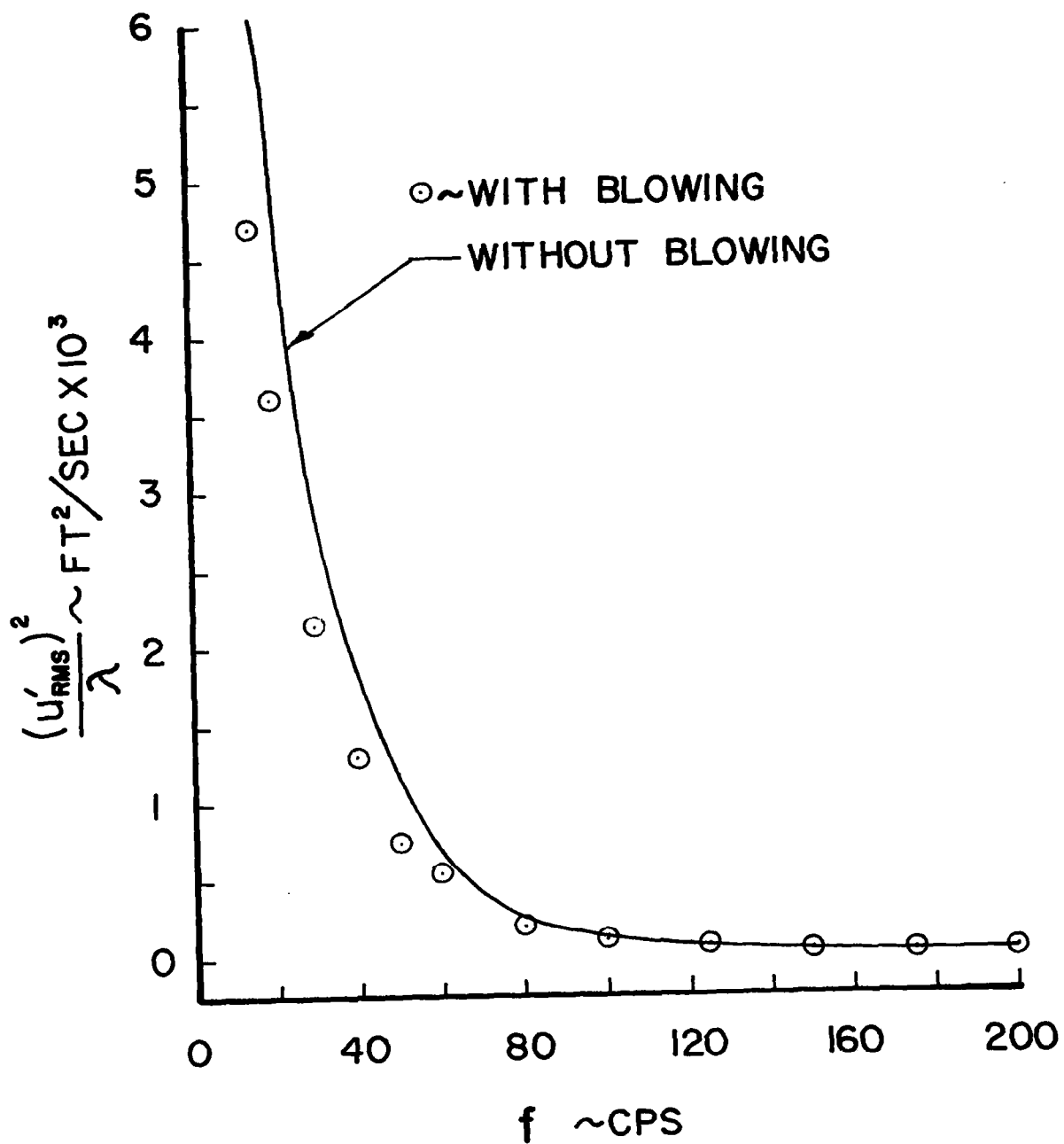
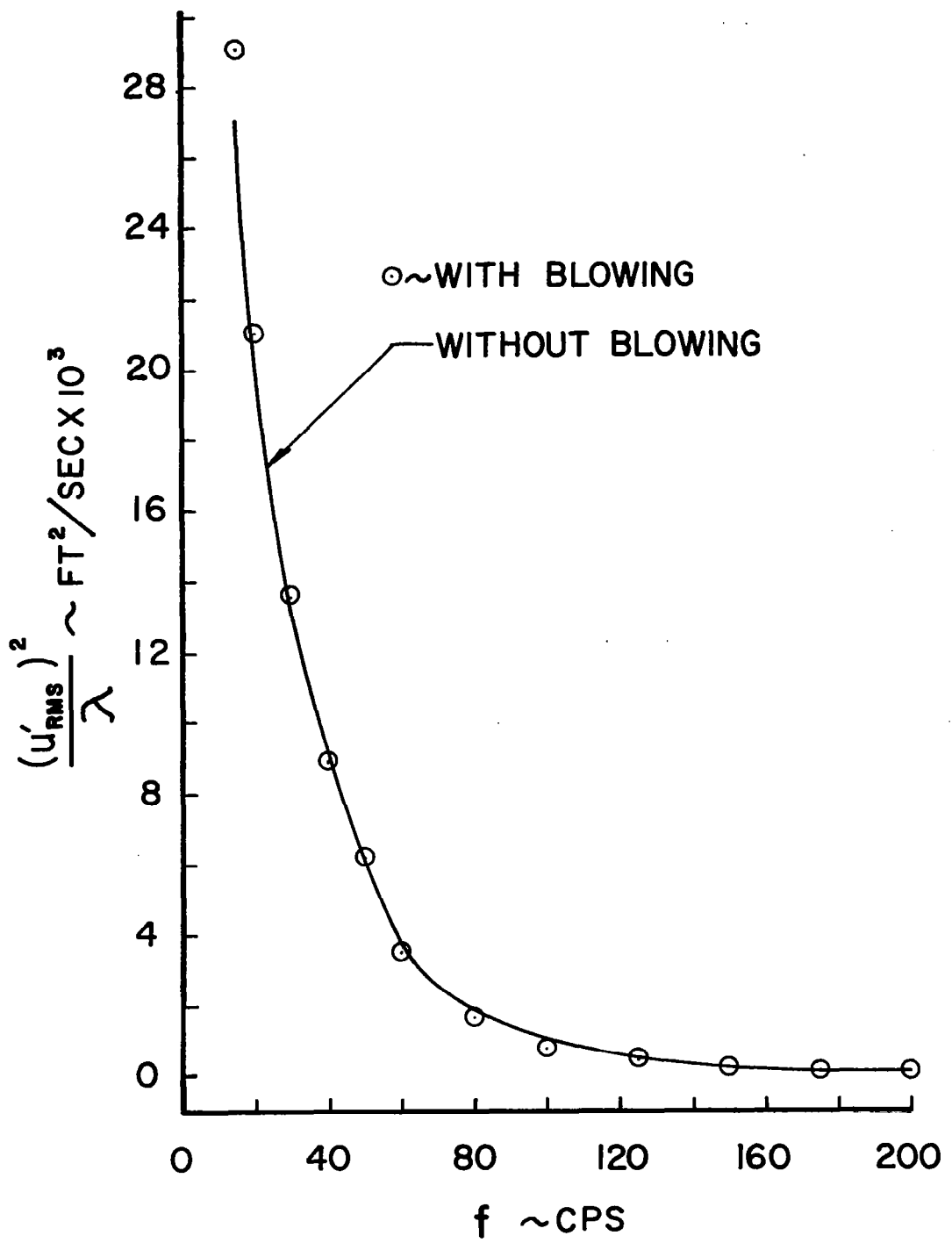


Figure 13 Longitudinal turbulence intensity, station 15.7 inches.



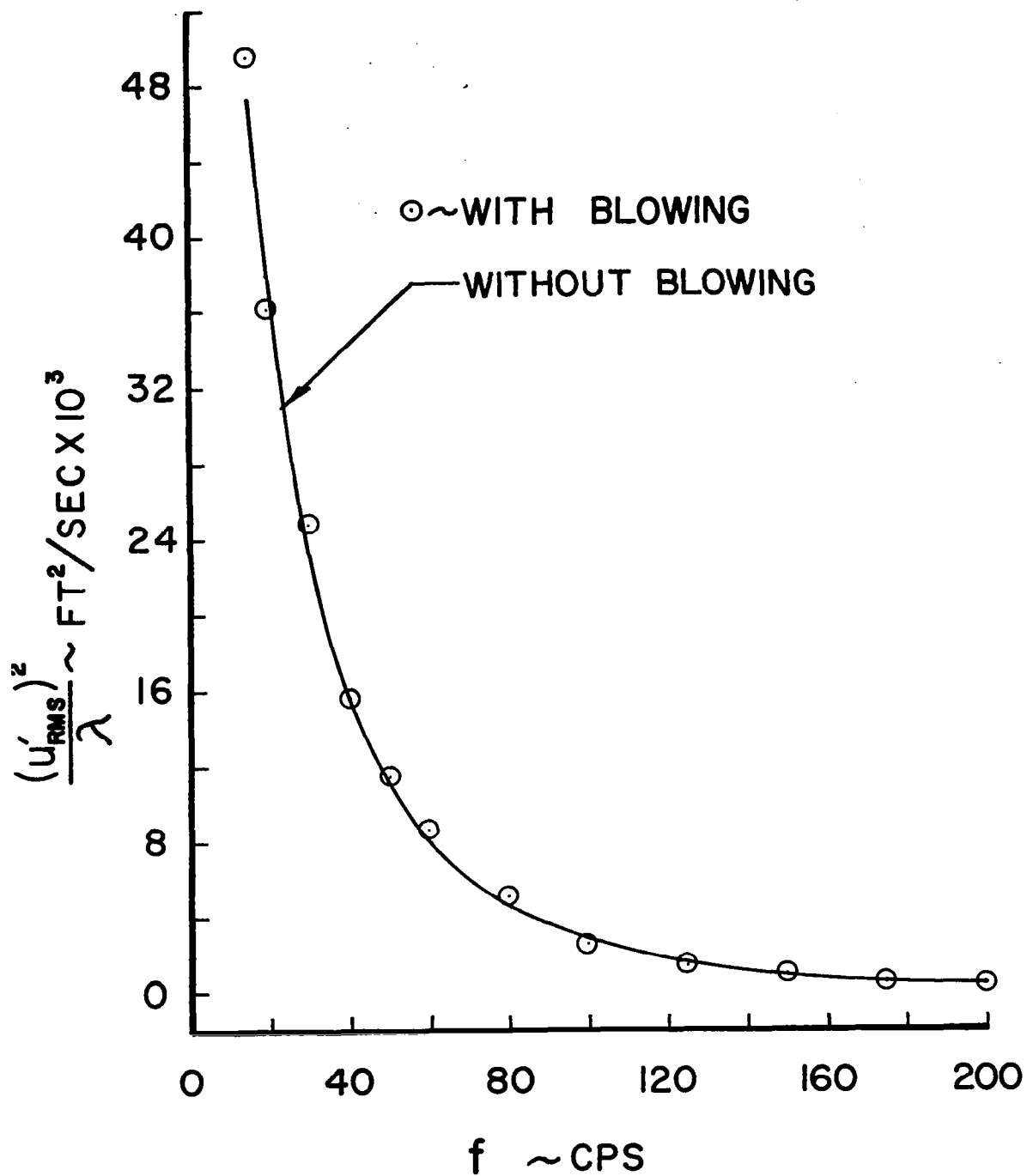
(a) Station 15.7 inches, $y = 0.010$ inches

Figure 14 Longitudinal turbulence spectrum.



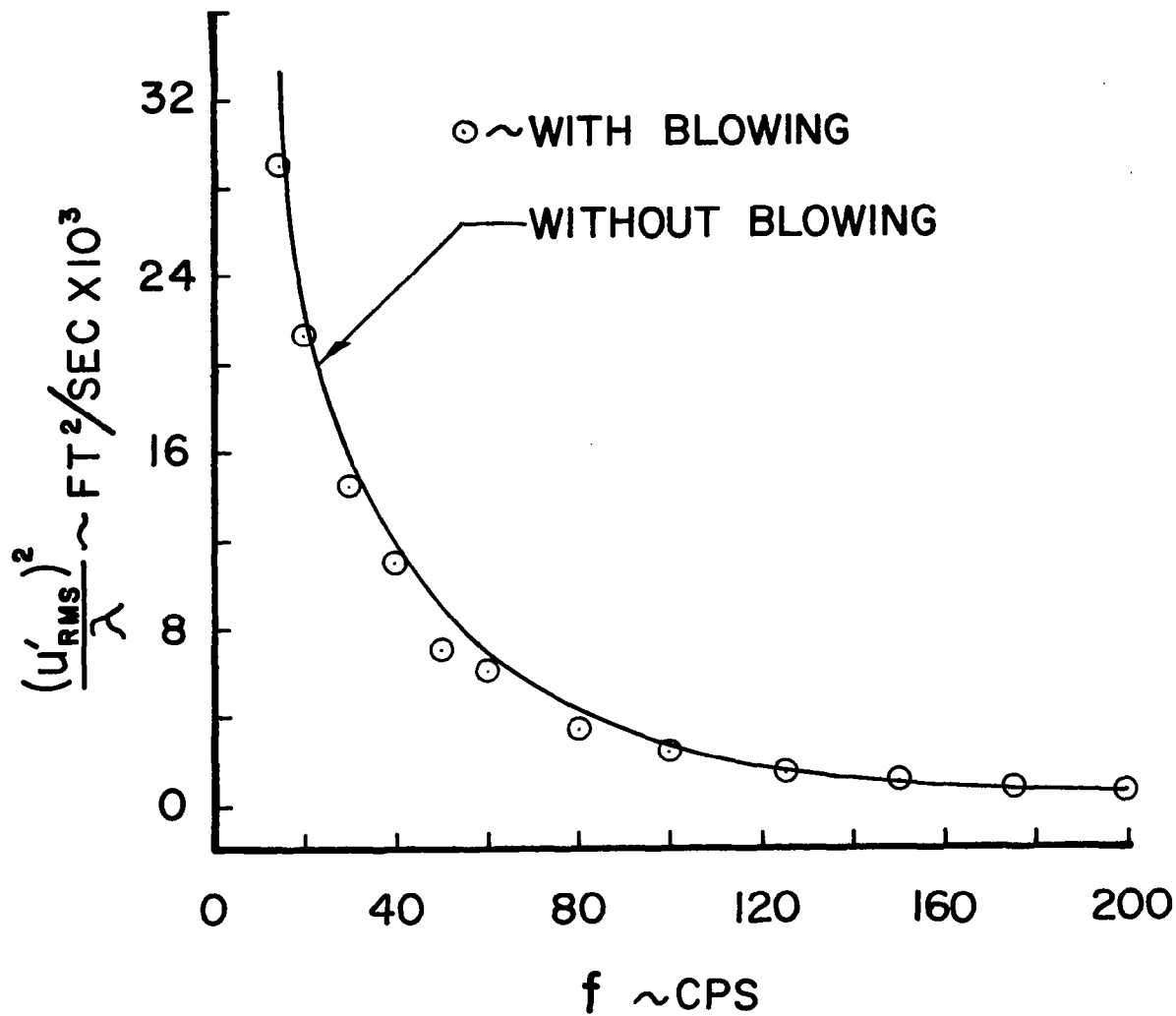
(b) Station 15.7 inches, $y = 0.025$ inches

Figure 14 (Continued) Longitudinal turbulence spectrum.



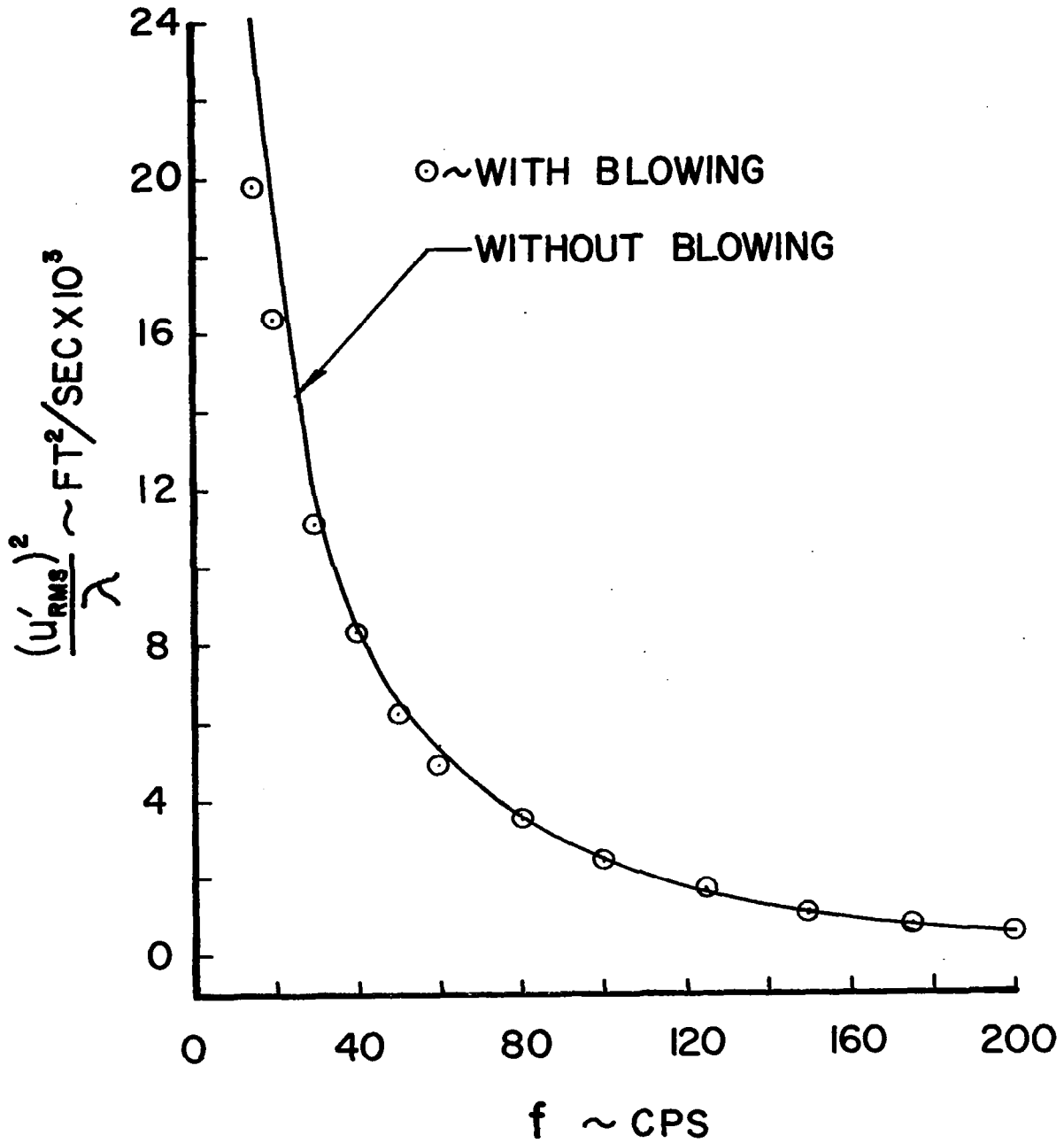
(c) Station 15.7 inches, y = 0.050 inches

Figure 14 (Continued) Longitudinal turbulence spectrum.



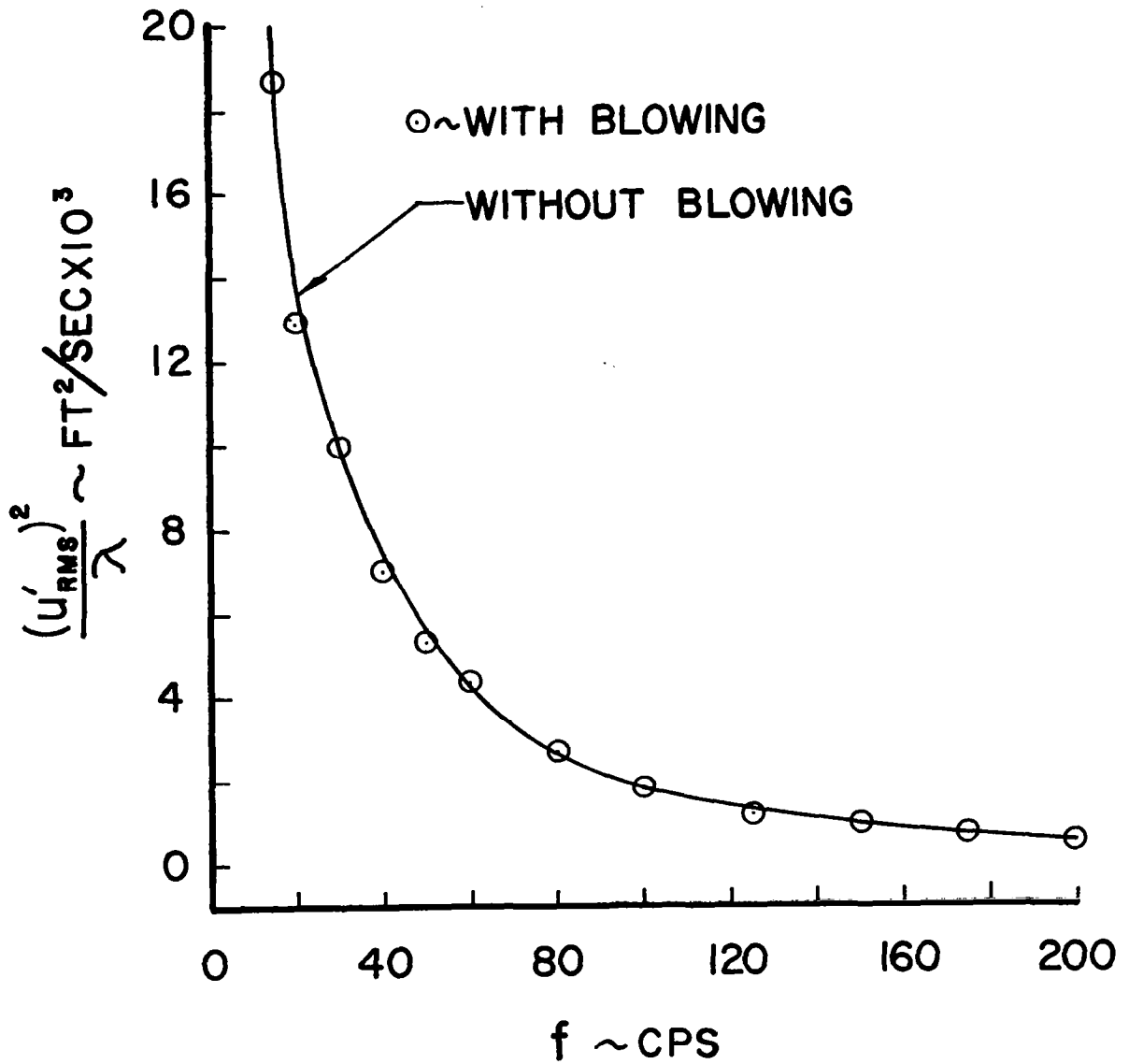
(d) Station 15.7 inches, $y = 0.100$ inches

Figure 14 (Continued) Longitudinal turbulence spectrum.



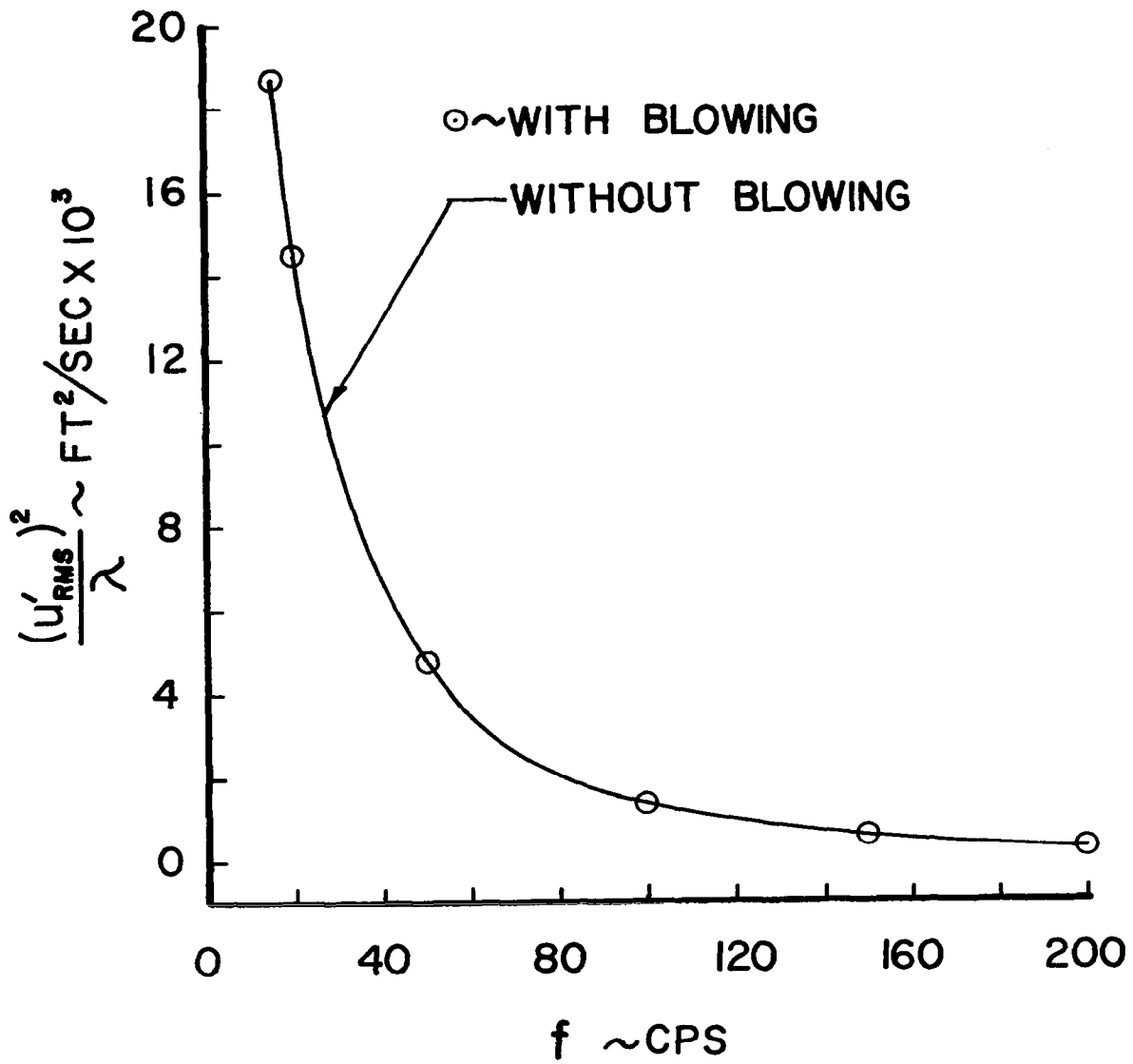
(e) Station 15.7 inches, $y = 0.250$ inches

Figure 14 (Continued) Longitudinal turbulence spectrum.



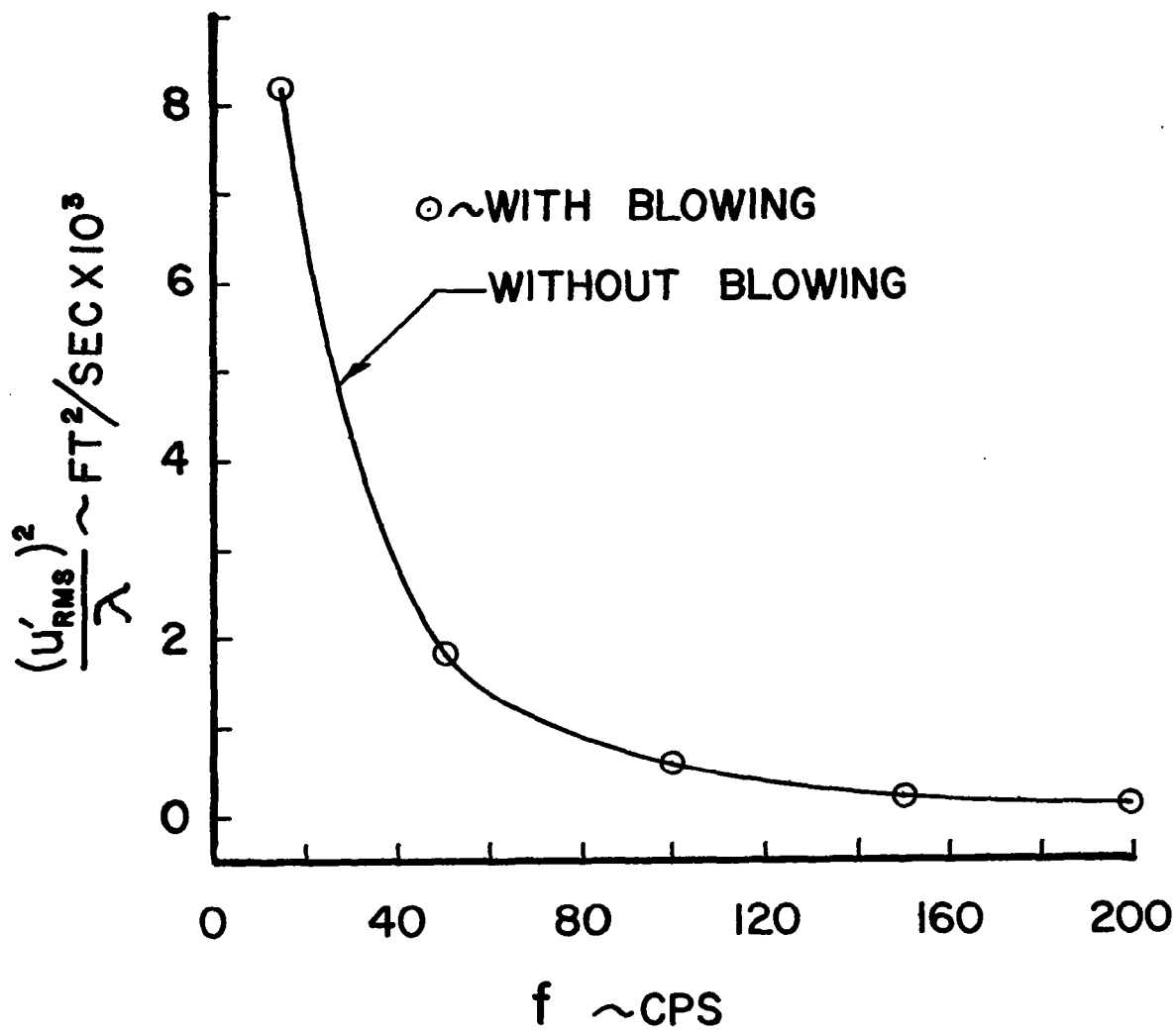
(f) Station 15.7 inches, y = 0.500 inches

Figure 14 (Continued) Longitudinal turbulence spectrum.



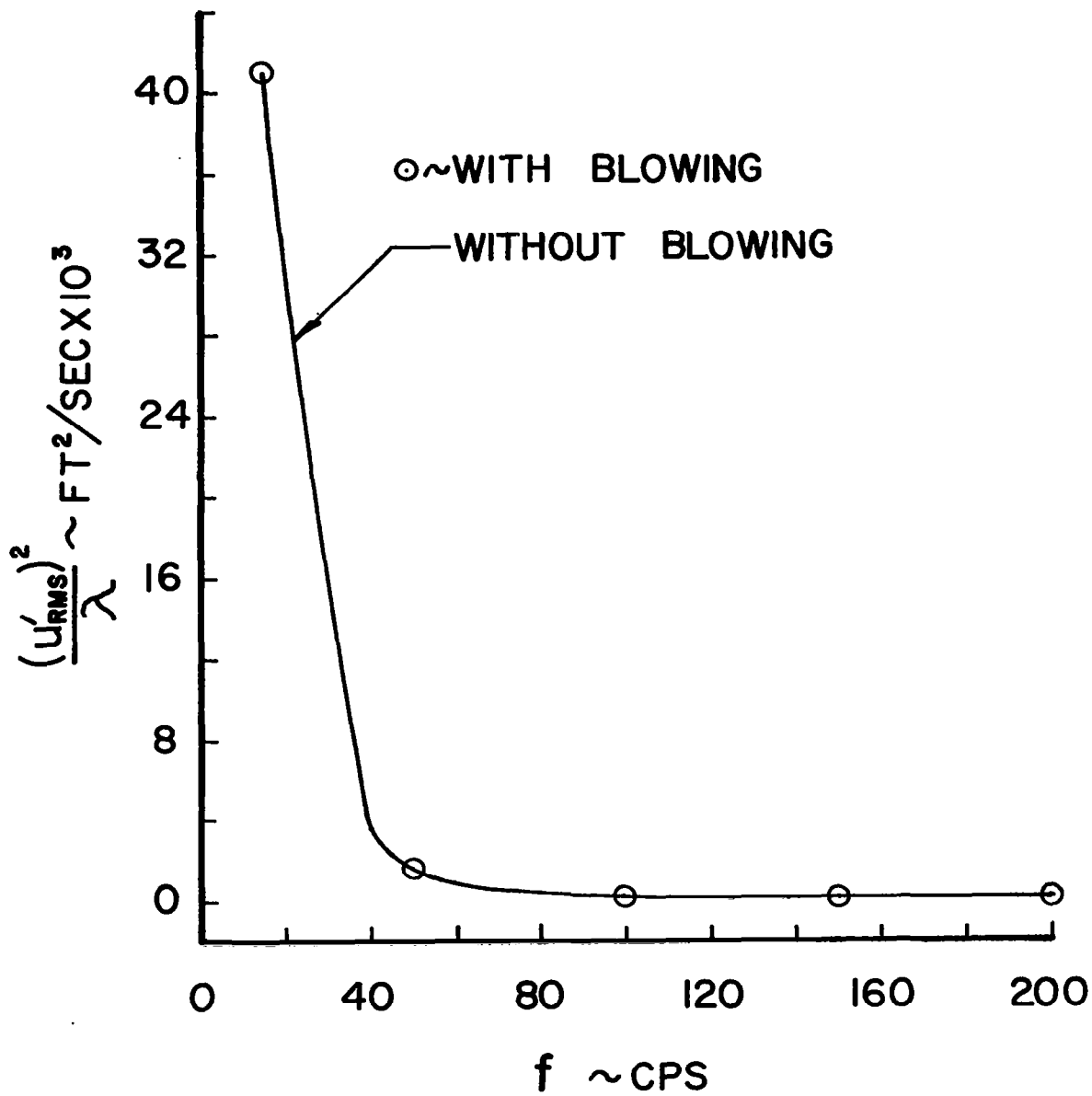
(g) Station 15.7 inches, y = 1.000 inches

Figure 14 (Continued) Longitudinal turbulence spectrum.



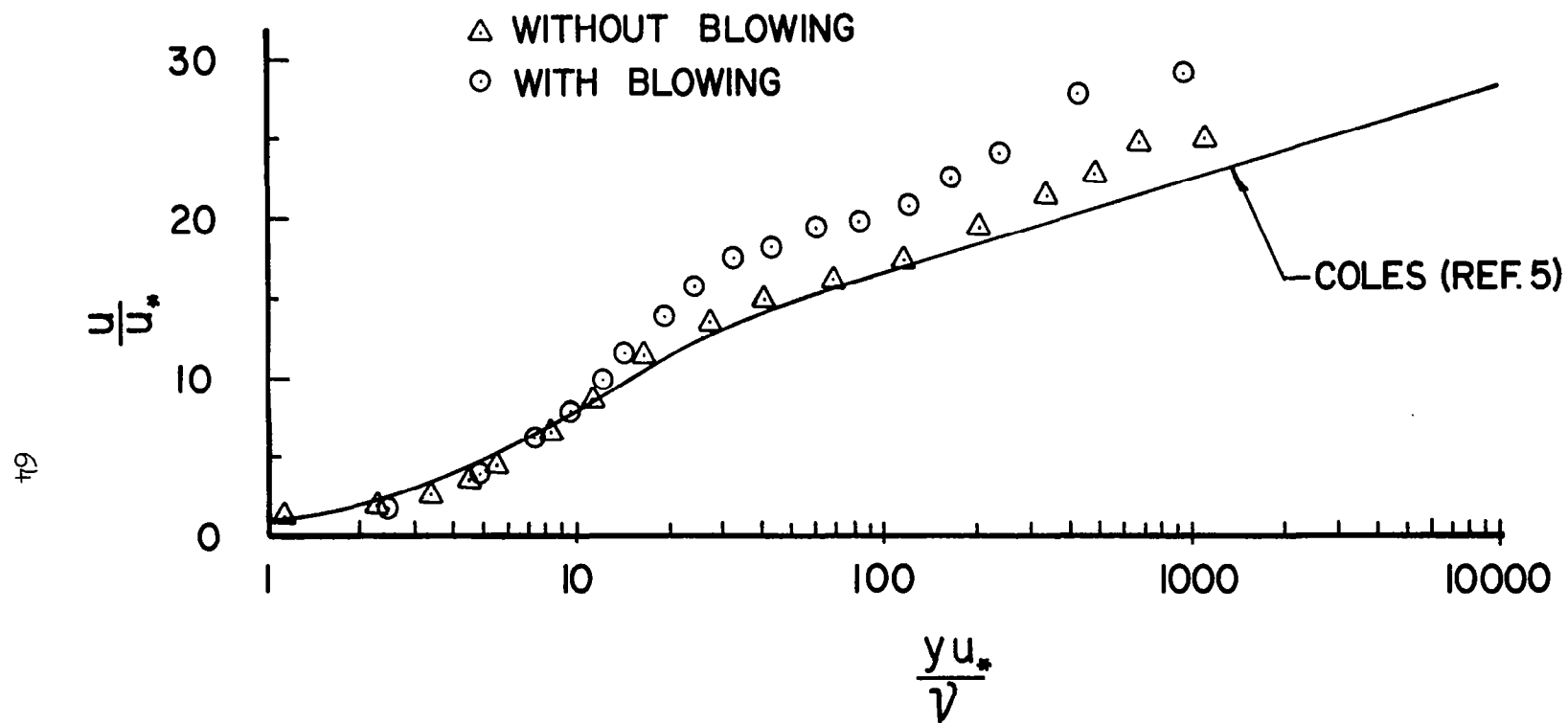
(h) Station 15.7 inches, $y = 2.000$ inches

Figure 14 (Continued) Longitudinal turbulence spectrum.

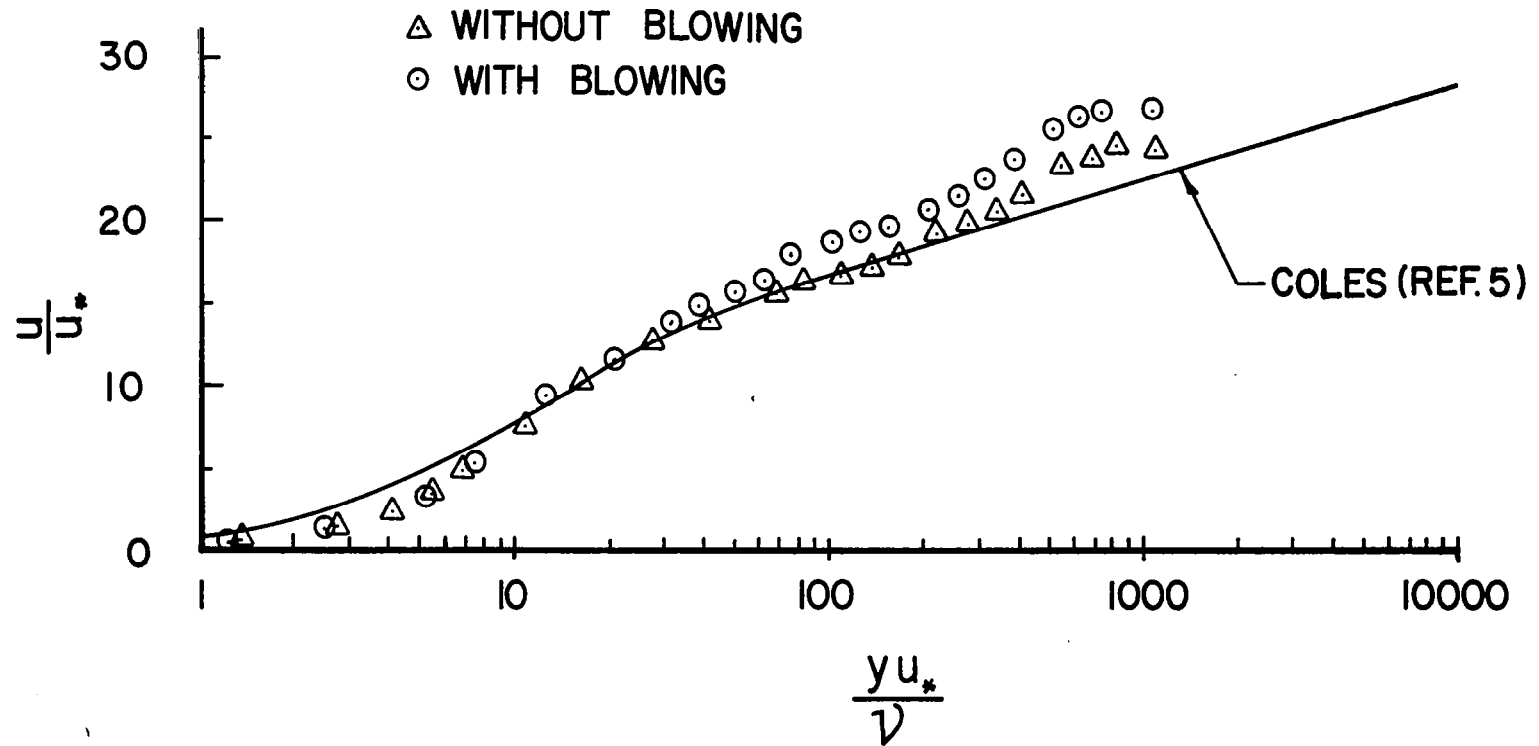


(1) Station 15.7 inches, $y = 4.015$ inches (channel centerline)

Figure 14 (Concluded) Longitudinal turbulence spectrum.

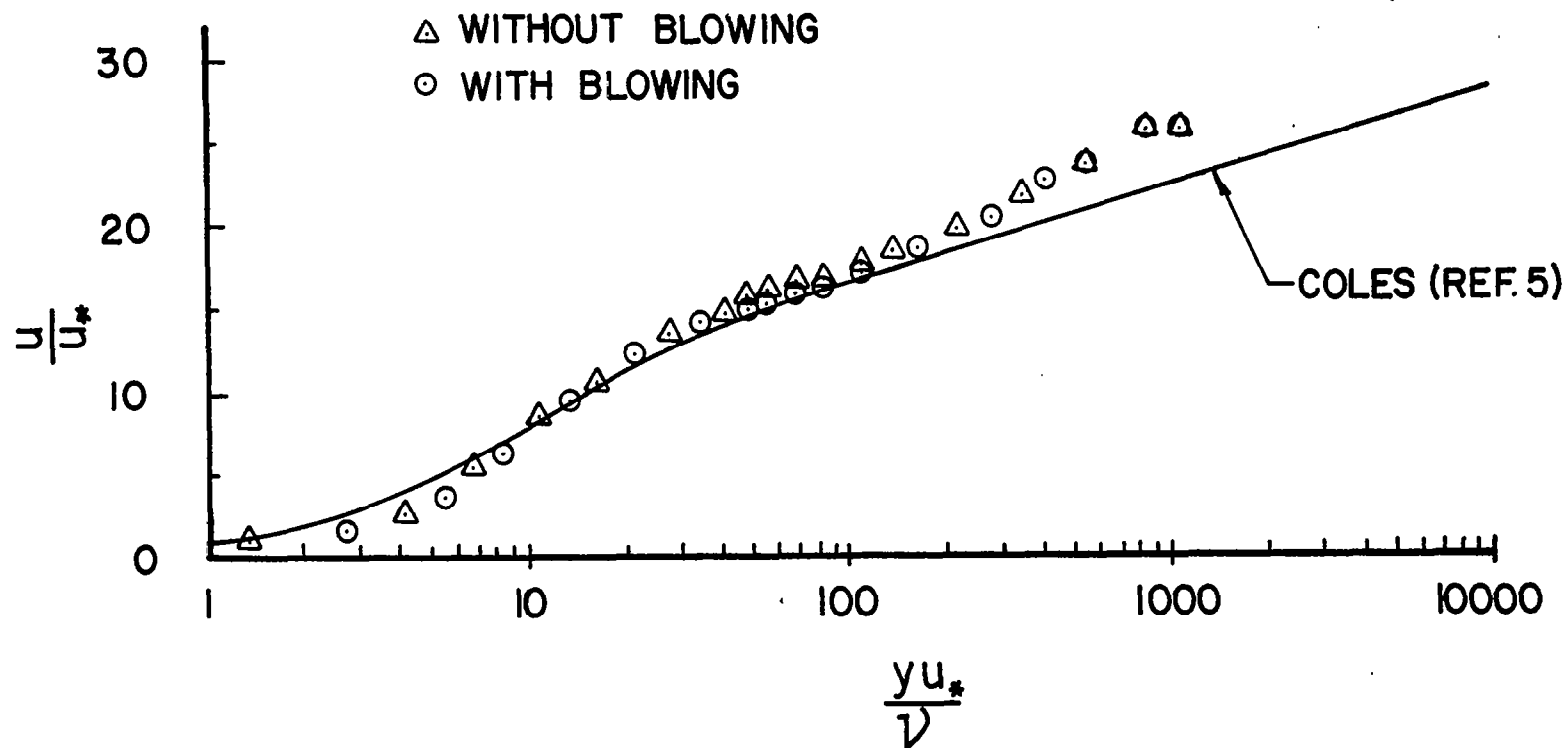


(a) Station 3.3 inches, $Q = 60 \times 10^{-3}$ ft³/sec (steady), $\Delta\tau_o = -24.3\%$
 Figure 15 Law of the wall velocity profile, $\tau_{oNB} = 6.72 \times 10^{-4}$ lb/ft².



(b) Station 6.9 inches, $Q = 60 \times 10^{-3}$ ft³/sec (steady), $\Delta\tau_o = -15.2\%$

Figure 15 (Continued) Law of the wall velocity profile, $\tau_{o_{NB}} = 6.68 \times 10^{-4}$ lb/ft².



(c) Station 15.7 inches, $Q = 60 \times 10^{-3}$ ft³/sec (steady), $\Delta\tau_o = 0\%$
 Figure 15 (Concluded) Law of the wall velocity profile, $\tau_{o_{NB}} = 6.59 \times 10^{-4}$ lb/ft²

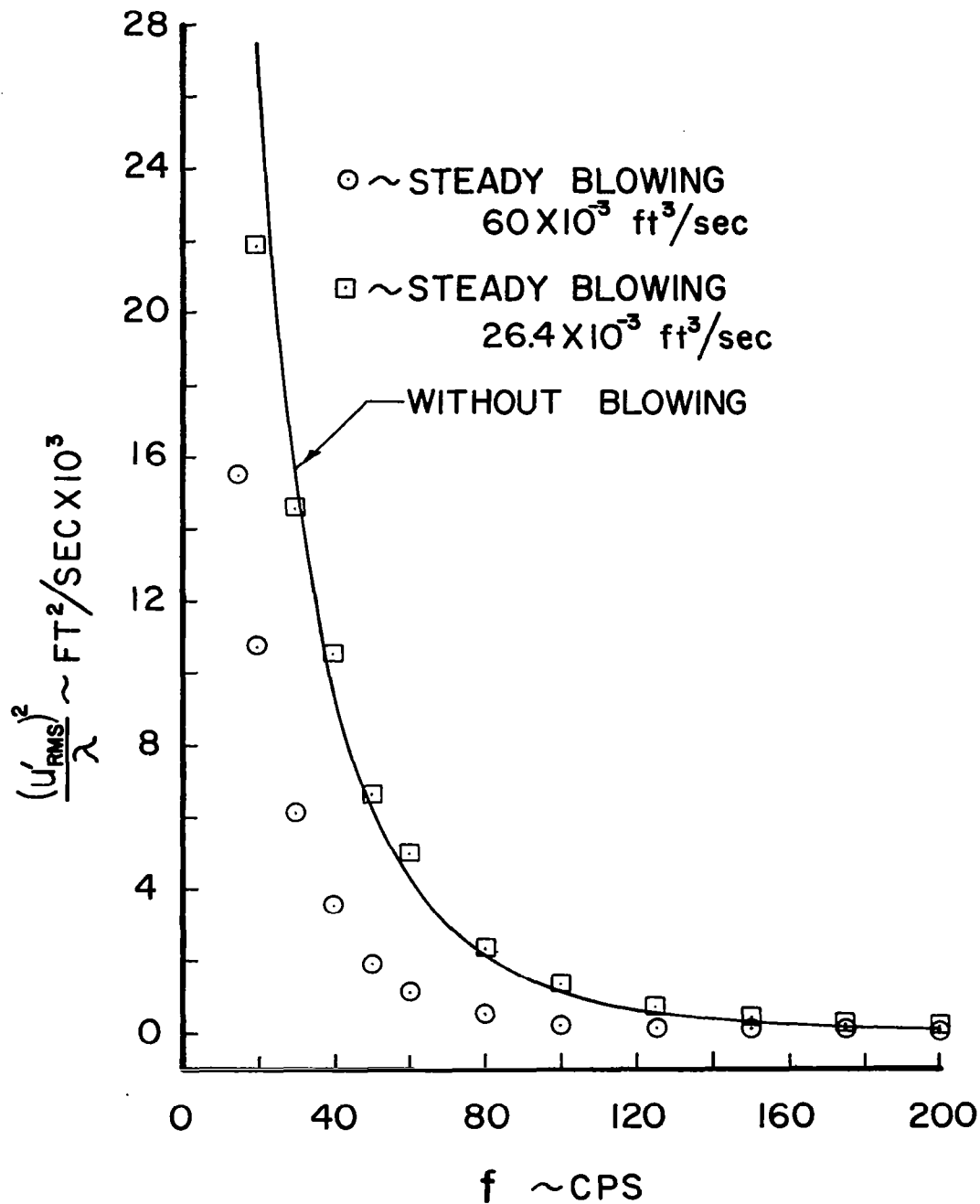


Figure 16 Longitudinal turbulence spectrum for various blowing conditions, station 3.3 inches, $y = 0.025$ inches.